TABLE OF CONTENTS

[redacted]

0012

3 8

LIST OF TABLES

LIST OF FIGURES

(At rear of Section)

0014

FIGURES (Cont'd)

0015

FIGURES (Cont'd)

0016

FIGURES (Cont'd)

0017

14 SAFETY ANALYSIS

14.1 CORE AND COOLANT BOUNDARY PROTECTION ANALYSIS

14.1.1 ABNORMALITIES

In previous sections of this report both normal and abnormal operations of the various systems and components have been discussed. This section summarizes and further explores abnormalities that are either inherently terminated or require the normal protection systems to operate to maintain integrity of the fuel and/or the reactor coolant system. These abnormalities have been evaluated for the rated power of 2,633 MWt. Fission product dispersion in the atmosphere is assumed to occur as predicted by the dispersion models developed in 2.3. Table 14-1 summarizes the potential abnormalities studied.

Table 14-1
Abnormalities Affecting Core and Coolant Boundary

Event	Analysis Assumptions	Effect
Uncompensated Operating Reactivity Changes	Automatic control system inoperative or unused.	Changes in reactor system average temperature. Automatic reactor trip if uncompensated. No equipment damage or radiological hazard.
Start-Up Accident	Uncontrolled single-group and all-group rod withdrawal from subcriticality with the reactor at zero power. Only high flux and high pressure trips were used to terminate the accident.	Power rise terminated by negative Doppler effect, control rod inhibit on short period, high reactor coolant system pressure, or overpower. No equipment damage or radiological hazard.
Rod Withdrawal Accident at Rated Power Operation	Uncontrolled single-group and all-group rod withdrawal with the reactor at rated power. Only high flux and high pressure trips were used to terminate the accident.	Power rise terminated by overpower trip or high-pressure trip. No equipment damage or radiological hazard.
Moderator Dilution Accident	Uncontrolled addition of unborated water to the reactor coolant system due to failure of equipment designed to limit flow rate and total water addition.	Slow change of power terminated by reactor trip on high temperature or pressure. During shutdown a decrease in shutdown margin occurs, but criticality does not occur. No radiological hazard.

8

[redacted]
Amendment No. 0018

Table 14-1 (Cont'd)

Event	Analysis Assumptions	Effect
Loss of Coolant Flow	Reactor coolant system flow decreases because of mechanical or electrical failure in one or more reactor coolant pumps. The only reactor protection systems assumed are the flux-flow and power-pump trips.	None. Core protected by reactor low-flow trip or loss-of-power trip. No radiological hazard.
Stuck-Out, Stuck-In, or Dropped-In Control Rod	Asymmetric rod monitor operates to inhibit rod out-motion and run back of secondary load.	None. Subcriticality can be achieved if one rod is stuck out. (if stuck in or dropped in, continued operation is permitted if effect on power peaking not severe.) No radiological hazard.
Loss of Electric Power	Both a loss of load condition and a complete loss of all plant power are considered. One per cent defective fuel plus a 1 gpm steam generator tube leakage are assumed.	Possible power reduction or reactor trip, depending on condition. Redundancy provided for safe shutdown. Integrated thyroid dose at exclusion distance is 0.004 rem.
Steam Line Failure	Reactor coolant leakage into the steam generator continues for 3 hours following reactor operation with 1% defective fuel and 1 gpm steam generator tube leakage.	Reactor trips following a large rupture. Integrated doses at exclusion distance are 0.002 rem whole body and 0.25 rem thyroid.
Steam Generator Tube Failures	Reactor coolant leakage into the steam generator continues for 1.7 hours following reactor operation with 1% defective fuel.	Reactor automatically trips if leakage exceeds normal makeup capacity to reactor coolant system. Integrated doses at exclusion distance are 0.38 rem whole body and 0.005 rem thyroid.

0019

14.1.2 ANALYSIS OF EFFECTS AND CONSEQUENCES

14.1.2.1 Uncompensated Operating Reactivity Changes

14.1.2.1.1 Identification of Cause

During normal operation of the reactor, the overall reactivity of the core changes because of fuel depletion and changes in fission product poison concentration. These reactivity changes, if left uncompensated, can cause operating limits to be exceeded. In all cases, however, the reactor protection system prevents safety limits from being exceeded. No damage occurs from these conditions.

14.1.2.1.2 Analysis and Results

During normal operation, the automatic reactor control system senses any reactivity change in the reactor. Depending on the direction of the reactivity change, the reactor power increases or decreases. Correspondingly, the reactor coolant system average temperature increases or decreases, and the automatic reactor control system acts to restore reactor power to the power demand level and to reestablish this temperature at its set point. If manual corrective action is not taken or if the automatic control system malfunctions, the reactor coolant system average temperature changes to compensate for the reactivity change. It is assumed in the analysis that the secondary system follows the temperature changes in the reactor coolant system. Table 14-2 summarizes these typical changes. | 8

Table 14-2 | 8
Typcial Uncompensated Reactivity Changes

Cause	Maximum Reactivity Rate, (Δk/k)/min	Rate of Average Temperature Change (Uncorrected), F/min
Fuel Depletion	-1.7×10^{-7}	-0.0004
Xenon Buildup	-2.2×10^{-5}	-0.060

These results are based on $+0.5 \times 10^{-4}$ (Δk/k)/F moderator coefficient and -1.17×10^{-5} (Δk/k)/F Doppler coefficient. The Doppler coefficient is representative of beginning of core life for the first cycle; however, the results shown are conservative because the reactor has a negative moderator coefficient at the beginning of core life for the first cycle. These reactivity changes are extremely slow and allow the operator to detect and compensate for the change.

14.1.2.2 Start-Up Accident

14.1.2.2.1 Identification of Cause

The objective of a normal start-up is to bring a subcritical reactor to the critical or slightly supercritical condition, and then to increase power in a [redacted] 0020

controlled manner until the desired power level and system operating temperature are obtained. During a start-up, an uncontrolled reactivity addition could cause a nuclear excursion. This excursion is terminated by the strong negative Doppler effect if no other protective action operates.

The following design provisions minimize the possibility of inadvertent continuous rod withdrawal and limit the potential power excursions:

a. The control system is designed so that only one control rod group can be withdrawn at a time, except that there is a 25 per cent overlap in travel between two rod groups successively withdrawn. This overlap occurs at the minimum worth positions for each group since one group is at the end of travel and the other is at the beginning of travel. The maximum calculated worth of any single control rod group is 1.5 per cent $\Delta k/k$ when the reactor is critical as specified in 7.3.2.1.

b. Control rod withdrawal rate is limited to 30 in./min.

c. A short-period withdrawal stop and alarm are provided in the source range.

d. A short-period withdrawal stop and alarm are provided in the intermediate range.

e. A high flux level and a high-pressure trip are provided in the power range.

The criterion for the analysis of this accident is that the reactor protection system shall be designed to limit (a) the reactor thermal power to 112 per cent of rated power, and (b) the reactor coolant system pressure so as not to exceed code pressure limits.

14.1.2.2.2 Methods of Analysis

A B&W digital computer model of the reactor core and coolant system was used to determine the characteristics of this accident. This model used full reactor coolant flow, but no heat transfer out of the system and no sprays in the pressurizer. The rated-power Doppler coefficient -1.17×10^{-5} $(\Delta k/k)/F$ was used although the Doppler is much larger than this for the principal part of the transient. The rods were assumed to be moving along the steepest part of the rod-worth versus rod-travel curve. The values of the principal parameters used are shown in Table 14-3.

0021

Table 14-3
Startup Accident Analysis Parameters

Control Rod Group Worth, % Δk/k	1.5
Control Rod Speed, in./min	30
Doppler Coefficient, (Δk/k)/F	-1.17×10^{-5}
Moderator Coefficient, (Δk/k)/F[a]	$+0.5 \times 10^{-4}$
CRA Insertion Time (2/3 Insertion), s	1.4
Trip Delay Time (High Flux Trip), s	0.3
Trip Delay Time (High Pressure Trip), s	0.5

(a) This is a conservative value because the reactor has a negative moderator coefficient.

In addition, the criterion for minimum movable control rod worth is that a shutdown margin of 1 per cent Δk/k at the hot standby condition is required (3.2.2.1.2). The start-up accident has been analyzed using the minimum tripped rod worth as part of the analysis.

The start-up accident was analyzed from 1 per cent Δk/k subcritical at the hot, pressurized condition.

14.1.2.2.3 Results of Analysis

Figure 14-1 shows the results of withdrawing the maximum worth control rod group at a rod speed of 30 in./min from 1 per cent subcritical. This group is worth a maximum of 1.5 per cent Δk/k. This rod velocity and worth result in a maximum reactivity addition rate of 1.09×10^{-4} (Δk/k)/s. The Doppler effect begins to slow the neutron power(*) rise, but the heat to the coolant increases the pressure past the trip point, and the transient is terminated by the high-pressure trip.

Figure 14-2 shows the results of withdrawing all 49 control rod assemblies at the maximum speed (with a total worth of 8 per cent Δk/k) from 1 per cent subcritical. Although the calculated total rod worth (Table 3-2) is slightly higher, the sensitivity analysis in Figures 14-3 and 14-4 indicate that the difference will have little effect on the analysis. This results in a maximum reactivity addition rate of 5.8×10^{-4} (Δk/k)/s. The neutron power peaks at 288 per cent, where the power rise is stopped by the negative Doppler effect. The high neutron flux trip takes effect 0.3 s after the peak power is reached and terminates the transient. The peak thermal heat flux is only 42 per cent of the rated power heat flux.

- - - - -

0022

(*) Neutron power is defined as the total energy release from fission.

A sensitivity analysis was performed on both of these start-up accidents to determine the effect of varying several key parameters. Variation of the trip delay time from 0.1 to 0.7 s resulted in a change in peak thermal power of only 5 per cent. Figures 14-3 through 14-6 show typical results for the single group, 1.5 per cent Δk/k start-up accident.

Figures 14-3 and 14-4 show the effect of varying the reactivity addition rate on the peak thermal power and peak neutron power. This reactivity rate was varied from more than an order of magnitude below the nominal single rod-group rate used for analysis (i.e., the rate for the maximum-worth 1.5 per cent Δk/k group) to a rate above that for simultaneous withdrawal of all rods. The slower rates--up to about 2.0×10^{-4} (Δk/k)/s--will result in the pressure trip being actuated. Only the very fast rates actuate the high neutron flux level trip.

Figures 14-5 and 14-6 show the peak thermal power variation as a function of a wide range of moderator and Doppler coefficients for the 1.5 per cent Δk/k rod group. The peak thermal power varied about 10 per cent from the nominal case for the moderator coefficient variation, and also by about 10 per cent from the nominal for the range of Doppler coefficients. Figures 14-7 and 14-8 are the corresponding results from the withdrawal of all rods (8 per cent Δk/k).

None of these postulated start-up accidents, except for reactivity addition rates greater than 2×10^{-3} (Δk/k)/s, which is three times greater than for withdrawal of all rods at once, causes a thermal power peak in excess of 100 per cent rated power or a nominal fuel rod average temperature greater than 1,150 F. The nominal 1.5 per cent Δk/k rod group withdrawal causes a peak pressurizer pressure of 2,515 psia, the relief valve set point. The capacity of the relief valves is adequate to handle the maximum rate of coolant expansion resulting from a start-up accident at 2×10^{-3} (Δk/k)/s.

It is concluded that the reactor is completely protected against any start-up accident involving the withdrawal of any or all control rods, since in no case does the thermal power approach 112 per cent, and the peak pressure never exceeds code allowable limits.

14.1.2.3 Rod Withdrawal Accident at Rated Power Operation

14.1.2.3.1 Identification of Cause

A rod withdrawal presupposes an operator error or equipment failure which results in accidental withdrawal of a control rod group while the reactor is at rated power. As a result of this assumed accident, the power level increases, the reactor coolant and fuel rod temperatures increase, and, if the withdrawal is not terminated by the operator or protection system, core damage would eventually occur.

The following provisions are made in the design to indicate and terminate this accident:

a. High reactor outlet coolant temperature alarms.

b. High reactor coolant system pressure alarms.

0023

c. High pressurizer level alarms.

d. High reactor outlet coolant temperature trip.

e. High reactor coolant system pressure trip.

f. High power level (i.e., neutron flux level) trip.

The rod withdrawal accident analysis is performed with the criterion that the reactor protection system will limit (a) the reactor thermal power to 112 per cent of rated power, and (b) the reactor coolant system pressure to code allowable limits.

14.1.2.3.2 Methods of Analysis

A B&W digital computer code was used to determine the characteristics of this accident. A complete kinetics model, pressure model, average fuel rod model, steam demand model with secondary coastdown to decay heat level, coolant transport model, and a simulation of the instrumentation for pressure and flux trip were included. The initial conditions were normal rated power operation without automatic control. Only the moderator and Doppler coefficients of reactivity were used as feedback. The nominal values used for the main parameters are shown in Table 14-4.

Table 14-4
Rod Withdrawal Accident Analysis Parameters

Trip Delay Time (High Pressure Trip), s	0.5
Trip Delay Time (High Flux Trip), s	0.3
CRA Insertion Time (2/3 Insertion), s	1.4
Doppler Coefficient, $(\Delta k/k)/F$	$(-)\ 1.17 \times 10^{-5}$
Moderator Coefficient, $(\Delta k/k)/F$ [(a)]	$(+)\ 0.5 \times 10^{-4}$
Control Rod Speed, in./min	30
Control Rod Group Worth, $\sim \Delta k/k$	1.5

(a) This is a conservative value because the reactor has a negative moderator coefficient.

The criterion for minimum movable control rod worth is that a shutdown margin of 1 per cent $\Delta k/k$ at the hot stand-by condition is required (3.2.2.1.2). The rod withdrawal accident has been analyzed using the minimum tripped rod worth as part of the analysis.

14.1.2.3.3 Results of Analysis

Figure 14-9 shows the results of the nominal rod withdrawal from rated power using the 1.5 per cent Δk/k rod group at 1.09 x 10^{-4} (Δk/k)s. The transient is terminated by a high neutron flux level trip, and the reactor thermal power is limited to 106 per cent, well below the design overpower of 112 per cent of rated power. The changes in the parameters are all quite small. For example, the average reactor coolant temperature rise is only about 2 F and system pressure increase is only 70 psi.

A sensitivity analysis of important parameters was performed around this nominal case, and the resultant reactor coolant system pressure responses are shown in Figures 14-10 through 14-13.

Figure 14-10 shows the pressure variation for a very wide range of rod withdrawal rates--more than an order of magnitude smaller and greater than the nominal case. For the very rapid rates, the neutron flux level trip is actuated. This is the primary protective device for the reactor core. It also protects the system against high pressure during fast rod withdrawal accidents. The high-pressure trip is relied upon for the slower transients. In no case does the thermal power exceed 109 per cent rated power.

Figures 14-11 through 14-13 show the pressure response to variations in the trip delay time, Doppler coefficient, and moderator coefficient. In all cases the neutron flux level trip is actuated.

An analysis has been performed extending the evaluation of the rod withdrawal accident for various fractional initial power levels up to rated power. This evaluation has been performed assuming simulated withdrawal of all 49 control rods giving a maximum reactivity addition rate of 5.8 x 10^{-4} (Δk/k)/s. This rate is a factor of six higher than that used in the cases evaluated for withdrawal of a single group. The results of this analysis are shown in Figures 14-14 and 14-15.

As seen in Figure 14-14, the peak thermal power occurs for the rated power case and is well below the maximum design power of 112 per cent. The peak neutron power for all cases is approximately 116 per cent of rated power and represents a slight overshoot above the trip level of 112 per cent. Figure 14-15 shows that the maximum fuel temperature reached in the average rod and the hot spot are well below melting. Even in the most severe case at rated power, the average fuel temperature increased by only 24 F. It is therefore, readily concluded that no fuel damage would result from simultaneous withdrawal of all rods from any initial power level.

This analysis demonstrates that the high-pressure trip and the high flux level trip adequately protect the reactor against any rod withdrawal accident from rated power.

14.1.2.4 Moderator Dilution Accident

14.1.2.4.1 Identification of Cause

The reactor utilizes boron in the form of boric acid in the reactor coolant to control excess reactivity. The boron content of the reactor coolant is

0025

periodically reduced to compensate for fuel burnup. The dilution water is supplied to the reactor coolant system by the makeup and purification system. This system is designed with several interlocks and alarms to prevent improper operation. These are as follows:

a. Flow of dilution water to the letdown tank must be initiated by the operator. The dilution water addition valve can be opened only when the control rods have been withdrawn to a preset (95 per cent withdrawn) position and the timing device to limit the integrated flow has been set. Dilution water is added at flow rates up to 70 gpm at 2,200 psia.

b. Flow of dilution water is automatically stopped when either the flow has integrated to a preset value or when the rods have been inserted to a preset position (at 75 per cent full stroke).

c. A Dilute Permit light and feed and bleed valve position lights on the console are on whenever dilution is in progress.

The makeup and purification system normally has one pump in operation which supplies makeup to the reactor coolant system and the required seal flow to the reactor coolant pumps. Thus, the total makeup flow available is normally limited to 70 gpm. When the makeup rate is greater than the letdown rate, the net water increase will cause the pressurizer level control to close the makeup valves. The nominal moderator dilution event considered is the pumping of water with zero boron concentration from the makeup tank to the reactor coolant system by use of the makeup pump.

It is possible, however, to have a slightly higher flow rate during transients when the system pressure is lower than nominal value and the pressurizer level is below normal. This flow might temporarily be as high as 100 gpm.

Furthermore, with a combination of multiple valve failures or maloperations, plus more than one makeup pump operating with reduced reactor coolant system pressure, the resulting inflow rate could be as high as 500 gpm. This constitutes the maximum dilution accident. A reactor trip would terminate unborated water addition to the makeup tank, and total flow into the coolant system would be terminated by a high pressurizer level.

The criteria for reactor protection in this accident are:

a. The reactor thermal power will be limited to less than the design overpower of 112 per cent rated power.

b. The reactor coolant system pressure will be limited to less than the code allowable limit.

c. The reactor minimum shutdown margin of 1 per cent $\Delta k/k$ subcritical will be maintained.

14.1.2.4.2 Analysis and Results

The reactor is assumed to be operating at rated power with an initial boron concentration of 1,200 ppm in the reactor coolant system. The dilution water

is uniformly distributed throughout the reactor coolant volume. Uniform distribution results from a discharge rate of 70 - 500 gpm into a reactor coolant flow of 88,000 gpm. A change in concentration of 100 ppm produces a 1 per cent $\Delta k/k$ reactivity change. The analysis is based on $+0.5 \times 10^{-4}$ $(\Delta k/k)/F$ moderator coefficient, -1.17×10^{-5} $(\Delta k/k)/F$ Doppler coefficient, and 1200 ppm boron concentration, representative of beginning of core life conditions. This value for the moderator coefficient yields conservative results because the actual coefficient is negative. The effects of the three dilution rates discussed above on the reactor are shown in Table 14-5.

Table 14-5
Moderator Temperature Change Resulting From Dilution

Dilution Water Flow, gpm	Reactivity Rate, $(\Delta k/k)/s$	Average Reactor Coolant System Temp Change, °F/s
70	$+1.6 \times 10^{-6}$	0.004
100	$+2.3 \times 10^{-6}$	0.006
500	$+1.2 \times 10^{-5}$	0.033

The highest rate of dilution can be handled by the automatic control system, which would insert rods to maintain the power level and thus limit the reactor coolant system temperature rise. If an interlock failure occurred while the reactor was under manual control, these reactivity additions would cause a high reactor coolant temperature trip or a high-pressure trip. In any event, the thermal power will not exceed 112 per cent rated power, and the system pressure will not exceed code allowable limits. Therefore, moderator dilution accidents will not cause any damage to the reactor system.

During refueling or maintenance operations when the reactor closure head has been removed, the sources of dilution water makeup to the makeup tank--and therefore to the reactor coolant system--are locked closed, and the makeup pumps are not operating. At the beginning of core life when the boron concentration is highest, the reactor is about 9.5 per cent $\Delta k/k$ subcritical with the maximum worth rod stuck out. To demonstrate the ability of the reactor to accept moderator dilution during shutdown, the consequences of accidentally filling the makeup tank with dilution water and starting the makeup pumps have been evaluated. The entire water volume from the makeup tank could be pumped into the reactor coolant system (assuming only the coolant in the reactor vessel is diluted), and the reactor would still be 5.6 per cent $\Delta k/k$ subcritical.

14.1.2.5 Cold-Water Accident

The absence of individual loop isolation valves eliminates the potential source of cold water in the reactor coolant system. This is not a credible accident in this reactor.

0027

14.1.2.6 Loss-of-Coolant Flow

14.1.2.6.1 Identification of Cause

A reduction in the reactor coolant flow rate occurs if one or more of the reactor coolant pumps should fail. A pumping failure can occur from mechanical failures or from a loss of electrical power. With four independent pumps available, a mechanical failure in one pump will not affect operation of the others.

Each reactor coolant pump receives electrical power from one of the two electrically separate busses of the 13,800 volt system discussed in 8.2.2.3. Loss of the unit auxiliary transformer to which the 13,800 volt busses are normally connected will initiate a rapid transfer to the start-up transformer source without loss of coolant flow. Faults in an individual pump motor or its power supply could cause a reduction in flow, but a complete loss of forced flow is extremely unlikely. In spite of the low probability of this event, the nuclear unit has been designed so that such a failure would not lead to core damage. 2

The reactor protection criterion for loss-of-coolant-flow conditions starting at rated power is that the reactor core shall not reach a Departure From Nucleate Boiling Ratio (DNBR) smaller than the DNBR in the hot channel at the steady-state design overpower (112 per cent rated power). This corresponds to a DNBR of 1.50 (3.2.3.2.3 d).

14.1.2.6.2 Methods of Analysis

The loss-of-coolant-flow accident is analyzed by a combination of analog and digital computer programs. Analog simulation is used to determine the reactor flow rate following loss of pumping power. Reactor power, coolant flow, and inlet temperature are input data to the digital program which determines the core thermal characteristics during the flow coastdown.

The B&W digital computer model used to determine the neutron power following reactor trip includes six delayed neutron groups, control rod worth and rod insertion characteristics, and trip delay time. The analog model used to determine flow coastdown characteristics includes description of flow-pressure drop relations in the reactor coolant loop. Pump flow characteristics are determined from manufacturers' performance curves. Flow-speed, flow-torque, and flow-head relationships are solved by affinity laws.

A transient, thermal-hydraulic, B&W digital computer program is used to compute channel DNBR continuously during the coastdown transient. System flow, neutron power, fission product decay heat, and core entering enthalpy are varied as a function of time. The program maintains a transient inventory of stored heat which is determined from fuel and clad temperatures beginning with the initial steady-state conditions. The transient core pressure drop is determined for average channel conditions. The representative hot channel flows and corresponding DNBR are obtained by using the average core pressure drop. The hot channel DNBR as a function of time is compared with the design DNBR at maximum overpower to determine the degree of heat transfer margin.

The loss-of-coolant-flow analysis has been carried out in the power range for coastdown from power levels between 100 to 112 per cent rated power. Conditions utilized in the analysis are as follows:

[redacted]

0-28

a. Initial core inlet temperature for given power level is assumed to be plus 2 F in error.

b. Initial system pressure is assumed to be minus 65 psi in error.

c. Trip delay time, i.e., time from sensor detection of loss of power to the pumps until initial downward movement of control rod, is 500 milliseconds.

d. The per cent of beginning-of-life neutron power as a function of time after loss of pumps is as shown in Figure 3-5. This figure also contains the shutdown characteristics for a minimum of 1.0 per cent shutdown margin at the hot standby condition.

e. The pump inertia is 70,000 lb-ft^2.

14.1.2.6.3 Results of Analysis

The results of this analysis show that the reactor can sustain a loss-of-coolant-flow accident without damage to the fuel. The results of the evaluation are presented in Figures 14-16 and 14-17. Figure 14-16 shows the per cent reactor flow as a function of time after loss of all pump power. Figure 14-17 shows the minimum DNBR which occurs during the coastdown from various initial power levels using the minimum tripped rod worth assuming 1% $\Delta k/k$ subcritical margin at hot standby. The degree of core protection during coastdown is indicated by comparing the minimum DNBR for the coastdown (1.77) with the criterion value of 1.50. This DNBR (1.50) in the hot channel corresponds to a 99 per cent confidence that 99.96 per cent of the fuel rods in the core will not experience a departure from nucleate boiling under steady-state conditions at the design overpower (3.2.3.1).

Under normal conditions, the maximum indicated reactor power level from which a loss-of-coolant-flow accident could occur is 100 per cent rated power (as indicated by reactor instrumentation). The rated power is an instrument-indicated value and is subject to a 2 per cent heat balance error. The true power level could be as high as 102 per cent. As shown in Figure 14-17, however, the DNBR at 102 per cent is 1.70 for the minimum rod worth available. The coastdown from rated power results in a minimum DNBR of 1.77 which is considerably larger than the 112 per cent overpower minimum DNBR of 1.50.

The reactor coolant system is capable of providing natural circulation flow after the pumps have stopped. The natural circulation characteristics of the reactor coolant system have been calculated using conservative values for all resistance and form loss factors. No voids are assumed to exist in the core or reactor outlet piping. The following tabulation shows the natural circulation flow capability as a function of the decay heat generation.

Time After Loss of Power, s	Decay Heat Core Power, %	Natural Circulation Core Flow Available, % Full Flow	Flow Required for Heat Removal, % Full Flow
3.6×10^1	5	4.6	2.3
2.2×10^2	3	3.8	1.2
1.2×10^4	1	2.4	0.36
1.3×10^5	0.5	1.6	0.20

The flows above provide adequate heat transfer for core cooling and decay heat removal by the reactor coolant system.

The reactor is protected against reactor coolant pump failure(s) by the reactor protective system and the integrated control system. The integrated control system initiates a power reduction on pump failure to prevent reactor power from exceeding that permissible for the available flow. The reactor is tripped if insufficient reactor coolant flow exists for the power level.

14.1.2.7 Stuck-Out, Stuck-In, or Dropped-In Control Rod

14.1.2.7.1 Identification of Cause

The control rod drives have been described in 3.2.4.3. The results of continuous control rod withdrawal have been analyzed in 14.1.2.2 and 14.1.2.3. In the event that a control rod cannot be moved because of electrical faults or mechanical seizure, localized power peaking and subcritical margin must be considered.

14.1.2.7.2 Analysis and Results

Adequate hot subcritical margin is provided by requiring a subcriticality of 1% $\Delta k/k$ subcritical with the control rod of greatest worth fully withdrawn from the core. The nuclear analysis reported in 3.2.2 demonstrates that this criterion can be satisfied.

In the event that an unmovable control rod is partially or fully inserted in the core or a single rod is dropped during operation, its location and effect on local power distribution determine whether continued power operation is permissible. The location of a stuck rod in the core will be studied further to define permissible conditions of operation. The criteria for these studies are (a) operation with a stuck rod will not increase the DNB probability above the probability specified for design conditions, and (b) a hot subcritical margin of 1% $\Delta k/k$ will be maintained with the stuck rod in its inoperative position and the operating rod of greatest reactivity worth in the fully withdrawn position.

If a control rod is dropped into the core during power operation, the same consideration of localized power peaking as for a stuck rod will apply.

0030

14.1.2.8 Loss of Electric Power

14.1.2.8.1 Identification of Cause

The Davis-Besse Station is designed to withstand the effects of a loss of electric load or electric power. Emergency power systems are described in 8.2.3. Two types of power losses are considered:

a. A loss of load condition caused by separation of the unit from the transmission system.

b. A hypothetical condition which results in a complete loss of all system and station power except the station battery.

The reactor protection criteria for these conditions are that fuel damage will not occur from an excessive power-to-flow ratio nor will the reactor coolant system pressure exceed design pressure.

14.1.2.8.2 Results of Loss-of-Load Condition Analysis

The station has the capability to accommodate a loss of-load condition without a reactor or turbine trip. The net effect of a loss-of-load condition on the station would be opening of the main generator breakers, thus disconnecting the station from the entire transmission system. When this occurs, a runback signal on the integrated master controller causes an automatic power reduction to 15 per cent power. Other actions which occur include:

a. All vital electrical loads, including power to the reactor coolant pumps, condenser circulating water pumps, condensate and condensate booster pumps, and other auxiliary equipment, will continue to obtain power from the unit generator. Feedwater is supplied to the steam generators by steam-driven feed pumps.

b. As the electrical load is dropped, the turbine generator accelerates and closes the governor valves and reheater intercept valves. The unit frequency will peak at less than the overspeed trip point and decay back to set frequency in 40-50 s.

c. Following closure of turbine governor valves and reheat intercept valves, steam pressure increases to the turbine bypass valve set point, and may increase to the steam system safety valve set point. Steam is relieved to the condenser and to the atmosphere. Steam venting to the atmosphere occurs for about three minutes following loss-of-load from 100 per cent initial power until the turbine bypass can handle all excess steam generated. About 350,000 pounds of steam will be relieved to the atmosphere. Steam relief permits energy removal from the reactor coolant system to prevent a high pressure reactor trip. The initial power runback is to 15 per cent power, which is a higher power level than needed for the unit auxiliary load. This allows sufficient steam flow for regulating turbine speed control. Excess steam above unit auxiliary load requirements is rejected by the turbine bypass valves to the condenser.

0031

d. During the short interval while the turbine speed is high, the vital electrical loads connected to the unit generator will undergo speed increase in proportion to the generator frequency increase. All pumps, motors and electrical gear so connected will withstand the increased frequency.

e. After the turbine generator has been stabilized at 15 per cent power set frequency, the station operator may reduce reactor power to the auxiliary load as desired.

The loss-of-load accident does not result in any fuel damage or excessive pressures on the reactor coolant system. There is no resultant radiological hazard to station operating personnel or to the public from this accident as only secondary system steam is discharged to the atmosphere.

If the station was being operated with 1 per cent defective fuel and 1 gpm steam generator leakage, the leaking reactor coolant would be vaporized and carried into the condenser with the normal steam flow. Most of the radioactive iodine would go into the condensate and be removed by the full flow condensate demineralizers. However, a loss-of-load would result in direct venting of steam to the atmosphere for three minutes. During this period 0.06 dose equivalent curies of I-131 would be released. The integrated thyroid dose at the site boundary from this release would be 0.004 rem.

14.1.2.8.3 Results of Complete Loss of All Station Power Analysis

The second power loss considered is the hypothetical case where all station power except the station batteries is lost. The sequence of events and the evaluation of consequences relative to this accident are:

a. A loss of power results in gravity insertion of the control rods and trip of the turbine stop valves.

b. The steam generator safety valves actuate after the turbine stop valves trip and prevent excessive temperatures and pressures in the reactor coolant system.

c. The reactor coolant system flow decays without fuel damage occurring. Decay heat removal after coastdown of the reactor coolant pumps is provided by the natural circulation characteristics of the system. This capability is discussed in the loss-of-coolant-flow evaluation (14.1.2.6).

d. Two turbine-driven auxiliary feedwater pumps are provided to supply feedwater any time the main feed pumps cannot operate. The auxiliary feed pumps take suction from the deareater and the condensate storage tanks and are driven by steam from either or both steam generators. The auxiliary feedwater system is discussed in Section

0032

9.10. The controls and auxiliary systems for the auxiliary feed pumps operate on d-c power from the station batteries.

A recirculation line from the auxiliary pump discharge back to the deareator is provided to permit periodic testing.

e. There will normally be 120,000 gallons of water in the two deaerator storage tanks for cooldown. This is adequate to cool down to 280F whereupon the decay heat system will continue the cooldown. The deaerator storage is backed up by additional storage in the condensate storage tanks. 6

The features described above permit decay heat cooling of the nuclear unit for an extended period of time following a complete loss of outside electric power.

The above evaluation demonstrates the features incorporated in the design to sustain loss of power conditions with only the station battery to operate system controls. Immediate operation of the auxiliary feedwater pump and the emergency condenser cooling water system is not of critical nature. The reactor can sustain a complete electric power loss without emergency cooling for about 23 min before the steam volume in the pressurizer is filled with reactor coolant. These 23 minutes are derived as follows:

Steam generators evaporate to dryness	9 min
Pressurizer relief valves open	5 min
Pressurizer fills with water (due to reactor coolant system expansion)	9 min
	23 min

Beyond this time reactor coolant will boil off, and an additional 83 min will have elapsed before the boiloff will start to uncover the core.

The auxiliary feedwater pump can be actuated within this period of time. Accordingly, core protection is ensured for the unlikely condition of total loss of station electric power.

14.1.2.9 Steam Line Failure

14.1.2.9.1 Identification of Cause

Analyses have been performed to determine the effects and consequences of loss of secondary coolant due to a 36 in. O.D. double-ended, steam line rupture.

The criteria for plant protection and the release of fission products to the environment are as follows:

a. The core will remain intact for effective core cooling, assuming minimum tripped rod worth with a stuck rod.

b. No steam generator tube loss of primary boundary integrity will occur due to the loss of secondary side pressure and resultant temperature gradients.

0033

c. Doses will be within 10 CFR 100 limits.

14.1.2.9.2 Analysis and Results

Accident Dynamics

The loss of secondary coolant due to a failure of a steam line between the steam generator and the turbine causes a decrease in steam pressure, thus placing a demand on the control system for increased feedwater flow. The turbine control valves will open to maintain power generation. Increased feedwater flow, accompanied by steam flow through the turbine stop valves and the break, lowers the average reactor coolant temperature. The limiting action in this condition is the 102 per cent power demand to the rod drive control system.

The steam line failure was analyzed for the maximum break size to determine the maximum cooling effects on reactor coolant and related core reactivity effects. In addition, two plant conditions were considered; one uses a positive moderator coefficient, the other represents end-of-core-life (EOL) condition with a negative moderator coefficient.

The rate of reactor system cooling following a steam line break accident is also a function of the steam generator water inventory available for cooling. The steam generator inventory increases with power level. The inventory at rated power is 55,000 lb. This decreases linearly to 20,000 lb at 15 per cent of rated power. The larger inventory results in a greater mass available for cooling.

A steam line rupture of small area causes a relatively slow decrease in steam pressure. With a positive moderator temperature coefficient the reactor power will decrease when the control system reaches the power demand limit because of the continuing temperature decrease. The reactor will then trip on low reactor coolant system pressure, causing a turbine trip. It is impossible for the reactor in this condition to return to criticality.

When the moderator temperature coefficient is negative, the reactor power will increase with decreasing average coolant temperature. This will cause control rod insertion in an attempt to limit reactor power to 102 per cent. Additional cooling causes a reduction in reactor coolant pressure and an increase in neutron power. The reactor trips on low reactor coolant pressure or high neutron power.

Following the trip the turbine stop valves and feedwater control valves close. The steam generator in the steam loop associated with the rupture blows dry, and decay heat is removed by the unaffected steam generator by steam flow through the turbine bypass valve.

The analysis for the maximum break size (36 in. outside diameter) at rated power shows results similar to those discussed above, but represents the worst condition for a steam line rupture accident. With a positive moderator coefficient the reactor will trip on low pressure, making it impossible for the reactor to return to criticality because of continuing decrease in reactor coolant temperature. A negative moderator coefficient (EOL) would result in a reactor power increase with decreasing average reactor coolant temperature. A controlled cooldown rate can be established by feedwater isolation.

[redacted] 0934

Analysis Inputs

The following initial conditions are assumed:

a. Before the accident, the reactor is operating at 100% power (2,633 MWt) with a high flux trip setting of 112%.

b. Doppler coefficient (EOL) is -1.2×10^{-5} $(\Delta k/k)/F$.

c. Moderator coefficient is -3.0×10^{-4} $(\Delta k/k)/F$, corresponding to EOL.

d. Rod drop starts 0.3 s after the trip point is reached, and 2/3 insertion occurs in 1.4 seconds. The tripped rod worth (3.46% $\Delta k/k$) corresponds to the minimum worth available with the maximum worth rod stuck out at EOL.

The following sequence of events occurs following a steam line rupture:

a. As a result of reactor trip, the turbine stop valves close.

b. Feedwater flow is held at 100% until reactor trip occurs. The trip also causes the closing of the feedwater main control valves and feedwater startup valves.

c. The auxiliary feedwater pump is started on a loss of discharge pressure on the main feedwater pumps (800 psia).

d. Auxiliary feedwater isolation valves open and normal feedwater isolation valves close. (See Figure 10-1.)

e. The feedwater isolation valves upstream of startup valves close when the auxiliary feedwater pump has started and auxiliary feedwater isolation valve is opening.

f. The feedwater startup and main control valves follow control system requirements for steam generator minimum level control.

g. The unaffected steam generator is isolated, on the steam side, by the automatic closing of the steam line isolation valves. The turbine bypass valve opens on high pressure. Steam flow through this valve to the condenser is the means of removing core decay heat.

h. The operator ensures that the feedwater valves are closed and remain closed on the affected steam generator.

Evaluation Results

After a steam line rupture both steam generators blow down at the same rate until a reactor trip occurs (6 s), which closes the turbine stop valves and feedwater startup and main control valves on both steam generators. The unaffected steam generator is isolated, resulting in a pressure increase until the turbine bypass valve opens. This bypass valve remains open until the reactor coolant temperature goes below 550 F at which time this valve closes.

0035

The steam generator with the assumed break will continue to blow down after the feedwater valves are closed. The operator assures that the startup and main control valves in this generator remain closed by switching the feedwater valve controller to manual. The steam generator blows dry approximately 50 seconds after the steam line rupture has occurred.

The unaffected steam generator (that has been isolated on the steam side) has the capability of removing core decay heat by venting steam through the turbine bypass valve. When the reactor coolant temperature is above 550 F, the turbine bypass valve will remain open allowing up to 25 per cent steam flow, which is more than adequate to remove core decay heat. With continuing steam flow through the turbine bypass valve, the steam generator downcomer water level will reach 2 feet, at which time the feedwater control, which is left in automatic, will open the feedwater startup and main control valves to meet the 2 ft downcomer minimum level control system requirement. Sufficient feedwater can be obtained from the feedwater pumps or the emergency feedwater pump to satisfy decay heat requirements. | 8 | 1

Figure 14-18 shows the response of the reactor coolant system for an assumed 36-in. double-ended steam line rupture. Initially, both steam generators blow down until a high flux reactor trip occurs with a maximum thermal power of 106% of rated power. The reactor coolant temperature leaving the unaffected steam generator increases after the turbine stop valves close as a result of pressure recovery and a reduction of feedwater flow. The coolant temperature leaving the affected steam generator decreases until it has blown dry (50 seconds), at which time it approaches the inlet temperature. Since the unaffected steam generator turbine stop valves are closed, and the steam generator with the rupture is dry, the reactor coolant system temperature can be lowered as a result of the steam flow from the isolated steam generator through the turbine bypass valve or the atmospheric dump valves. At 108 seconds after the rupture, thermal equilibrium is re-established; i.e., the heat removal rate (steam flow through the turbine bypass valve or atmospheric dump valve) is equal to the heat input (core decay heat). The maximum cooling rate occurs during the first 10 seconds of blowdown. After reactor trip the core remains 0.4% $\Delta k/k$ subcritical.

3 The effect of a steam line rupture inside the containment building has been evaluated by conservatively assuming an instantaneous release to the containment building of the energy associated with this accident. The mass and energy releases for the steam generator in this analysis are:

	Mass, lb	Energy, Btu x 10^{-6}
Steam Generator	55,000	31.58
Feedwater Flow (6 s full flow plus coastdown to 0% flow @ 16 s)	12,800	5.6
Reactor Coolant System Energy Transferred	--	17.6
Available Mass in Feedwater Line Between Feedwater Control Valves and Steam Generator	35,500	15.5
	103,300	70.28

Based on the above, a single steam generator release would result in about a 7 psi rise in containment vessel pressure.

The environmental consequences from this accident are calculated by assuming that:

a. The unit has been operating with a 1-gpm steam generator tube leak.

b. The unit has been operating with 1 per cent defective fuel rods.

c. The steam line break occurs between the containment vessel and a main steam isolation valve.

d. Reactor coolant leakage into the steam generator continues unabated for 3 hours before the reactor coolant system can be cooled down and the leakage terminated.

With once-through steam generators and full flow condensate demineralizers the iodine inventory in a leaking steam generator would not be significant compared to the iodine in the primary coolant which would continue to leak into the steam generator following the steam line break. Assuming this leakage continued at an average rate of 1 gpm for three hours and that all of the iodine was released to the atmosphere, a total of 3.6 curies of dose equivalent I-131 would be released. Using the 0-2 hour diffusion model the thyroid dose at the exclusion distance is 0.25 rem. The corresponding whole body dose is 0.002 rem.

14.1.2.10 Steam Generator Tube Failures

14.1.2.10.1 Identification of Accident

The environmental effects associated with steam generator tube leakage and subsequent releases to the environment are evaluated in the preceding sections. An evaluation has also been performed for the complete severance of a steam generator tube. For this occurrence, the activity contained in the reactor coolant would be released to the secondary system. Radioactive gases and some of the radioactive iodine would be released to the atmosphere through the condenser air removal system.

14.1.2.10.2 Analysis and Results

In analyzing the consequences of this failure, the following sequence of events is assumed to occur:

a. A double-ended rupture of one steam generator tube occurs with unrestricted discharge from each end.

b. The initial leak rate, approximately 435 gpm, exceeds the normal makeup of 70 gpm to the reactor coolant system, and system pressure decreases. No operator action is assumed, and a low reactor coolant system pressure trip will occur in about 8 minutes.

c. Following reactor trip, the reactor coolant system pressure continues to decrease until high-pressure injection is actuated at a pressure of 1,500 psig. The capacity of the high-pressure injection is sufficient to compensate for the leakage and maintains both pressure and volume control of the reactor coolant system. Thereafter, the reactor is assumed to be cooled down and depressurized at the normal rate of 100 F per hour.

d. Following reactor trip, the turbine stop valves will close. Since a reactor coolant to secondary system leak has occurred, steam line pressure will increase, opening the steam bypass valves to the condenser. The bypass valves actuate at a lower pressure than do the steam safety valves. The reactor coolant that leaks as a result of the tube failure is condensed in the condenser. Only the fission products that escape from the condensate are released to the atmosphere.

0038

e. After the reactor coolant system pressure decreases below the set point of the main steam line safety valves, the affected steam generator can be isolated by closing the steam bypass isolation valves. Cooldown continues with the unaffected steam generator until the temperature is reduced to 280 F. Thereafter, cooldown to ambient conditions is continued using the decay heat removal system.

f. At the design cooling rate for the pressurizer of 100 F per hour, depressurization of the reactor coolant system to the steam line safety valve set point requires approximately 1.7 hours. During this time period, 5,930 ft^3 of reactor coolant leaks to the secondary system. This leakage corresponds to approximately 4.15×10^4 curies of xenon-133 if the reactor has been operating with 1 per cent of the fuel pins in the core defective.

The radioactivity released during this accident is discharged through the turbine bypass to the condenser and then out the station vent. A partition factor of 10^4 is assumed for iodine in the condenser.(1,2) Noble gases are assumed to be released directly to the station vent. The total dose to the body from all the xenon and krypton released is only 0.38 rem at the 730 meter exclusion distance. The corresponding dose to the thyroid at the same distance is only 0.005 rem. This calculation conservatively assumes that the station vent discharge mixes in the wake of the building structures rather than remaining at its elevated release height.

0039

14.2 STANDBY SAFETY FEATURES ANALYSIS

14.2.1 SUMMARY

In this section accidents are analyzed in which one or more of the protective barriers are breached. All accidents evaluated are based on the ultimate power level of 2,772 MWt. Table 14-6 summarizes the potential effects of accidents studied.

Table 14-6
Summary of Accidents

Event	Release Assumptions	Effect
Fuel Handling Accidents	Gap activity is released from the outer row of fuel rods in one assembly (operated at 24.6 MWt for 930 days and then zero power for 1 day), while in spent fuel storage pool.	Integrated dose at exclusion distance boundary is 2.25 rem thyroid and 0.134 rem whole body.
Rod Ejection Accident	All fuel rods which experience DNB are assumed to release their total gap activity to the reactor coolant.	Some fuel clad damage. Two-hour dose at exclusion distance is 0.05 rem thyroid.
Loss-of-Coolant	Double-ended rupture of 36 in. diam. reactor coolant system pipe. Release of all gap activity.	No clad melting. Two-hour dose at exclusion distance is 1.11 rem thyroid.
Maximum Hypothetical Accident	Release of 100% noble gases, 50% iodine, and 1% solid fission products.	Two-hour dose at exclusion distance is 221 rem thyroid and 17.1 rem whole body. Thirty-day dose at 2 mile low population zone distance is 166 rem thyroid and 8.04 rem whole body.
Gaseous Radwaste Decay Tank Rupture	Release of all noble gases in the reactor coolant system at Table 11.3 concentration without decay.	Integrated whole body dose at exclusion distance is 0.82 rem.

0040

14.2.2 ACCIDENT ANALYSES

14.2.2.1 Fuel Handling Accident

14.2.2.1.1 Identification of Accident

Spent fuel assemblies are handled entirely under water. Before refueling, the reactor coolant and the fuel transfer canal water above the reactor are increased in boron concentration so that, with all control rods removed, the k_{eff} of a core is no greater than 0.99. In the spent fuel storage pool, the fuel assemblies are stored under water in storage racks having an eversafe geometric array. Under these conditions, a criticality accident during refueling is not considered credible. Mechanical damage to the fuel assemblies during transfer operations is possible but improbable. The mechanical damage type of accident is considered the maximum potential source of activity release during refueling operations.

14.2.2.1.2 Analysis and Results

2 The fuel assembly is assumed to have operated for 930 days at 24.6 MWt. The reactor is assumed to have been shut down for 72 hours, which is the minimum time for reactor coolant system cooldown, reactor closure head removal, and removal of the first fuel assembly. It is further assumed that the entire outer row of fuel rods in the assembly, 56 of 208, suffers mechanical damage to the cladding. Since the fuel pellets are cold, only the gap activity is released. The fuel rod gap activity is calculated using the escape rate coefficients and calculational methods discussed in 11.1.1.3.

The gases released from the fuel assembly pass upward through the spent fuel storage pool water prior to reaching the auxiliary building atmosphere. As a minimum, the gases pass through 10 ft of water. Although there is experimental evidence that a portion of the noble gases will remain in the water, no retention of noble gases is assumed. In experiments whereby air-steam mixtures were bubbled through a water pond, Diffey, et al[3] demonstrated decontamination factors of about 1,000 for iodine. Similar results for iodine were demonstrated by Barthoux, et al[4] and predicted by Eggleton.[5] To be conservative, only 99 per cent of the iodine released from the fuel assembly is assumed to remain in the water. The iodine activity released from the 56 damaged fuel rods to the auxiliary building atmosphere is therefore 27.2 dose equivalent curies of I-131. The noble gas activity released is given in Table 14-7.

Table 14-7
Noble Gas Release for Fuel Handling Accident

Isotope	Activity Released
Kr-85	1.76×10^3 curies
Xe-131m	1.77×10^2 curies
Xe-133m	1.01×10^2 curies
Xe-133	1.47×10^4 curies

2

0041

The auxiliary building is ventilated, and the discharge is to the station vent. The discharge from the station vent is assumed to mix in the wake of the building structures rather than remain at its elevated release point. This assumption produces less favorable dilution and, therefore, higher ground concentrations at the exclusion distance. Atmospheric dilution is calculated using the 2-hour dispersion factor of 1.32×10^{-4} s/m^3 developed in Appendix 2B. The total integrated dose to the whole body at the exclusion distance is 0.134 rem, and the thyroid dose at the same distance is 2.25 rem.

14.2.2.2 Rod Ejection Accident

14.2.2.2.1 Identification of Accident

Reactivity excursions initiated by uncontrolled rod withdrawal (14.1) were shown to be safely terminated without damage to the reactor core or reactor coolant system integrity. For reactivity to be added to the core at a more rapid rate, physical failure of a pressure barrier component in the control rod drive assembly must occur. Such a failure could cause a pressure differential to act on a control rod assembly and rapidly eject the assembly from the core region. The power excursion due to the rapid increase in reactivity is limited by the Doppler effect and terminated by reactor protection system trips.

Since control rod assemblies are used to control load variations only and boron dilution is used to compensate for fuel depletion, only a few control rod assemblies are inserted (some only partially) at ultimate power. Thus, the severity of a rod ejection accident is inherently limited because the amount of reactivity available in the form of control rod worth is relatively small.

The criterion for reactor protection in this assumed accident is that the reactor will be operated in such a manner that a control rod ejection accident will not further damage the reactor coolant system.

a. Accident Bases

Using an analytical method based on diffusion theory (3.2.2.2.1) the worth of the most reactive control rod assembly in each rod group was determined for different control rod configurations.

The maximum rod worths and other important parameters used in the study are shown in Table 14-8.

0042

Table 14-8
Rod Ejection Analysis Parameters

Worth of Ejected Rod, Δk/k	
Ultimate Power, No Xenon	0.46%
Ultimate Power, With Xenon	0.36%
Hot, Zero Power, Critical	0.56%
Rod Ejection Time, s	0.150
Ultimate Power Level, MWt	2,772
Reactor Trip Delay Time, s	
High Flux Trip	0.3
High Pressure Trip	0.5
Trip Time to 2/3 Insertion, s	1.4

The tripped rod worth used corresponds to the minimum worth available with the maximum worth rod stuck out at BOL and EOL.

The severity of the rod ejection accident is dependent upon the worth of the ejected rod and the reactor power level. The control rod group of greatest worth is the first of the entire rod pattern to be withdrawn. The maximum worth of a rod in this group can be as high as 2.5 per cent Δk/k but would only have this worth when the reactor was subcritical. The details of the control rod worth calculations and the methods of selecting the number of control rods in each group are presented in 3.2.2 and 7.2.2.1.2.

When the reactor is subcritical, the boron concentration is maintained at a level which ensures that the reactor is at least 1 per cent subcritical with the control rod of greatest worth fully withdrawn from the core. Thus, a rod ejection will not cause a nuclear excursion when the reactor is subcritical and all the other rods are in the core.

As criticality is approached, the worth of the remaining rods decreases so that at criticality the maximum reactivity addition from a rod ejection would be 0.56 per cent Δk/k.

The rod worth continues to decrease as ultimate power is attained. Before equilibrium xenon is established, the total pattern worth remaining in the core at ultimate power is 2.8 per cent Δk/k, and the greatest single control rod worth is 0.46 per cent Δk/k. At equilibrium xenon the pattern worth is 1.8 per cent Δk/k and the maximum rod worth is 0.36 per cent Δk/k. A detailed analysis has been performed at worths up to 0.7 per cent Δk/k, however, to show the large margin that exists between the actual rod worths and those worths needed to approach any failure thresholds.

A rod must be fully inserted in the core to have the foregoing reactivity worth values. Assuming that the failure occurs so that the pressure barrier no longer offers any restriction to the ejection and that there is no viscous drag force limiting the rate of ejection, the control rod travel time to the top of the active region of the core is calculated to be 0.176 s. Since most of the reactivity is added during the central 75 per cent of this travel, only this distance is used in the analysis, resulting in an ejection time of 0.15 seconds for the analysis.

b. Fuel Rod Damage

The consequences of a rod ejection accident are largely dependent upon the rate at which the thermal energy resulting from the nuclear excursion is released to the coolant. If the fuel rods remain intact while the excursion is being terminated by the negative Doppler coefficient and by reactor trip, then the energy release rate is limited by a relatively low surface-to-volume ratio for heat transfer. The energy stored in the fuel rods will then be gradually released to the coolant (over a period of several seconds) at a rate which poses no threat to the integrity of the reactor coolant system. However, if the magnitude of the nuclear excursion is such that the fuel rod cladding does not remain intact, then fuel and clad may be dispersed into the coolant to such an extent as to cause a significant increase in the heat transfer rate.

Power excursions caused by reactivity disturbances of the order of magnitude occurring in rod ejection accidents could lead to three potential modes of fuel rod failure Failure by the first mode occurs when internal pressures developed in the fuel rod are insufficient to cause cladding rupture, but subsequent heat transfer from fuel to cladding raises the temperature of the cladding and weakens it until local failure occurs. "Departure-from-nucleate-boiling" (DNB) usually accompanies and contributes to this mode of failure, and little or no fuel melting would be expected. In this mode of failure, fuel fragmentation is usually only minor, and any dispersal of fuel to the coolant would occur very gradually, with system contamination being the worst probable consequence.

The second failure mode occurs when significant fuel melting causes a rapid increase in internal fuel rod pressure(*) which, combined with clad loss of strength at higher temperatures, causes the fuel rod clad to rupture. Some fuel vaporization may occur, contributing to the pressure buildup. Considerable fragmentation and dispersal of the fuel would be expected in this mode.

The third and most serious mode of fuel rod failure occurs when, as a result of a very large and rapid reactivity transient in which

[redacted]

- - - - -

(*) The increase in volume associated with the melting of UO_2 is 9.6 per cent.[6]

there is insufficient time for heat to be transferred from fuel to cladding, extensive fuel melting followed by vaporization occurs. Destructive internal pressures can be generated without increasing cladding temperatures significantly in this mode.

In evaluating the effects of the failure modes discussed above, two failure thresholds are considered. The first is associated with a gradual, and usually minor, cladding failure and may be approximately defined by the minimum heat flux for DNB at the cladding surface. The second failure threshold, defined as the enthalpy threshold for prompt fuel failure with significant fragmentation and dispersal of fuel and cladding into the coolant, is used to describe the energy required to cause failure by either the second or the third failure mode described above.

A correlation of the results of different experiments conducted on Zircaloy-2-clad UO_2 fuel rods at TREAT[7] has been interpreted by the experimenters to show a threshold at 280 cal/g of fission energy input. That is, below this value the fuel rod can be expected to remain intact, and above this value fragmentation can be expected. The enthalpy corresponding to the melting point of UO_2 is about 260 cal/g[8], and the heat of fusion is at least 78/cal/g.[9] Thus the 280 cal/g represents a condition where only part of the fuel is molten. Also of interest as a probable indication of the degree and rapidity of fuel and cladding dispersal are the measurements of pressure rise rates in the autoclave in the TREAT experiments.[7] Preliminary analysis indicates that there is only a modest pressure rise up to an energy input of 400 cal/g. Above 500 cal/g, however, there is a very definite pressure pulse. Thus between 400 and 500 cal/g there is a transition which probably corresponds to the change from the second to the third failure mode discussed previously. A fuel failure threshold of 280 cal/g, at the pellet radius corresponding to the average temperature of the hottest fuel pellet, has been used in this study to define the extent of fuel failure.

In computing the average enthalpy of the hottest fuel pellet during the excursion for the ultimate power cases, it is assumed that no heat is transferred from the fuel rod between the time the accident is initiated and the time when the neutron power returns to the ultimate power level. For the zero-power cases, the enthalpy increase was based on the peak value of the average fuel temperature. In all cases the average enthalpy rise--from the integrated energy or the fuel temperature traces--is multiplied by the maximum peaking factor to obtain the enthalpy increase in the hottest fuel pellet.

The latest correlation of the ANL TREAT data[7] for the meltdown experiments on Zircaloy-2-clad UO_2 fuel rods shows the threshold for the zirconium-water reaction to be 210-220 cal/g energy input. A conservative threshold value of 200 cal/g is used in this study.

In calculating the volume of the core that experiences burnout in a given rod ejection accident, it is assumed that any DNB conditions result in burnout for each rod where the DNB occurs. DNB in a rod ejection transient is assumed to occur whenever the peak thermal

power of a given fuel rod exceeds the peak at steady-state conditions which could result in a DNB, which in turn is assumed to occur for a DNBR of 1.3 using the W-3 correlation.

In determining the environmental consequences from this accident, an even more conservative approach is taken in computing the extent of DNB experienced in the core. All fuel rods that undergo DNB to any extent are assumed to experience cladding failure with subsequent release of all the gap activity. Actually, most of the fuel rods will recover from DNB and no fission product release will occur. The fuel rods that experience DNB at BOL are assumed to have EOL gap activities.

14.2.2.2.2 Method of Analysis

A B&W digital computer program has been used to analyze the rod ejection accident. This program agrees to within a few per cent in all cases with CHIC-KIN.(10) The B&W program is a point kinetics model with a reactor coolant loop and pressurizer model. The core heat transfer model allows for up to 30 radial mesh points in the fuel and clad, and the mesh size can be different in the two regions. The model accounts for the gap conductivity and film coefficient of heat transfer. Reactivity feedback is calculated in each mesh point and in the coolant and is weighted for inclusion in the kenetics simulation. The thermal properties are input separately for each mesh point but remain constant with time. The loop model includes a simulation of the steam generator which can have a nonlinear heat demand input on the secondary side. Trip action is initiated on high or low reactor coolant system pressure or on high neutron flux. Decay heat can be taken into account as well. This code was used to calculate the neutron and thermal power, integrated energy, reactivity components, pressure, and fuel rod and loop temperatures. Six delayed neutron groups are considered. The control rod trip is represented by a 25-segment curve of reactivity insertion during trip versus time, obtained by combining the rod worth curve with the actual rod velocity curve. Nominal values for the various nuclear and physical parameters used as inputs are listed in Table 14-9.

As a check on the point kinetics calculation, the rod ejection accident was also analyzed for a limited number of cases using the exact, one-dimensional, space-and-time dependent WIGL2 digital computer program.(11) The point kinetics model assumes that the flux shape remains constant during a transient. This flux shape contains peaking factors which reflect unusual rod patterns such as the flux adjacent to a position where a high worth rod has been removed. Therefore, these point kinetics peaking factors are much higher than any that would actually occur in the core during normal operation. The purpose of using an exact space-time calculation is to find the flux shape during a transient. But to have a transient where a rod is ejected from the core, one must start with a flux shape that is necessarily depressed in the region of the ejected rod. In fact, the higher the worth of the rod, the more severe becomes the depression. This flux depression also causes a fuel temperature depression. When the rod is ejected from this position, the flux quickly assumes a shape that shows some local peaking.

0046

Table 14-9
Nominal Values of Input Parameters for
Rod Ejection Accident Analysis

	BOL	EOL
Delayed Neutron Fraction, β_{eff}	0.0071	0.0053
Neutron Lifetime, μs	24.8	23.0
Moderator Coefficient, $(\Delta k/k)/F$	$+0.5 \times 10^{-4}$(a)	-3.0×10^{-4}
Doppler Coefficient, $(\Delta k/k)/F$	-1.17×10^{-5}	-1.33×10^{-5}
Coolant Inlet Temperature, F	557	557
Initial System Pressure, psia	2,200	2,200
Total Nuclear Peaking Factor, F_q	3.24	2.92
Average Fuel Temperature of Average Pellet, F	1,610	1,735
Average Fuel Temperature of Hottest Pellet, F	2,905	2,760

3 | (DELETED)

(a) This value for the moderator coefficient yields conservative results because the actual coefficient is negative.

Results from WIGL2 indicate that for rod worths greater than 0.2 per cent Δk/k this local peaking is in excess of the maximum peaking applied to the point kinetics results. However, when this "exact" peaking is applied to a region initially at depressed fuel temperatures, as it is in the case of the region adjacent to the ejected rod, the resultant energy deposited in this region causes a lower peak temperature and peak thermal power than does applying a lower maximum peaking factor to an undepressed peak power region. The result is that this local region simulated in the WIGL2 code actually undergoes a less severe transient than the hottest fuel rod assumed in the point kinetics model. As seen in Table 14-10, this result is uniformly true for all rod worths up through 0.5 per cent Δk/k.

Thus it can be seen that the space-time dependent code gives a less conservative treatment of the accident analysis than does the point kinetics code.

For certain cases where the ejected rod has a low worth, or where at least one reactivity coefficient is very negative, or the initial power level is low, there is considerable pressure buildup in the reactor coolant system because

0047

of the increased heat being added to the coolant with no increase in heat demand. Many of these transients never reach the overpower trip point. For this class of possibilities, the high-pressure trip must be relied on, and this is incorporated in the calculation.

Table 14-10
Comparison of Space-Dependent and Point Kinetics Results on the Fuel Enthalpy

Rod Worth (% Δk/k)	BOL Ultimate Power Peak-to-Average Values		Fuel Enthalpy (cal/g)	
	WIGL2	Point Kinetics	WIGL2	Point Kinetics
0.2	4.2	3.24	72	141
0.3	4.8	3.24	86	149
0.4	5.4	3.24	109	159
0.5	6.0	3.24	143	172

14.2.2.2.3 Analysis and Results

a. Zero Power Level

This analysis was performed at 10^{-3} ultimate power. For the nominal case of a 0.56 per cent Δk/k rod ejection, the neutron power reaches 60 per cent and the thermal power peaks at 39 per cent for BOL; the excursion is terminated by high-pressure trip. The EOL case trips on high flux, is a faster transient; and results in peak neutron and thermal powers of 165 and 11 per cent, respectively. No DNB and no fuel damage would result from these transients.

A sensitivity analysis has been performed around these two cases in which the Doppler and moderator coefficients, trip delay time, and rod worth were varied. Figure 14-20 shows the peak neutron power as a function of ejected rod worth from 0.4 to 0.8 per cent Δk/k. The curve shows two distinct parts corresponding to worths less than β and values near to and greater than β. Figure 14-21 shows the corresponding results for the peak thermal power. It is seen that for rod worth values near prompt critical, the period is small enough to carry the transient through the high neutron flux trip. For lower values the pressure trip is relied on. In no case does the thermal power exceed 70 per cent. Therefore, no DNB would occur.

Figure 14-22 shows that the peak enthalpy in the fuel for the rod worths in the range being evaluated never exceeds 75 cal/g. Therefore, no threshold for damage is approached.

Figures 14-23 and 14-24 show the peak neutron and thermal power as a function of Doppler coefficient from -0.9 to -1.7 x 10^{-5} (Δk/k)/F. It is seen that the variation is relatively small. Similar results

[redacted]

0048

are shown in Figures 14-25 and 14-26 for the variation of the moderator coefficient from -4.0 to +1.5 x 10^{-4} $(\Delta k/k)/F$. The slope of the curve for 10^{-3} ultimate power at BOL is the greatest slope for any of the four curves because this case relies on the pressure trip, which makes it a longer transient. It is also steeper because of the effect of the positive moderator coefficient, which is only noticeable in long transients due to the long time constant from fuel to coolant.

Similarly, it is seen that the peak neutron power is higher for the EOL cases in both the Doppler and moderator studies. whereas the peak thermal powers are higher for the BOL cases. This again is because the EOL rod ejection cases are faster and the neutron power overshoots the trip point by a greater margin. It also trips more quickly, however, terminating the transient faster.

Figure 14-27 shows the effect of the trip delay time on the peak thermal power. It is seen that there is very little effect.

b. Ultimate Power

An analysis was performed for a 0.46 per cent $\Delta k/k$ rod ejection, although this worth is available at ultimate power only when no xenon is present. For BOL rod ejection, the neutron power peaks at 277 per cent, and the thermal power at 126 per cent. This causes only 0.5 per cent of the core to be in DNB, as described above. A sensitivity study was made around this case and around the same rod worth at EOL. Figures 14-23 through 14-27 show these results.

As seen in Figure 14-21, the peak thermal power shows relatively little change with increased rod worth. The peak neutron power in Figure 14-22 does show a marked change with increased worths, but the thermal effect is small because the transients are rapidly terminated by the Doppler effect. As further evidence of this small thermal effect, the peak fuel enthalpies are given in Figure 14-22. The threshold for the zirconium-water reaction is not reached until values of 0.64 and 0.69 per cent $\Delta k/k$ for BOL and EOL ejected rod worths, respectively, are encountered. These worths are well above any which are considered feasible.

The results of varying the Doppler and moderator coefficients and trip delay time show very little effect on the peak neutron and thermal powers.

The only situation in which DNB occurs is for the ultimate power case at BOL. The results of the DNB calculation are shown in Figure 14-28. For the nominal rod ejection analysis which considers a worth of 0.46 per cent $\Delta k/k$, only 0.5 per cent of the core volume is in DNB. This corresponds to 4.1 per cent of the rods.

14.2.2.2.4 Energy Required to Produce Further Reactor Coolant System Damage

The reactor vessel has been analyzed to estimate the margin that exists between the rod worths assumed for the calculated rod ejection accident transients and those worths that could initiate reactor coolant system failure. The pressure vessel material is SA-533 Grade B steel. Table 14-11 lists the values used in this analysis. The radial deformation which is assumed to represent failure of the vessel is 50 per cent of the total elongation, or 0.13 in./in. To calculate the weight of an explosive charge required to reach 50 per cent elongation, the vessel is simulated by a single cylinder with the same OD as the actual vessel, but with an increased thickness to account for the thermal shield and core barrel.

Table 14-11
Reactor Vessel Parameters

Vessel Temperature, F	600
Yield Strength (0.2% Offset), psi	55,000
Ultimate Strength, psi	80,000
Ultimate Strain (ε_u), %	26
Strain Energy (E_s) per unit Volume up to a Strain Equal to 1/2 Ultimate Strain, in.-lb/in.^{3}	8,000
Strain Energy (E_s) per Unit Volume up to Ultimate Strain, in.-lb/in.^{3}	17,000
Equivalent Pressure Vessel Dimensions, in.	
OD	188.25
ID	166.69
Thickness	10.78

The expression used for the weight of explosive required to strain the vessel a given amount is (12)

$$W = \left[\frac{1.407E_s(3.41 + 0.117R_i/t)(R_e^2 - R_i^2)^{1.85}}{10^5 w^{-0.85} (1.47 + 0.0373R_i/t)^{0.15} (R_i)^{0.15}} \right]^{0.811}$$

where

W = charge weight (TNT or Pentolite), lb

w = weight density of vessel material, lb/ft^3

R_i = initial internal radius of vessel, ft

R_e = initial external radius of vessel, ft

t = initial wall thickness of vessel wall, ft

E_s = wall strain energy, in.-lb/in.^{3}

Using this formula on the equivalent vessel, the required weight of explosive charge was calculated. The results of this calculation indicate that 1,410 pounds of TNT would strain the mid-meridian ring up to the 50 per cent ϵ_u, i.e., 0.13 in./in. The 1,410 pounds of TNT have an energy equivalent of 6.74×10^8 cal.

An analysis of ejected rod worths higher than those reported in the preceding sections has been made to estimate the transient required to generate the deformation energy equivalent to 1,410 pounds of TNT. These cases were evaluated to find the amounts of fuel melting and zirconium-water reaction. Using the conservative assumption that all the fuel that exceeds the melting threshold is fragmented, dispersed into the coolant, and quenched to the coolant average temperature, a total thermal energy release can be determined. The conversion of this energy release to an equivalent deformation energy is dependent upon the duration of the release. TNT has an energy release in microseconds, and a deformation conversion efficiency of about 50 per cent. The energy generated during a reactor transient from the zirconium-water reaction and a molten fuel dispersal is in the range from milliseconds to seconds. Thus, the conversion efficiency to deformation energy would be considerably less, and is assumed to be 1/5 that of TNT.(13) Using these figures, the reactor vessel capability is 3.37×10^8 cal, and, under the foregoing assumptions, a reactivity addition of 1.52 per cent $\Delta k/k$ is required to release this much energy to vessel deformation.

14.2.2.2.5 Conclusions

The hypothetical rod ejection accident has been investigated in detail at two different initial reactor power levels: ultimate power and zero power; both BOL and EOL conditions were considered. The results of the analysis prove that the reactivity transient resulting from this accident will be limited by the Doppler effect and terminated by the reactor protection system with no serious core damage or additional loss of the coolant system integrity. Furthermore, is has been shown that an ejected rod worth greater than 1.52 per cent $\Delta k/k$ would be required to cause a pressure pulse, due to prompt dispersal of fragmented fuel and zirconium-water reaction, of sufficient magnitude to cause rupture of the pressure vessel.

As a result of the postulated pressure housing failure associated with the accident (14.2.2.2.1), reactor coolant is lost from the system. The rate of mass and energy input to the reactor building is considerably lower than that previously reported for the smallest rupture size considered in the loss-of-coolant analysis (14.2.2.3). The maximum hole size resulting from a rod ejection is approximately 1.75 in. This lower rate of energy input results in a much lower reactor building pressure than those obtained for any rupture sizes considered in the loss-of-coolant accident.

The environmental consequences of this accident are calculated assuming that all fuel rods undergoing DNB release all of their gap activity to the reactor

coolant. Subsequently, this gap activity and the activity in the reactor coolant from operation with 1% defective fuel pins is released to the reactor building. For the case of a 0.46 per cent Δk/k rod ejection from rated power at BOL, 4.1 per cent of the fuel rods are assumed to fail, releasing the noble gas activity to the containment vessel as given in Table 14-12.

Table 14-12
Noble Gas Release for Nominal Rod Ejection

Isotope	Curies
Kr-85	2.47×10^4
Xe-131m	4.31×10^3
Xe-133m	4.19×10^5
Xe-133	4.77×10^5

The iodine released to the containment vessel is 65,200 dose equivalent curies of I-131.

Fission product activities for this accident are calculated using the methods discussed in Section 11.1.1.3. Using environmental models and dose rate calculational methods discussed under the loss-of-coolant accident, the total integrated dose to the thyroid at the exclusion distance from this accident is only 0.05 rem in 2 hours, which is more than a factor of 6,000 below the guideline values of 10 CFR 100.

14.2.2.3 Loss-of-Coolant Accident

14.2.2.3.1 Identification of Accident

Failure of the reactor coolant system would allow partial or complete release of reactor coolant into the containment vessel, thereby interrupting the normal mechanism for removing heat from the reactor core. If all the coolant were not released immediately, the remaining amount would be boiled off owing to residual heat, fission product decay heat, and possible heat from chemical reactions unless an alternate means of cooling were available. In order to prevent significant chemical reactions and destructive core heatup, emergency core cooling equipment rapidly recovers the core and provides makeup for decay heat removal.

14.2.2.3.2 Accident Bases

All components of the reactor coolant system have been designed and fabricated to ensure high integrity and thereby minimize the possibility of their rupture. The reactor coolant system, the safety factors used in its design, and the special provisions taken in its fabrication to ensure quality are described in Section 4.

0052

[redacted]

In addition to the high-integrity system, emergency core cooling is provided to insure that the core does not melt even if the reactor coolant system should fail and release the coolant. This emergency core cooling is provided by the core flooding system and two full capacity and independent emergency core cooling systems. Each system contains a high pressure injection train, normally used in the makeup and purification system, and a low pressure train, normally used in the decay heat removal system. These systems are described in detail in Section 6 and their characteristics are summarized in the succeeding paragraphs.

The core flooding system has two independent core flooding tanks, each of which is connected to a different reactor vessel injection nozzle by a line containing two check valves and a normally open, remotely operated isolation valve. Since these tanks and associated piping are missile-protected and are connected directly to the reactor vessel, a rupture of reactor coolant system piping will not affect their performance. These tanks are normally pressurized with nitrogen and provide for automatic flooding when the reactor coolant system pressure de-
2 creases below 600 psig. The flooding water is injected into the reactor vessel and directed to the bottom of the reactor vessel, flooding the core from the bottom upward. The combined contents of the two tanks (1,880 ft^3 of borated water) rapidly reflood the core immediately after the blowdown to provide cooling until coolant flow can be established by one of the two emergency core cooling systems.

Each of the two emergency core cooling systems has a high pressure pump and a low pressure pump. The high pressure injection pump is actuated by a low reactor coolant system pressure of 1,500 psig and supplies coolant at pressures up to the design pressure of the reactor coolant system and delivers 500 gpm at 600 psig. The low pressure pump is actuated by a low system pressure of 200 psig and supplies coolant at pressures below 150 psig and delivers 3,000 gpm at 100 psig. To provide redundancy, each pump is also actuated by a high containment pressure signal of 4 psig. Both systems can be operated at full capacity from the on-site emergency electrical power supply and can be in operation within 25 s after the accident. The total combined (high and low pressure) capacity of each system is 3,500 gpm.

The performance criterion for the emergency cooling equipment is to limit the temperature transient below the clad melting point so that fuel geometry is maintained to provide core cooling capability. This equipment has been conservatively sized to limit the temperature transient to 2,300 F or less since temperatures in excess of this value promote a faster zirconium-water reaction rate, and the termination of the transient near the melting point would be difficult to demonstrate.

Injection water is supplied from the borated water storage tank. When this tank empties, water is recirculated from the containment sump through heat exchangers and returned to the reactor vessel.

Engineered safety features are also provided to cool the containment environment following a loss-of-coolant accident and thereby limit and reduce pressure in the containment. The containment spray system is actuated on a high high containment pressure signal of 10 psig and sprays borated water into the containment atmosphere. This spray water reaches thermal equilibrium within the building atmosphere during its passage from the nozzles to the sump. Spray

water is supplied from the borated water storage tank until it is emptied. Thereafter, water collected in the sump is recirculated to the sprays. Cooling is also provided by the containment air cooling system in which recirculating fans direct the steam-and-air mixture through coolers, where steam is condensed. Heat absorbed in the coolers is rejected to the service water system. The heat removal capacity of either of these two containment cooling systems is adequate to prevent overpressurization of the containment vessel during a loss-of-coolant accident.

In order to evaluate this accident, a range of rupture sizes from small leaks up to the complete severance of a 36-in. ID reactor coolant system line has been evaluated. A detailed core cooling analysis is presented for the complete severance of the 36-in. ID reactor coolant piping. Since the large rupture removes the least amount of stored energy from the core, this represents the minimum temperature margin to core damage and, therefore, places the most stringent requirements on the core cooling equipment. This is shown by analysis of peak temperature conditions for a spectrum of rupture size in both hot and cold leg piping.

The containment pressures have been evaluated for a complete spectrum of rupture sizes with the action of core flooding tanks. Rupture sizes smaller than the 36-in. ID leak result in longer blowdown times, and the amount of energy transferred to the containment atmosphere is increased. As a result the intermediate leak sizes result in a containment pressure greater than that produced by the 36-in. ID rupture.

This analysis demonstrates that in the unlikely event of a failure of the reactor coolant system, both the reactor fuel and the containment maintain their integrity. Accordingly, the public would be protected against potential radiation hazards.

14.2.2.3.3 Accident Simulation - Reactor Coolant System

a. Hydraulic Model

Blowdown of the reactor coolant system following an assumed rupture has been simulated by using a modified version of the FLASH(14) code. This code calculates transient flows, coolant mass and energy inventories, pressures, and temperatures during a loss-of-coolant accident. The code calculates inflow from the emergency cooling systems and calculates heat transferred from the core to the coolant.

Modifications were made to FLASH to make the model more applicable to this system. The changes are as follows:

1. The calculation of reactor coolant pump cavitation was based on the vapor pressure of the cold leg instead of the hot leg water.

2. Core flooding tanks have been added. Water flow from the core flooding tanks is calculated on the basis of the pressure difference between the core flooding tanks and the point of discharge into the reactor coolant system. The line resistance

and the inertial effects of the water in the pipe are included. The pressures in the tanks are calculated by assuming an adiabatic expansion of the gas above the water level in the tank. Pressure, flow rate, and mass inventories are calculated and printed out in the computer output.

3. Additions to the water physical property tables (mainly in the subcooled region) have also been made to improve the accuracy of the calculations.

4. A change in the steam bubble rise velocity has been made from the constant value in FLASH to a variable velocity as a function of pressure. The bubble velocity term determines the amount of water remaining in the system after depressurization is complete. For large ruptures, this change in velocity shows no appreciable change in water remaining from that predicted by the constant value in the FLASH code. For smaller ruptures, an appreciable difference exists. The variable bubble velocity is based on data in Reference 15 and is adjusted to correspond to data from the LOFT semiscale blowdown tests.

   Test No. 546 from the LOFT semiscale blowdown tests is a typical case for the blowdown through a small rupture area. A comparison of the predicted and experimentally observed pressures is shown in Figure 14-29. Figure 14-30 shows the per cent mass remaining in the tank versus time, as predicted by the code. At the end of blowdown, the predicted mass remaining is 13 per cent. The measured mass remaining is approximately 22 per cent.

The FLASH code describes the reactor coolant system by the use of two volumes plus the pressurizer. The system was grouped into two volumes on the basis of the temperature distribution in the system as follows:

Volume 1 includes half of the core water volume, the reactor outlet plenum, the reactor outlet piping, and approximately 55 per cent of the steam generators.

Volume 2 includes half of the core water volume, the reactor inlet plenum and downcomer section, the reactor inlet piping, pumps, and 45 per cent of the steam generators.

Volume 3 represents the pressurizer.

The resistances to flow were calculated by breaking the reactor coolant system into 24 regions and calculating the volume-weighted resistance to flow for a given rupture location based on normal flow resistances. For the double-ended ruptures, all of the leak was assumed to occur in the volume in which that pipe appeared.

The reactor core power was input as a function of time as determined by the CHIC-KIN code in conjunction with the FLASH output. Steam generator heat removal was assumed to cease when the rupture occurred.

[redacted]

The modified FLASH code has the capability of simulating injection flow from the core flooding tanks. Reactor vessel filling was calculated by adding the mass remaining in the vessel as predicted by FLASH to the mass injected from the core flooding tanks. This method of calculation is conservative in that condensation of steam by the cold injection water is not taken into account. An analysis using the FLASH code with condensation effects confirms that conservatism is used in this analysis.

Pressure, temperature, mass and energy inventories, and hydraulic characteristics as determined by FLASH are input into the core thermal codes (SLUMP and PRIT) and the containment vessel pressure buildup code.

b. Core Thermal Model

The core heat generation and heat transfer to the fluid are dependent upon the blowdown process. The FLASH program includes a core thermal model and the functional relationship between heat transfer and fluid flow. While the FLASH thermal model is acceptable for determining the effect of core heat transfer on the blowdown process, a more extensive simulation is necessary for evaluation of the core temperature transient.

Additional analytical models and two digital computer programs (SLUMP and PRIT) were developed to simulate the core thermal transient for the period beginning with the initiation of the leak and ending after the core temperature excursion had terminated.

The SLUMP program determines the clad and fuel temperature as a function of time after a rupture with provisions for a time dependent tabular input of heat transfer coefficient, sink temperature, and power level. The PRIT program was developed from SLUMP and, in addition to determining fuel and clad temperature, maintains an inventory of mass and energy in the reactor vessel and that which is released to the containment.

These models include the effects of heat generation from neutrons before reactor trip, neutron decay heat, and fission and activation product decay heat; the exothermic zirconium-water reaction based on the parabolic rate law; heat transfer within the fuel rods, heat convection from the fuel clad surface to any fluid within the core region, heat transfer from reactor vessel walls and internals to the coolant, and heat transfer from fuel rods to the steam necessary to sustain a metal-water reaction; and emergency injection flow, and boiloff.

The basic model structure provides for up to 50 equal-volume core regions with input provisions to allow any choice of power distribution. The model may be used to simulate the entire core or any subdivision of the core. Therefore, the core geometry may be detailed to the degree consistent with the results desired.

[redacted] 0056

The following parabolic law for the zirconium-water reaction equation (16) with the following constants is simulated for each of the regions:

$$-\frac{dr}{dt} = \frac{K}{(r_o - r)} \exp \frac{\Delta E}{RT}$$

where

r = radius of unreacted metal in fuel rod

r_o = original radius of fuel rod

t = time

K = rate law constant (0.3937 cm^2/s)

ΔE = activation energy (45,000 cal/mole)

R = gas constant (1.987 cal/mole K)

T = temperature, K

The zirconium-water reaction heat is assumed to be generated completely within the clad node. The heat necessary to increase the steam temperature from the bulk temperature to the reaction temperature is transferred from the clad at the point of reaction. The above equation implies no steam-limiting. However, the program does have provision for steam rate-limiting to any degree desired, but no steam-limiting of the reactions has been assumed. All heat from beta and gamma sources and 97.3 per cent of the neutron heat is assumed to be generated within the fuel according to the preaccident power distribution after infinite irradiation.

Within each of the regions there is a single fuel node and a single clad node with simulation of thermal resistance according to the normal fuel rod geometry. Provision is made in PRIT to simulate four different modes of heat transfer from the clad node to the fluid sink node by specifying the time-dependent surface coefficient. As noted above, SLUMP utilizes a tabular input of heat transfer coefficient as a function of time.

The surface heat transfer coefficient input data are determined from calculations which are based on flow and water inventory as furnished from the blowdown and the core flooding tank performance analysis.

In the event that insufficient cooling is provided, the program will allow clad heating to progress to the melting point. At this point the latent heat of zirconium must be added before the clad melts. Provisions are also incorporated to allow the clad to be heated to temperatures above the melting point before slump occurs.

As each region slumps it may be assumed to surrender heat to a water pool or to some available metal heat sink. If water is available, an additional 10 per cent reaction is assumed to occur.

The program outputs incl\ e the following as a function of time, unless otherwise specifiea:

PRIT and SLUMP - Average fuel temperature of each region.

PRIT and SLUMP - Average clad temperature of each region.

PRIT and SLUMP - Per cent metal-water reaction in each region.

PRIT - Time for the clad of each region to reach the metal-water threshold, the beginning and end of melting, and the [illegible]mp temperature.

PRIT - Heat transferred to the containment from the core.

PRIT - Heat generation by hydrogen and oxygen recombination.

PRIT - Total zirconium-water reaction.

PRIT - Total heat transferred to the containment from all sources.

PRIT - Total mass transferred to the containment via boiloff and overflow.

14.2.2.3.4 Accident Analysis - Reactor Coolant System

a. Core Flooding Tank Design Base Accident

The design basis accident selected for emergency core cooling equipment sizing is based on reactor conditions at the ultimate power level of 2,772 MWt. The moderator temperature coefficient is expected to be zero or negative over the lifetime of the core. However, this analysis conservatively uses a positive moderator coefficient which places a more stringent requirement on emergency core cooling equipment. The analysis of core cooling during a loss-of-coolant accident is based upon the following conditions:

1. End-of-life fuel temperatures.

2. A void shutdown (for cases where control rod insertion will be impeded by higher than normal core pressure drop during the blowdown) including the positive reactivity effects from initial void formation when a moderator coefficient of $+0.5 \times 10^{-4}$ $\Delta k/k/F$ is assumed.

3. The hot spot power generation is a factor of 3.28 times the average.

[redacted]0058

The 36-in. ID, double-ended pipe rupture produces the fastest blowdown and lowest heat removal from the fuel. This case, therefore, represents the most stringent emergency core cooling requirements. Results from the modified version of FLASH indicate that the core flooding tank simulation provides for the retention of all injection plus a portion of the original reactor coolant that would otherwise have been released. Thus, the cool injection water provides a cooling and condensing effect which reduces overall leakage. For the present analysis, no credit has been taken from the extra accumulation of water due to the condensing effect.

The SLUMP digital computer program, as described in 14.2.2.3.3 b above, is used to evaluate core flooding tank performance in terms of core cooling capability. In the analysis, the hottest spot of the core was simulated.

A detailed analysis of the void shutdown and core response was made with the digital computer program CHIC-KIN. This program accounts for changes in flow, pressure, enthalpy, and void fraction. It also computes axially weighted Doppler and moderator coefficients of reactivity for the kinetics calculation. The Doppler coefficient is input as a nonlinear function of fuel temperature, and the moderator void coefficient is input as a function of void fraction. The parameters describing the coolant were obtained from the digital computer program FLASH, which in turn used the neutron power output from CHIC-KIN. The core is assumed to be initially at the ultimate power level of 2,772 MWt.

Figures 14-31 and 14-32 show the results of the hot leg, 36-in. ID, rupture simulation without trip action. Figure 14-31 is the neutron power trace, and Figure 14-32 shows the various components of the reactivity feedback.

Figure 14-33 shows the integrated power for the spectrum of leak sizes in both the hot and cold legs. These integrated power curves reflect the entire heat generation from beta, gamma, and neutron power until the reactor power decays to 10 per cent of ultimate power. Above a 5-ft^2 hot leg rupture the blowdown forces on the control rod are greater than those resulting from the normal core pressure drop so that control rod insertion is not as rapid for the larger break sizes. The blowdown forces on the control rods during cold leg ruptures do not inhibit rod drop velocity for the complete spectrum of leak sizes. Accordingly, the data presented for the spectrum of cold leg ruptures are based upon reactor trip characteristics. The results of this study have been used for determination of hot spot clad temperatures for the loss-of-coolant accident spectrum analysis presented in the following pages under 14.2.2.3.4 b.

The transient core flow from the FLASH analysis of the 36-in. ID, double-ended rupture was used to determine the core cooling mechanism used in SLUMP. The very high flow rate during the initial blowdown period provides nucleate boiling conditions. Based upon the average channel flow predicted by FLASH, the core pressure drop was used to

establish the hot channel flow conditions, and the W-3 DNB correlation was applied to the hot channel to determine the length of time nucleate boiling would exist.

This analysis was made for only the first 4 seconds following the break because the correlation does not apply at the low pressures and heat fluxes that exist beyond the 4-s period. The minimum DNBR ratios predicted by W-3 did not reach a value of one or less during this time period examined. However, a conservative design approach has been taken, and a DNB has been assumed to occur at 0.25 s, followed by dispersed flow film boiling. The degree of conservatism in assuming this early DNB time is shown in the sensitivity analysis of the design base accident.

Prior to reaching a DNB condition, nucleate boiling surface coefficients at high flow rates may exceed 50,000 Btu/h-ft^2-F. A nucleate boiling surface coefficient of 20,000 Btu/h-ft^2-F was used in the analysis. However, the series heat transfer from the clad node to the fluid sink is limited to 6,100 Btu/h-ft^2-F by the relatively low conductance of the clad.

From 0.25 s until 9.5 s when the flow rate predicted by FLASH drops to a negligible value for the 14.1-ft^2 rupture, Quinn's correlation given below for dispersed flow film boiling is used to calculate the heat transfer from the clad. For a significant period of time, the mass velocity and exit qualities are in regions that available data indicate, that if there had been a DNB, the heat transfer mechanism would be transition boiling rather than fully developed film boiling. Tong's correlation for transition boiling predicts a heat transfer coefficient two to four times larger than Quinn's correlation of dispersed flow film boiling for the same flow conditions. Therefore, the correlation used in this analysis of core cooling is conservative and yields predicted maximum clad temperatures which are in excess of those that would occur if the piping ruptured.

Quinn's correlation [17] for dispersed flow film boiling is as follows:

$$\frac{1}{h} = \frac{1}{H} + \frac{1}{h_{TP}}$$

where

h = overall heat transfer coefficient from wall to coolant.

H = heat transfer coefficient from vapor phase to the liquid drops. The value ranges from 3,000 to 18,000 Btu/h-ft^2-F. This analysis uses the lower value of 3,000.

h_{TP} = heat transfer coefficient from wall to vapor phase.

$$h_{TP} = 0.023 \frac{k_B}{D_e} \left(\frac{G_T \times D_e}{\mu_B} \right)^{0.8} \left(\frac{C_p \times \mu_B}{k} \right)_B^{1/3} \left(\frac{\mu_B}{\mu_W} \right)^{0.14} \left[1 + \frac{1-X}{X} \left(\frac{\rho_g}{\rho_f} \right)^{2/3} \right]$$

where

k = fluid conductivity, Btu/h-ft-F

D_e = hydraulic diameter, ft

G_T = mass velocity, lb/h-ft^2

X = steam quality of fluid

ρ = density

μ = viscosity

C_p = specific heat

Subscript

B = "bulk steam phase"

g = "saturated steam"

f = "saturated liquid"

W = "wall"

After blowdown no core cooling is assumed until after core recovering starts. When the water level reaches the core bottom and starts to rise up on the core, the submerged portion will be cooled by pool boiling, and any steam thus produced will provide some cooling for that portion of the core above the water line. However, in determining peak clad temperatures no cooling is assumed for that portion of the core which is above the water line.

When the quiet water level reaches the 1/4-point of the core, a pool boiling heat transfer coefficient of 20 Btu/h-ft^2-F is applied even though the equation developed for pool film boiling from vertical plane surfaces predicts a heat transfer coefficient of 38 Btu/h-ft^2-F.

From the above it may be seen that conservative heat transfer assumptions have been used in the core cooling analysis. The assumptions used are summarized below.

1. DNB occurs after 1/4 s, when in fact it probably does not occur until at least four seconds have passed.

2. A fully developed dispersed flow film boiling correlation exists from 1/4 s until the blowdown is over, while for most of the period the heat transfer mechanism is transition boiling which is two to four times as effective as film boiling.

3. h = 0 until the water wets the hot spot, thus neglecting steam cooling up to that time.

4. A low coefficient for pool film boiling, i.e., 20 versus 38, after the water level reaches the 1/4-point of core.

Figure 14-34 shows the core flow versus time for the 14.1-ft^2 leak as calculated by FLASH. Figure 14-35 shows the clad surface heat transfer coefficient versus time based on the flow of Figure 14-34 and Quinn's correlation.

The preliminary core flooding tank design selected is for a 600 psig charge pressure, 940 ft^3 of water, 470 ft^3 of nitrogen, and a 14-in. supply line from the tanks to the reactor vessel. Figure 14-36 shows the reactor vessel water level versus time for this case. The core flooding system will provide for covering approximately 80 per cent of the core at 25 s after the double-ended rupture of the 36-in. ID pipe first occurs. Beyond this time, high pressure and low pressure injection will provide a continuous increase in the water level.

Figure 14-37 shows hot spot clad temperature transients for a range of injection cooling coefficients. All cases have a nominal clad surface heat transfer coefficient per Figure 14-35. Heat removal is then zero until the effect of injection cooling is simulated. Figure 14-37 shows that without any cooling the temperature reaches the melting point in approximately 40 s. An h value of 20 provides immediate quenching action and a slow cooling rate thereafter. An h value of 40 provides fast cooling. Even though the value of 40 is realistic for film boiling in a pool--the probable mode for the submerged portion of the core--a more conservative value of 20 has been used as the reference for evaluating performance of the core flooding tank.

The clad hot spot temperature excursion is terminated at 2,069 F. Only a minute amount (less than 1 per cent) of zirconium-water reaction occurs, and the maximum temperature is at least 1,281 F below the clad melting point.

Additional analysis was performed to evaluate the sensitivity of the maximum clad temperature to three important thermal parameters. All cases discussed below have in common the following parameters:

Leak size, ft^2	14.1
Time of DNB, s	0.25
Integrated power, full-power seconds	1.55
Time that blowdown cooling ends, s	9.5
Core region	Hot spot
Time to initiate quenching, s	16.8
Dependent variable examined	Clad temperature for hottest spot in the core

[redacted]

0062

Figure 14-38 shows the clad maximum temperature sensitivity to the surface heat transfer coefficient after the 0.25-s nucleate boiling period for 50 to 150 per cent of the nominal calculated values. After blowdown, zero cooling is maintained until quenching is initiated with a clad surface coefficient of 20 Btu/h-ft^2-F. Figure 14-38 shows that this nominal heat transfer is not on the most sensitive part of the curve, and a 20 per cent decrease in h would only result in increasing the peak clad temperature by 124 F.

The assumption that DNB occurs at 0.25 s is quite conservative. The duration of the nucleate boiling period has been evaluated to show the sensitivity of the maximum fuel temperature to this parameter. Figure 14-39 shows the effect of variation of time to reach a DNB. It should be noted that if DNB occurred at the time of rupture, then the peak temperature would only increase about 15 F above 2,069 F, while if DNB has not occurred for a more realistic value of 4 s, then the temperature would be reduced by 296 F to a peak value of 1,763 F.

The analysis of core cooling has been based on 1.55 full-power seconds resulting from a void shutdown using an assumed positive moderator temperature coefficient of $+0.5 \times 10^{-4}$ $(\Delta k/k)/F$. (The predicted value is always zero or negative.) The effect of variation of the moderator coefficient on the hot spot clad temperature is shown in Figure 14-40. The resultant integrated power before a void shutdown occurs could increase to 2.5 full-power seconds before the hot spot clad temperature would reach 2,300 F. In order to produce this many full-power seconds, a moderator coefficient in excess of $+1.0 \times 10^{-4}$ $(\Delta k/k)/F$ is required.

Many of the fuel rods may be expected to experience cladding perforation during the heatup in the loss-of-coolant accident, as a result of fission gas internal pressure and weakening of the clad as its temperature increases. The mechanical strength of the Zircaloy cladding is reduced as the temperature exceeds 1,000 F, so that the fuel rods with appreciable fission gas internal pressure will begin to fail locally and relieve the gas pressure when the temperature exceeds 1,100 F. Some local deformation of the rods will occur before perforation. However, cooling would still be effective, since the fuel rods are submerged, and cross-channel flow around the ballooned area will cool the rod. At worst a local hot spot may occur.

To verify that the perforation/deformation failure made will not significantly inhibit the emergency core cooling system from preventing clad melting, B&W has undertaken a program to evaluate the effects of perforation and deformation of fuel rods during the temperature transient following the loss-of-coolant accident. Preliminary tests have been run on nine samples of Zircaloy-4 cladding filled with ceramic pellets, and additional experiments are planned to gain a clearer understanding of the effects of temperature excursions on Zircaloy-clad fuel elements. Current plans include performance of a three-phase program. In the first two phases, which are experimental, single-rod excursions will be performed to better establish temperature-pressure relationships at the time of clad perforation. The

0063

single-rod tests of the first phase will also investigate the extent of deformation to be expected under the varying conditions associated with simulated in-reactor temperature excursions. These will include the effects of hydrogen concentration and oxide films. The second phase of the program will consist principally of multirod tests to explore the effect of the restraining action of spacer grids and adjacent fuel rods and to determine the randomization of the localized deformation in an assembly of fuel rods. In the third phase of the program the data obtained from the two experimental phases will be applied to the analysis of the effects in a loss-of-coolant accident.

It is calculated that a small number of fuel rods operating at peak power will experience a cladding temperature transient to 2,000 F in about 17 s. The transient would be limited to regions of the core that operate at peak power. The major portion of the core will not experience as severe a transient. Heating of the fuel rod spacer grid requires heat flow from the clad to the structure by conduction and radiation; therefore, the structure temperatures will lag the cladding temperature transient. As the fuel rod temperature rises, the fuel rods are expected to experience some bowing due to axial growth between supports. The spacer grids have substantial mechanical strength, even at the maximum expected temperatures, and will therefore retain sufficient strength to ensure spacing between fuel rods to allow emergency coolant to reach them. This will suffice to keep the fuel rods in their respective positions in the core to prevent gross change in fuel geometry. | 1

The ability of the clad to maintain its strength and structural integrity during reflooding has been confirmed by recent experimental work at B&W involving the rapid quenching of Zircaloy tubing specimens from temperatures as high as 2,300 F. Test results show that, for temperatures as high as 2,300 F, the cladding material will retain its strength and will not suffer from brittle fracture upon quenching.

The temperature transient in the core can produce significantly higher than normal temperatures in components other than fuel rods. Therefore, a possibility of eutectic formation between dissimilar core materials exists. Considering the general area of eutectic formation in the entire core and reactor vessel internals, the following dissimilar metals are present, with major elements being in the approximate proportions shown:

Type-304 Stainless Steel [redacted]

19 per cent chromium
10 per cent nickel
remainder iron

0064

Control Rod Poison Material

80 per cent silver
15 per cent indium
5 per cent cadmium

Zircaloy-4

98 per cent zirconium
1-3/4 per cent tin

Inconel

53 per cent nickel
19 per cent chromium
3 per cent molybdenum
5 per cent CB-TA
1 per cent titanium
.5 per cent aluminum
Remainder iron

All these elements have relatively high melting points (greater than 2700 F) except those for silver, cadmium, and indium. The melting point of the silver-indium-cadmium alloy is about 1,470 F.

The binary phase diagram indicates that zirconium in the proportion 75 to 80 per cent has a eutectic point with either iron, nickel, or chromium at temperatures of approximately 1,710, 1,760, and 2,370 F, respectively. If these dissimilar metals are in contact and if those eutectic points are reached, then the materials could theoretically melt even though the temperature is below the melting point of either material taken singularly.

One point of each dissimilar metal contact is between Zircaloy-clad fuel rods and Inconel 718 spacers. The analysis of the performance of the core flooding tanks during a loss-of-coolant accident indicated that some of the cladding will exceed the zirconium-iron and the zirconium-nickel eutectic points. Since the spacers are located at 21-in. intervals along the assembly and each grid has a very small contact area, only a fraction of the hottest fuel rods would be in contact with Inconel 718 spacer grids.

B&W has conducted recent experimental tests in which specimens of Zircaloy tubing in contact with sections of spacer grid material were subjected to a thermal transient closely approximating that of the clad hot spot following a LOCA. These tests verified that the eutectic reaction is limited to the region of contact between the clad and the spacer grid tips (dimples), and that it terminates as these materials melt at the point of contact. Both the clad and the grid material maintained their structural integrity because the amount of material involved was small and at localized positions.

Another area of dissimilar metal contact is that of a zirconium guide tube with the stainless steel cladding of the control rod. To determine whether the temperatures in the control rod following a LOCA could become high enough to approach either the temperature required for possible eutectic formation between the clad and the guide tube or the melting temperature of the Ag-In-Cd alloy, the thermal performance of a control rod assembly following a LOCA was analyzed. A very conservative approach was taken in this analysis. In spite of the fact that the core flow is as high or higher than normal core flow during the first two seconds following the rupture, normal steady-state cooling of a control rod is assumed. In two seconds, the core power is essentially down to decay heat levels. Therefore, the following assumptions were made:

1. The average core power after two seconds is 8 per cent of ultimate power and remains at this level.

2. All decay heat is absorbed in the core and 50 per cent of the decay heat is in the form of gamma rays available for absorption in the control rod. By ratioing the control rod density to the average core density, an average energy deposition rate of 8.50 W/cc in the control assemblies was obtained.

3. The maximum activation product energy in the control rod itself was estimated to be 2.99 W/cc.

4. The highest energy deposition rate at the decay heat level was assumed to be the average times the ratio of peak-to-average power, or 36.18 W/cc.

5. An adiabatic heatup of the control rod with a heat rate of 36.18 W/cc was assumed until the water level reached the point in the core at which the highest peak-to-average power occurs.

6. The temperature of the control alloy is ≈650 F at the time the rod is assumed to be insulated (2 s).

Using the assumptions above, the average temperature of the Ag-In-Cd goes up to 1,035 F at 17 s, at which time the water level in the core reaches the elevation of the hottest spot on the control rod. The temperature of the rod would then rapidly decrease.

Since the melting point of the alloy is ≈1,472 F, a margin of 437 F exists between the conservatively calculated maximum temperature and the melting point of the alloy. The lowest temperature for an eutectic formation is that for Zr-Fe, which occurs at 1,710 F. Therefore, the integrity of the control rod assemblies is maintained during and following a loss-of-coolant accident.

[redacted]

0066

The reactor core will remain subcritical after flooding without control rods in the core because the injection water contains sufficient boron to hold the reactor subcritical at reduced temperatures. The most stringent boron requirement for shutdown without any control rods is at the beginning of core life when the reactor is in a cold, clean condition and 1,316 ppm boron are required to maintain a k_{eff} of 0.99. (See Table 3-6, Soluble Boron Levels and Worth.) The concentration existing in the containment sump after a loss-of-coolant accident from operating power at the beginning of core life is 1600 ppm boron. This concentration represents a boron margin of 284 ppm above the subcriticality design value margin of 1 per cent.

In conclusion, the results of the core flooding tank design base accident (36-in. double-ended rupture) are as follows:

1. The clad hot spot temperature excursion is terminated at 2,069 F. Less than 1 per cent zirconium-water reaction occurs, and the maximum clad temperature is at least 1,281 F below the clad melting point (Figure 14-37). This maximum temperature is based on conservative heat transfer assumptions and is 231 F below the design criterion of 2,300 F maximum clad temperature allowed. This also demonstrates that no clad melting occurs to affect core geometry for postaccident cooling and that no fuel melting occurs to release large quantities of fission product.

2. If DNB occurs at time 0, then the maximum hot spot clad temperature increases only 15 F; whereas if DNB occurs at 4 seconds, for which there is empirical justification, then the maximum hot spot clad temperature decreases by 296 (Figure 14-39) which shows the amount of conservatism in this analysis.

3. The correlation used to predict the blowdown heat transfer coefficient has been checked against available data and shows a maximum deviation of 20 per cent. A 20 per cent decrease from the nominal clad surface heat transfer coefficient after DNB results in an increase of only 124 F in the maximum hot spot clad temperature (Figure 14-38).

4. A clad surface heat transfer coefficient of 20 Btu/h-ft^2-F is sufficient to quench the clad temperature rise when the water reaches the 1/4-point of the core, even though a coefficient of 38 Btu/h-ft^2-F has been predicted from the formula for pool film boiling from a vertical plane surface (Figure 14-37).

5. The effect of varying the moderator coefficient on the loss-of-coolant accident has been investigated in this analysis. To reach the peak clad temperature limit of the design criteria (2,300 F), the moderator coefficient would have to increase from its value of $+0.5 \times 10^{-4}$ $(\Delta k/k)/F$ to approximately $+1.2 \times 10^{-4}$ $(\Delta k/k)/F$ (Figure 14-40). 1

b. Core Cooling Analysis for Spectrum of Leak Sizes

The loss-of-coolant accident has been analyzed for a spectrum of leak sizes and locations. This information is reported according to the following grouping: (1) hot leg ruptures, (2) cold leg ruptures, (3) injection line failures, and (4) injection system capability.

1. Hot Leg Ruptures

In 14.2.2.3.4 a an analysis of the 36-in. ID, double-ended pipe rupture was presented. This accident produced the fastest blowdown and lowest heat removal from the fuel, therefore producing the highest cladding temperatures of any loss-of-coolant accident. This was therefore the basis for design of the core flooding equipment. A decrease in the rupture size assumed results in decreased maximum clad temperature during a loss-of-coolant accident.

Core cooling evaluations have been performed for a spectrum of five additional rupture sizes using the same basic calculational technique and assumptions as used for the large rupture case. These rupture sizes are 8.5, 5.0, 3.0, 1,0, and 0.4 -ft^2. The reactor coolant system mass release and pressure-time history for these rupture sizes are shown in Figures 14-41 and 14-42.

The reactor vessel water volume as a function of time after the rupture for the various rupture sizes is shown in Figure 14-43. These water volume curves were generated utilizing the flow available from the core flooding tanks, one high-pressure injection pump, and one low-pressure injection pump. The two independent pumping systems have a combined capacity of at least 7,000 gpm with the high-pressure pumps running on emergency power within 25 s after the rupture, and the low-pressure pumps delivering 6,000 gpm when the pressure has decayed to 100 psi, or at 25 s, whichever occurs later. However, the analysis is based on only one system in operation with a total flow of 3,500 gpm.

Figure 14-44 shows the hot spot clad temperature as a function of time for the various rupture sizes. As can be seen from this figure, the small-sized ruptures yield maximum clad temperatures which are considerably lower than those resulting from the larger sizes. The results of this study are shown in Table 14-13. The temperature curve in Figure 14-44, as well as the results in Table 14-13, are for the 5.0-ft^2 hot rupture witnout trip and are more conservative than the results obtained for the 5.0 ft^2 hot rupture with trip. The trip case results in a maximum temperature of 1,563 F.

[redacted]

0068

Table 14-13
Tabulation of Loss-of-Coolant Accident Characteristics
for Spectrum of Hot Leg Rupture Sizes

Rupture Size, ft^2	Full-Power Seconds(a)	Minimum Water Level Below Bottom of Core, ft	Hot Spot Maximum Temperature, F
14.1	1.55	-6.8	2,069
8.5	2.65	-5.2	1,954
5.0	4.12(b)	-4.0	1,632
3.0	3.35(b)	-2.2	1,454
1.0	6.25(b)	+4.7	988
0.4	6.50(b)	+12.0	1,002

(a) Includes power generation until power has decayed to 10 per cent of ultimate power.

(b) Blowdown forces on control rods are equal to or less than normal pressure drop, and control rods will insert with normal velocities. These values are for trip shutdown rather than for a void shutdown, but include void reactivity effects.

2. Cold Leg Ruptures

A similar analysis of a spectrum of rupture sizes has been made for the cold leg piping. The rupture sizes tabulated are the double-ended, 28-in.-ID inlet pipe, which yields 8.5 ft^2 of rupture area, and the 5.0, 3.0, 1.0, and 0.4-ft^2 sizes.

The reactor coolant system average pressure for this spectrum of rupture sizes as a function of time is shown in Figure 14-45. The water level as a function of time is shown in Figure 14-46.

The hot spot temperature as a function of time for the spectrum of cold leg leak sizes is shown in Figure 14-47. The results of this analysis are shown in Table 14-14.

0069

Table 14-14
Tabulation of Loss-of-Coolant Accident Characteristics
for Spectrum of Cold Leg Rupture Sizes

Rupture Size, ft^2	Full-Power Seconds[a]	Minimum Water Level Below Bottom of Core, ft	Hot Spot Maximum Temperature, F
8.5	0.60[a]	-6.7	1,686
5.0	0.40[a]	-6.0	1,803
3.0	1.00[a]	-4.8	1,575
1.0	5.38[a]	+3.6	1,280
0.4	5.50[a]	+7.0	1,160

[a] Blowdown forces on control rods are equal to or less than normal pressure drop, and control rods will insert with normal velocity. These values are for trip shutdown rather than void shutdown, but include reactivity effects. Values also include power generation until power decays to 10 per cent of ultimate power.

3. Evaluation of Emergency Coolant Injection Line Failure

A low-pressure injection line failure has been evaluated, and the results show that the reactor is protected. The rupture of a pipe that connects a core flooding tank and the low-pressure injection flow to the reactor vessel was assumed to fail adjacent to the reactor vessel and before the first check valve (see Figure 6-1). This pipe has an internal diameter of 11.5 in., and the resultant rupture area is 0.72 ft^2.

Interpolation of available blowdown calculations has been used to evaluate this rupture size, and the data show that a rupture of this size would result in the core being uncovered several feet below the top of the core. However, the hot spot will never be uncovered, and peak cladding temperatures will be slightly less than that shown in Figure 14-47 for the 1.0-ft^2 cold leg rupture.

Since this small rupture size leaves a considerable water inventory in the reactor vessel, the remaining core flooding tank inventory is more than adequate to reflood the core completely.

The other low-pressure line can supply 3,000 gpm of water to the reactor vessel and provide coolant to keep the core cooled. The combined capacity of the two high-pressure pumps is 1,000 gpm, which is in excess of the boiloff rate (680 gpm) due to decay heat immediately after blowdown. With a single 500-gpm high-pressure injection pump the excess water above the core is adequate to prevent the core from being uncovered below the three-

quarter elevation, and beyond 340 seconds the water level will begin to increase.

The high-pressure injection mode has two independent chains of flow to supply borated coolant to the system. If a rupture of high-pressure injection piping were to occur in one of the four lines between the attachment to the reactor coolant pipe and the check valve, then the other chain of this system would have adequate capacity to protect the core against this small leak. In the event of a component failure in the second high-pressure injection line, the ruptured flow path can be monitored by the operator and spillage flow can be stopped by isolation of the affected piping. The entire capacity of one high-pressure pump can then be utilized to handle the small rupture and protect the core.

4. Evaluation of Emergency Core Coolant Injection System Performance for Various Rupture Sizes

The loss-of-coolant analysis is based on the operation of one high-pressure injection pump (500 gpm) and one low-pressure injection pump (3,000 gpm), and the operation of both core flooding tanks. It has been shown that this combination of engineered safety features provides core protection for all leak sizes up to that corresponding to the double-ended rupture of the 36-inch-ID pipe.

The capability of other combinations of engineered safety features to provide core protection has been evaluated. This capability is shown in Figure 14-48. In this evaluation the core is considered protected if the combination of emergency cooling equipment considered will prevent core damage that would interfere with further core cooling.

The high-pressure injection system, with only one pump operating, can protect the core for leaks up to about 4 inches in diameter. A combination of one high-pressure and one low-pressure injection pump will protect the core for leaks up to about 10 inches in diameter, (0.5 ft^2) whereas, one high-pressure and two low-pressure pumps provide protection for leak areas up to 1 ft^2. For larger break areas, the operation of one HPI pump, one LPI pump, and the core flood tanks provides the coolant necessary to keep the core protected.

This evaluation of emergency core cooling capability demonstrates that the core is protected for the entire spectrum of leak sizes in both the hot and cold leg piping.

0071

14.2.2.3.5 Accident Simulation - Containment Vessel

a. COPATTA Program

The COPATTA Code is Bechtel's computer program to analyze the effects of a LOCA on a containment vessel. It has been derived from the original CONTEMPT Code (18) written by the Phillips Petroleum Company for the LOFT program. The present COPATTA is written in Fortran IV and uses the GE 625 computer.

COPATTA calculates a pressure-time transient with stepwise iteration between thermodynamic state points. The iterations are based on the laws of conservation of mass, momentum and energy together with their derived functions. Superposition of heat input functions is assumed so that any combination of blowdown, metal water reaction, decay heat generation, and sensible heat energy can be used with appropriate engineered safety features to determine the pressure-time history associated with any LOCA.

COPATTA also includes several options which allow pressure-time transient calculations for the steam generator or reactor compartments. The effect of containment vessel leaks and time and position dependent thermal gradients can be evaluated depending upon the input used and printout requested.

The program assumes a three-region containment vessel. The vessel atmosphere is the vapor region, the sump is the liquid region, and the reactor, the third region, can function independently as a vapor or a liquid region. Energy is transferred between the liquid and vapor regions by boiling but evaporation is neglected. A convective heat transfer coefficient can be assumed between these two regions. However, since any heat transfer in this mode is small, a conservative coefficient of zero is assumed. Each region is assumed homogenous, but a temperature difference can exist between regions. Any moisture condensed in the vapor region during a time step is assumed to fall immediately into the sump.

The containment vessel model includes representation of three engineered safety features: a spray system, an ECCS, and an air recirculation and cooling system. Water supplied to the spray and ECCS can come from an external source at a prescribed temperature, or it can be recirculated from the liquid region in the containment vessel. During recirculation, water for decay heat removal is taken from the liquid region and is pumped through a heat exchanger before being returned to reactor region. The cold side of the heat exchanger can itself be part of another heat exchange system.

The methods of NTU* heat exchanger design are used for program analysis. The heat exchange circuit delay time is zero, so no containment vessel coolant inventory change is considered.

- - - - -

*Number of exchanger heat transfer units.

[redacted]72

The air recirculation and cooling system is described with start and stop times and a table of heat removal rates as a function of vapor temperature. Moisture condensed by the air coolers is assumed to fall immediately into the liquid region.

The containment vessel and internal structures can be separated in up to 20 heat conduction sections whose thermal behavior can be described by a one-dimensional, multiregion heat-conduction equation. These heat conducting sections can act as heat sources or sinks. Any boundary conditions from insulated to zero resistance can be applied to each section as appropriate. These conditions can be constant, time-dependent, temperature-dependent, or dependent upon the steam-to-air ratio existing in the containment vessel atmosphere. Bulk temperatures may be the vapor region temperature, the liquid region temperature, the reactor vessel liquid temperature, a cyclical outside air temperature, or a constant.

The heat sinks used to represent the Davis-Besse containment vessel and its internals are presented in Table 14-15.

Heat transfer to the heat sinks from the containment vessel atmosphere is determined by a "Modified Tagami" heat transfer coefficient. This coefficient correlates the test results of Uchida and Kolflat with a turbulence factor that depends upon the time from accident initiation to peak pressure. As time progresses and turbulence decreases, this coefficient is reduced to Uchida's steady-state heat transfer correlation by a ratio of the instantaneous mass blowdown rate to the mass blowdown rate at the time of peak pressure. No heat transfer from the containment vessel outer surface to the environment was assumed for the preliminary analysis. The heat rejection from the steel shell to the shield building annular space is not rapid enough to affect the peak pressure of the various break sizes. The final analysis will consider the heat transfer from the steel shell to the shield building annular space.

b. Engineered Safety Features

Two modes of operation of the containment vessel cooling system are assumed to show the vessel's response to a LOCA. The first mode assumes that standby power is available; hence the full cooling capacity can be used. The second mode simulates minimum conditions with only the minimum cooling capacity used. An ECCS flow of 3,500 gpm is assumed for both modes. Core flooding tank operation has been included in the reactor blowdown input. The minimum cooling capacity is determined by the power available from one emergency diesel generator.

The ·ty features used are tabulated below showing the systems in operation, the total capacity, and the assumed time they start after an incident.

	ESF Systems	Design Heat Removal Capacity, Btu/h	Flow Capacity, gpm	Initial Operating Time, s
Normal Operation	Air Coolers and Containment Vessel Sprays	150×10^6		
		150×10^6	2600	35
	Core Injection		7000	25
Minimum ES	Air Coolers or Containment Vessel Sprays	150×10^6		
		150×10^6	2600	35
	Core Injection		3500	25

8

c. Initial Conditions

The same initial conditions are assumed for all accidents. These initial conditions are chosen to represent conservative conditions, both within the containment vessel and for heat removal from the vessel.

These initial conditions are summarized as follows:

Containment Vessel Free Volume	2.866×10^6 ft^3
Containment Vessel Temperature	120 F
Containment Vessel Pressure	14.7 psia
Relative Humidity	70%
Shield Building Annulus	110 F
Service Water Inlet Temperature	85 F
BWS Tank Water Temperature	90 F

8

8

The containment vessel pressure-time history of a LOCA calculated by the COPATTA program is conservative. The assumptions used in preparing the program input and in the program calculations are consistent with the two-phase, two-component thermodynamic model used. These assumptions are summarized below:

The containment vessel atmosphere pressure is also the sump pressure and, following blowdown, the reactor coolant system pressure. Each region is thoroughly mixed, with homogeneous thermodynamic properties.

All liquid condensed in the atmosphere or on the walls during any calculational time interval is removed from the atmosphere and added to the sump at the end of the interval.

The sump region contains no water at the beginning of the transient.

Water entering the containment vessel from the reactor coolant system during the blowdown phase of the transient flashes, and its final temperature is the saturation temperature at total vessel pressure.

If the total pressure inside the containment vessel drops below the saturation pressure of sump water, boiling of sump water occurs until a new equilibrium pressure and water temperature are established. The atmosphere region is constrained to saturation conditions when the containment spray system is in operation.

The heat transfer coefficient during blowdown, for heat transfer between the containment vessel atmosphere and heat conducting regions in contact with it, is calculated from an empirical relationship between the maximum heat transfer coefficient, the rate of steam input into the vessel, and the duration of blowdown. During the postblowdown phase the heat transfer coefficient is calculated as function of the air/steam mass ratio in the atmosphere.

Heat transfer rates from a superheated atmosphere to heat sinks are calculated using a temperature gradient corresponding to the steam saturation temperature less the heat sink surface temperature.

The decay power energy input assumes infinite radiation.

No leakage from the containment vessel is assumed.

There is no convective heat transfer between the atmosphere and the sump, and evaporation is neglected.

The containment vessel bottom head is assumed insulated.

Table 14-15

Heat Sink Summary

Heat Sink	Surface Area (ft^2)	Thickness (ft)
1. Containment Vessel (Carbon Steel):		
Dome	24,550	0.063
Cylinder	74,740	0.125
2. Refueling Cavity		
S.S. Liner Plate	6,770	0.021
Concrete	6,770	1.000
3. Floor Slab:	11,400	1.000
4. Miscellaneous Concrete:	114,000	1.000
5. Miscellaneous Exposed Steel	18,000	0.092
	3,600	0.041

14.2.2.3.6 Accident Analysis - Containment Vessel

a. Building Response to Loss-of-Coolant Accidents

The response of the containment vessel has been determined for loss-of-coolant from various breaks in the primary system piping. The breaks were analyzed with the different operational modes of the engineered safety features tabulated previously. The following table shows the break area, peak pressure, and time of pressure peak for those breaks investigated.

Break Area, ft^2	Peak Pressure, psig	Time, s	Safety Features Mode Used
14.1	34.8	8.05	Any
8.5	35.5	12.0	Any
5.0	35.6	20.0	Any
3.0	36.0	30.0	Any
1.0	32.4	76.2	Normal
1.0	32.7	76.0	Minimum

Pressure-time curves are given in Figure 14-49 to show the containment vessel response for each break above with minimum safety features used.

0076

The energy sources and heat sink inputs as a function of time are shown in Figure 14-50 for the 14.1 ft^2 break.

The sources and sinks determine the response of the containment vessel atmosphere and sump. Subcooling of the sump and the vessel vapor and sump temperatures as a function of time for the 14.1 ft^2 break case are shown in Figure 14-51.

b. Margin Demonstrated in Containment Vessel Design

The design pressure of the containment vessel is based on the 3.0 ft^2 break, which results in the highest peak pressure after blowdown (approximately 36.0 psig). This pressure is 4 psi below the design pressure of 40.0 psig. Hence the vessel can withstand an additional 22,000 lb saturated steam.

c. Metal-Water Reaction Capability

This section considers the capability of the containment to withstand the effects of a metal-water reaction. This capability is described in terms of percent of zirconium in the core which may react with water without exceeding the containment design pressure of 40 psig.

Since the greatest probability of metal to water reaction occurs with the largest break (14.1 ft^2), the calculation for containment vessel metal-water reaction capability is based on the pressure-time history corresponding to this break. The minimum safety features operating mode with air coolers results in the least margin between the calculated pressure at any time, and the design pressure of 40.0 psig.

At any given time, this pressure difference corresponds to a finite amount of zirconium reacted. The number of pounds reacted is calculated for (1) the heat of reaction is released as saturated steam to the containment vessel atmosphere with subsequent superheat from the released hydrogen burning and (2) the total heats of reaction used to superheat the containment vessel atmosphere. The change in the state properties of the atmosphere with increased pressure is included. However, the increased rate of heat removal by the air coolers from the atmosphere due to increased temperature is not included. The reaction heat is not assumed to raise the temperature of the reaction vessel injection water to saturation. Hence, with these assumptions, the following estimate of the containment vessel metal-water capability is conservative.

In the event of a metal-water reaction beginning at 30 s, with 2,808 Btu/lb Zr heat transferred to the atmosphere as saturated steam and 2,350 Btu/lb Zr transferred to the atmosphere as superheat, by subsequent hydrogen burning, the Davis-Besse containment

0077

vessel can withstand 68.6 per cent metal-water reaction in 1,000 s. If all the metal-water reaction and subsequent hydrogen burn energies are transferred to the atmosphere as superheat, then the Davis-Besse vessel can withstand 37.1 per cent metal-water reaction by 1,000 s. Figure 14-52 shows the per cent metal-water reaction allowable for both cases as a function of time after 30 s.

14.2.2.3.7 Environmental Analysis

The fission product release to the containment vessel, in the event of a LOCA would be the gap activity of all fuel rods plus the equilibrium coolant activity. Of this release 50 per cent of the iodine is assumed to plate out within the containment vessel. This assumption is consistent with TID-14844.

The dose from the activity available for release from the containment vessel is then calculated for a leak rate of 0.5 per cent per day. This leakage would be into the shield building and penetration rooms which would be maintained at a negative pressure and all discharge to the environment would be through charcoal filters. No credit is taken for holdup and decay within the shield building. Iodine removal efficiency of the charcoal filters is conservatively assumed to be 95 per cent. The atmospheric dispersion models described in Appendix 2-B have been used in calculating doses for 0-2 hours, 2-24 hours, and 1-30 days.

The total integrated thyroid doses resulting from this LOCA fission product release are plotted in Figure 14-53 as a function of distance for 2-hour, 24-hour, and 30-day exposures. In addition, the thyroid doses from a LOCA are summarized in Table 14-16. Whole Body doses are of lesser significance for this accident so they were not calculated.

14.2.2.4 Maximum Hypothetical Accident

14.2.2.4.1 Identification of Accident

The analyses in the preceding sections have demonstrated that even in the event of a loss-of-coolant accident, no significant core melting will occur. However, to demonstrate that the operation of a nuclear power plant at the proposed site does not present any undue hazard to the general public, a hypothetical accident involving a gross release of fission products has been evaluated. No mechanism whereby such a release occurs is postulated since it would require a multitude of failures in the engineered safety features provided to prevent its occurrence. Fission products are assumed to be released from the core as follows: 100 per cent of the noble gases, 50 per cent of the halogens, and 1 per cent of the solids. | 1

14.2.2.4.2 Environmental Analysis

In order to demonstrate the conservatism or margin in the design of the containment and engineered safety features, this accident has been evaluated using a leak rate of 2.5 per cent per day. Meteorological models and iodine removal efficiency are the same as for the loss-of-coolant accident.

The total integrated thyroid doses are plotted in Figure 14-54 as a function of distance from the reactor for 2-hour, 24-hour, and 30-day exposures. Corresponding whole body doses due to immersion in the cloud of beta and gamma radioactivity are shown in Figure 14-55.

The resulting doses also are summarized in Table 14-16.

14.2.2.5 Gaseous Radwaste Decay Tank Rupture

Rupture of a gaseous radwaste decay tank would result in the release of its radioactive contents to the plant ventilation system and to the atmosphere through the vent stack. This accident was analyzed in order to evaluate the resultant integrated dose at the site boundary.

A tank is assumed to contain its maximum possible inventory of gas activity. Atmospheric dilution is calculated on the basis of the two-hour meteorological model presented in Appendix 2-B. The integrated dose is evaluated, using the immersion model, as a gamma-beta whole body exposure resulting from the radioactive Xe and Kr release. This dose is equal to 0.82 Rem, well below the guideline values of 10 CFR 100.

14.2.2.6 Radiological Dose Summary

Table 14-16 summarizes the calculated radiological dose at the exclusion distance for each of the accident conditions.

14.2.2.7 Loss of Intake Canal

Since the intake canal is not designed to Seismic Class I standards beyond approximately 700 feet, it has been postulated that the Class II portion of the canal can collapse following an earthquake. An analysis was made to determine the adequacy of the stored water, in the Class I portion of the intake structure and canal, to bring the station to cold shutdown.

The ratio of the areas of cross-sections of the intake canal and each of the dikes is 3:1, therefore, even if both the dikes collapse into the canal there will still be one-third the total area available in the canal for water flow. Even though a complete loss of the intake canal cannot be anticipated, a complete loss of canal was, however, postulated for this analysis.

In case of an unlikely event of the loss of the intake canal, the reactor will be tripped and the station will be maintained at hot standby with the auxiliary feedwater pumps for as long as condensate storage and other demineralized water storage is available. Based on a minimum of one condensate storage tank (250,000 gal.) being available for the auxiliary feedwater pumps, the station can be kept at hot standby for 13 hours followed by a six (6) hour cooldown to 280 F. In this situation, the service water pumps will be brought into operation a minimum of 19 hours after the loss of the canal.

For conservatism the water level in the canal prior to the collapse was assumed at 560' I.G.L.D. The service water pump suction is at elevation 548' (see Figure 5.10-2). Approximately 7.7 x 10^6 gallons of water is available.

between 548' and 560'. The water available as heat sink below 548' was not considered.

The design parameters used in this analysis and the results are given below.

DESIGN PARAMETERS:

Volume of water available below elevation 560'	= 7.7×10^6 gal. = 64×10^6 lbs.
Surface area at elevation 560'	= 165,000 ft^2
Time period considered	= 14 days
Average Decay Heat Rate (for 14 day period)	= 43×10^6 Btu/hr.
Total Decay Heat	= 14.5×10^9 Btu
Weather data for Toledo (from Marley Handbook)	
Max. dry bulb temperature °F	= 93
Max. wet bulb temperature °F	= 77
Latitude	= 41°-36' N
Wind Velocity	= 3 mph
Max. expected heat gain by solar radiation (24 hr. average)	= 130 Btu/hr-ft^2
Minimum time after reactor shutdown the service water pumps are required	= 19 hrs.
Service water temperature at the start of decay heat removal system	= 85 F (max.)

CALCULATED DATA FOR COOLING POND:

Pond Temp. °F	Heat Removal Capability Btu/hr. Based on 160,000 ft^2 surface area	Water loss by evaporation-gal/min
160	160×10^6	330
*140	60×10^6	120
130	42.3×10^6	83
120	40.0×10^6	78

*Expected equilibrium pond water temperature, since the total solar heat gain plus decay heat at 65 hours after shutdown approximately equals the removal capability.

0080

8 Time to raise the pond temperature to 140 F based on water elevation 560' and assuming pond does not lose any heat during this time (includes heat gain 3 by solar radiation) = 65 hours

8 Total water evaporated in 24 hours (for 140 F water temperature) = 1.76 in. water depth

8 Approximate time to evaporate water from elevation 560' to 557'-6 (assuming no in-leakage) = 17 days

8 An additional 42 days cooling will be available by evaporating water between elevation 557'-6" and 554". Below elevation 553' the service water pumps 5 will not have enough submergence.

8 Total time for which cooling is available after loss of intake canal. = 60 days

FORMULAS USED

8 1. W = moisture evaporated lbs/hr-ft^2 $= \frac{(240 + 3.7t)(P_s - P)}{7000}$

Where P_s = saturation pressure of vapor at temperature t°F, inches of mercury

P = actual vapor pressure of air, in. Hg
t = average water temperature, °F

3

2. Total water evaporated = W $\frac{\text{lb}}{\text{Hr-ft}^2}$ x A ft^2 x $\frac{1 \text{ gal.}}{8.25 \text{ lb}}$ x $\frac{\text{Hr}}{60 \text{ min}}$

= gal/min

3. Heat removal rate = WhA Btu/hr

Where h = latent heat of water, Btu/lb

A = surface area, ft^2

REFERENCES:

1. Cooling Tower Fundamentals and Application Principles, Published by The Marley Company, Kansas City, Missouri.

2. Perry's Chemical Engineers' Handbook; Perry, Chilton, Kirkpatrick, McGraw-Hill Publications, 4th Edition.

3. Kent's Mechanical Engineers' Handbook; J. Kenneth Salisbury, Wiley Handbook Series, 12th Edition.

0081

Table 14-16

Dose Calculation Summary
(Based on Exclusion Distance of 730 Meters)

Item	Dose, rem		
	2-Hour	24-Hour	30-Day
Loss of Electric Power			
Thyroid	0.004	- - - -	- - - -
Steam Line Failure			
Thyroid	0.25	- - - -	- - - -
Whole Body	0.002	- - - -	- - - -
Steam Generator Tube Failure			
Thyroid	0.005	- - - -	- - - -
Whole Body	0.38	- - - -	- - - -
Rod Ejection Accident			
Thyroid	0.05	0.14	0.18
Loss-of-Coolant Accident			
Thyroid	1.11	3.37	4.42
Maximum Hypothetical Accident			
Thyroid	221.	605.	721.
Whole Body	17.1	29.2	31.1
Fuel Handling Accident			
Thyroid	2.25	- - - -	- - - -
Whole Body	0.14	- - - -	- - - -
Gaseous Radwaste Decay Tank Rupture			
Whole Body	0.82	- - - -	- - - -

14.3 REFERENCES

(1) Watson, L. C., Bancroft, A. R., and Hoelke, C. W., Iodine Containment by Dousing in NPD-11, AECL-1130.

(2) Styrikovich, M. A., et al., "Transfer of Iodine From Aqueous Solutions to Saturated Vapor," Soviet Journal of Atomic Energy 17, July 1964.

(3) Diffey, H. R., et al., "Iodine Clean-up in a Steam Suppression System," International Symposium on Fission Product Release and Transport Under Accident Conditions, Oak Ridge, Tennessee, CONF-65047, Vol 2, pp 776-804 (1965).

(4) Barthoux, A. J., et al., "Diffusion of Active Iodine Through Water, With the Iodine Being Liberated in CO_2 Bubbles at High Temperatures," AEC-TR-6149, June 1962.

(5) Eggleton, A. E. J., "A Theoretical Examination of Iodine-Water Partition Coefficients," AERE-R-4887, February 1967.

(6) Weidenbaum, B. and Naymark, S., "Potentialities of Molten UO_2 as a Reactor Fuel," Transactions of the ANS, 7, No. 2, p 527 - 528 (1964).

(7) Liimatainen, R. C. and Testa, F. J., Studies in TREAT of Zircaloy-2-Clad, UO_2-Core Simulated Fuel Elements, Argonne National Laboratory Chemical Engineering Division Semi-Annual Report, ANL-7225, January - June 1966.

(8) White, J. F., GE-NMPO, direct communication of experimental data to be published.

(9) Grossman, L. N., "High-Temperature Thermal Analysis of Ceramic Systems," Paper presented at the American Ceramic Society 68th Annual Meeting, May 1966.

(10) Redfield, J. A., CHIC-KIN -- A Fortran Program for Intermediate and Fast Transients in a Water Moderated Reactor, WAPD-TM-479, January 1965.

(11) Henry, A. F. and Vota, A. V., WIGL2 -- A Program for the Solution of the One-Dimensional Two-Group, Space-Time Diffusion Equations Accounting for Temperature, Xenon and Control Feedback, WAPD-TM-532, October 1965.

(12) Wise, W. R., Jr. and Proctor, J. F., Explosion Containment Laws for Nuclear Reactor Vessels, NOLTR 63-140, August 1965.

(13) Wise, W. R., Jr., An Investigation of Strain Energy Absorption Potential as the Criterion for Determining Optimum Reactor Vessel Containment Design, NAVORD Report 5748, June 1958.

(14) Margolis, S. G. and Redfield, J. A., FLASH : A Program for Digital Simulation of the Loss-of-Coolant Accident, WAPD-TM-534, May 1966.

(15) Grenda, R. J. and Patterson, J. F., "The Velocity of Rising Steam in a Bubbling Two-Phase Mixture," Transactions of the ANS, 5, No. 1, p 151, June 1962.

(16) Possible Zirconium Water Reactions in Water Reactors, AEC Regulatory Staff Symposium, April 27, 1965.

(17) Quinn, E. P., Forced-Flow Heat Transfer to High-Pressure Water Beyond the Critical Heat Flux, ASME 66WA/HT-36, November 27, 1966.

(18) L. C. Richardson, L. J. Finnegan, R. J. Wagner and J. M. Waage, "CONTEMPT," A computer program for predicting the containment pressure-temperature response to a loss-of-coolant accident, Phillips Petroleum Company, Atomic Energy Division, Idaho Falls, Idaho; AEC Research and Development Report TID-4500; issued June, 1967.

~~279~~

0084

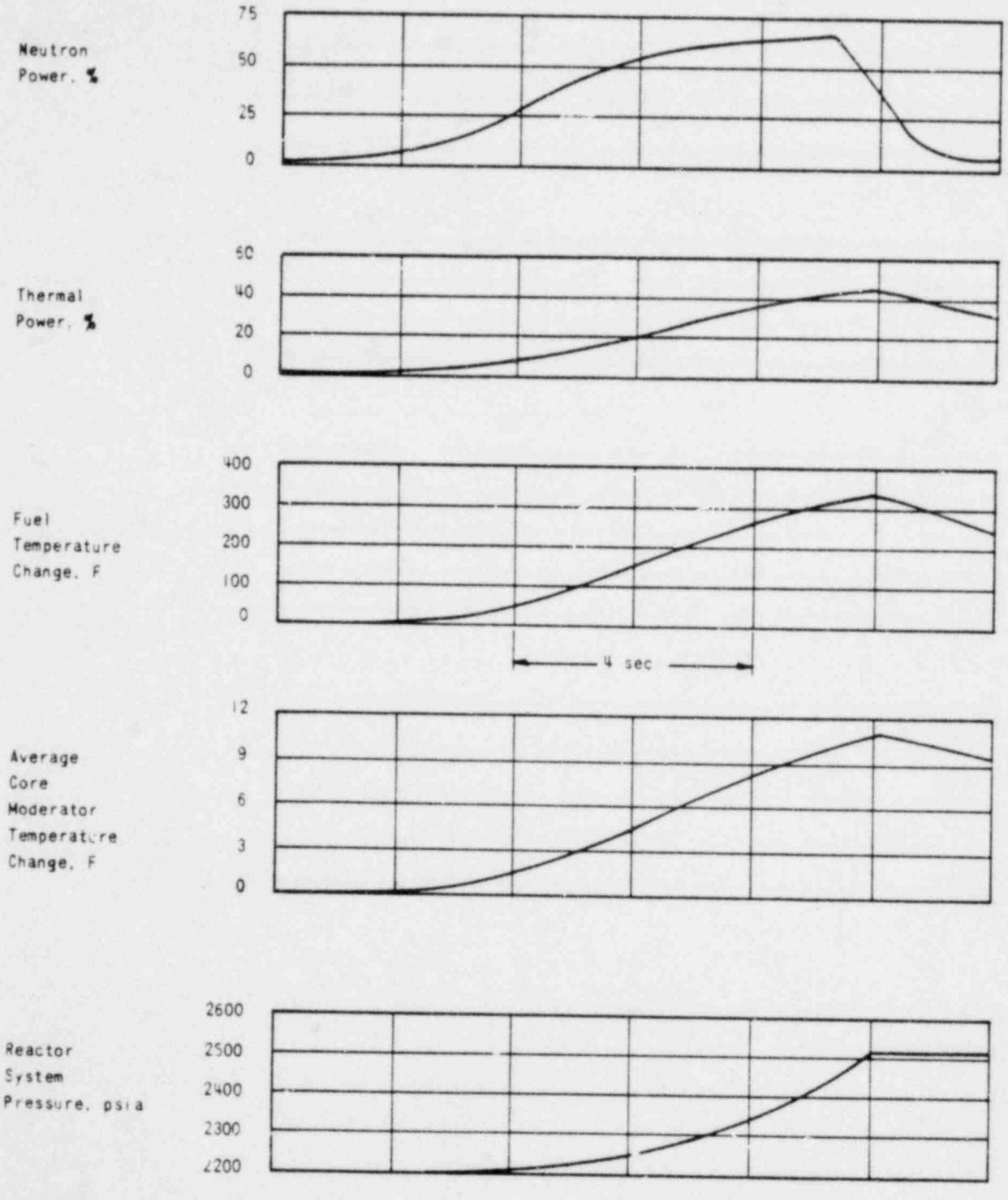

DAVIS-BESSE NUCLEAR POWER STATION
STARTUP ACCIDENT FROM 10^{-9} RATED POWER
USING A 1.5% Δk k ROD GROUP; HIGH PRESSURE
REACTOR TRIP IS ACTUATED
FIGURE 14-1

~~0085~~

0085

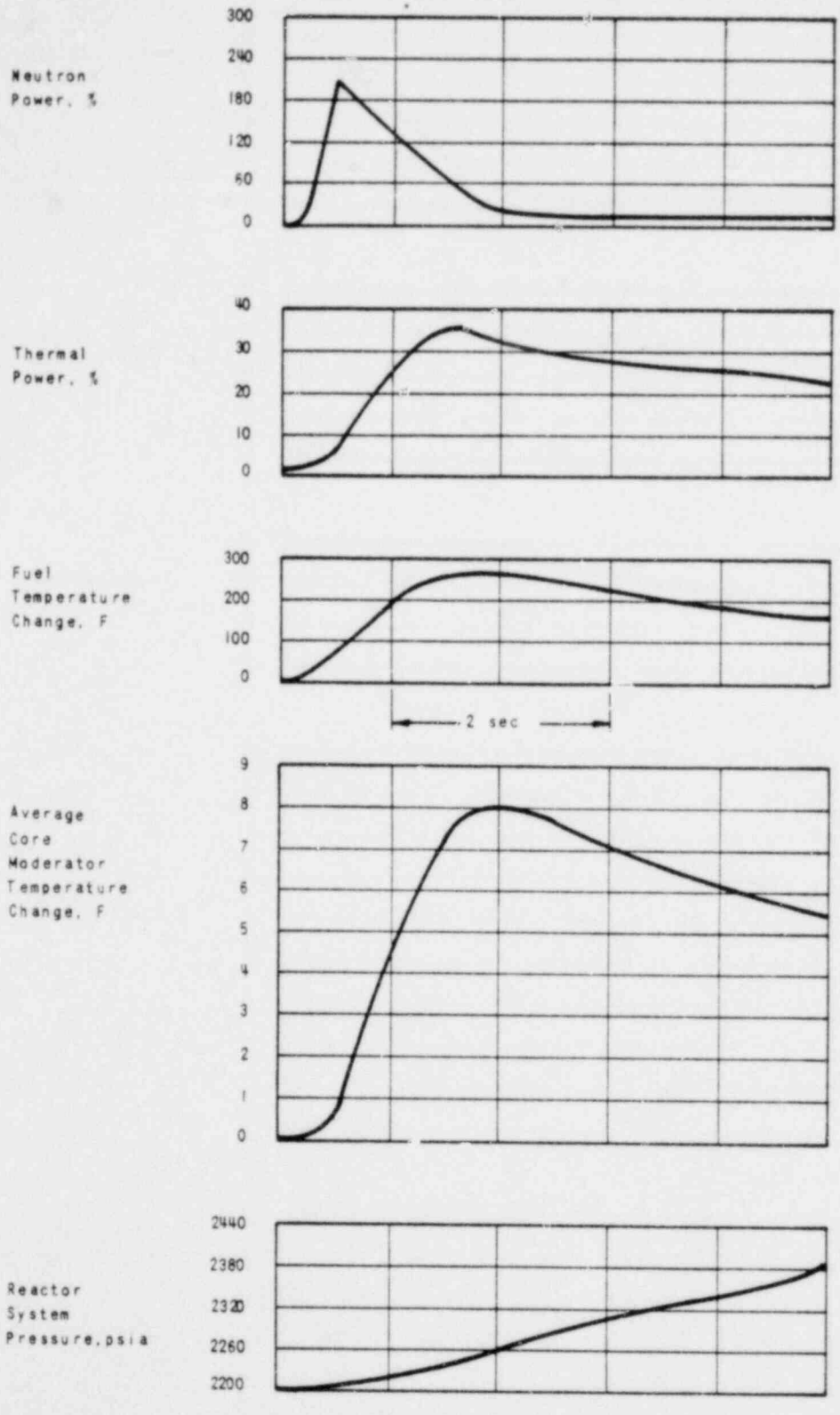

DAVIS-BESSE NUCLEAR POWER STATION
STARTUP ACCIDENT FROM 10^{-9} RATED POWER USING RODS WITH A WOP/H OF 8.0% $\Delta k/k$; FLUX REACTOR TRIP IS ACTUATED
FIGURE 14-2

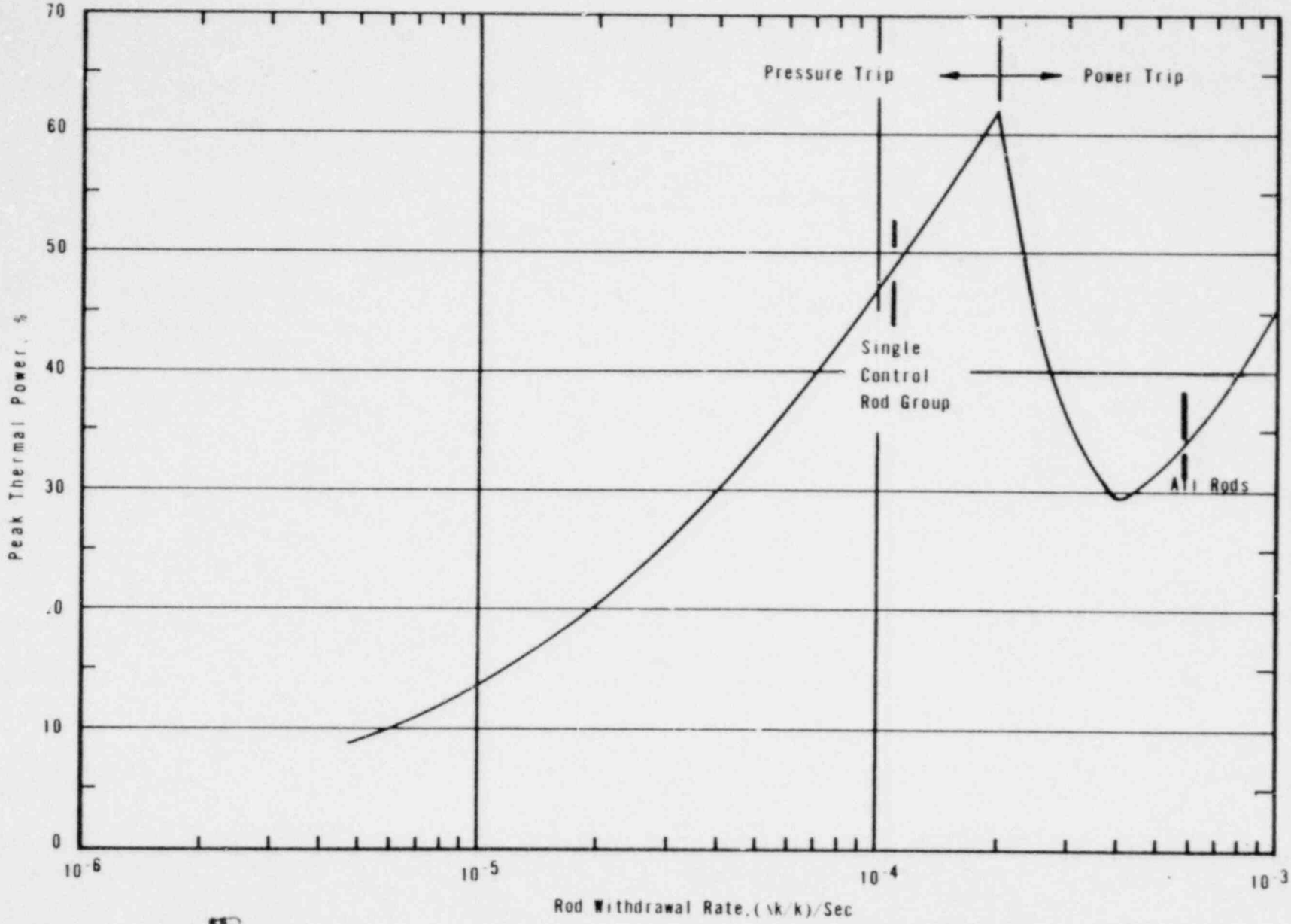

2800

DAVIS-BESSE NUCLEAR POWER STATION
PEAK THERMAL POWER VS ROD WITHDRAWAL RATE FOR A
STARTUP ACCIDENT FROM 10^{-9} RATED POWER
FIGURE 14-3

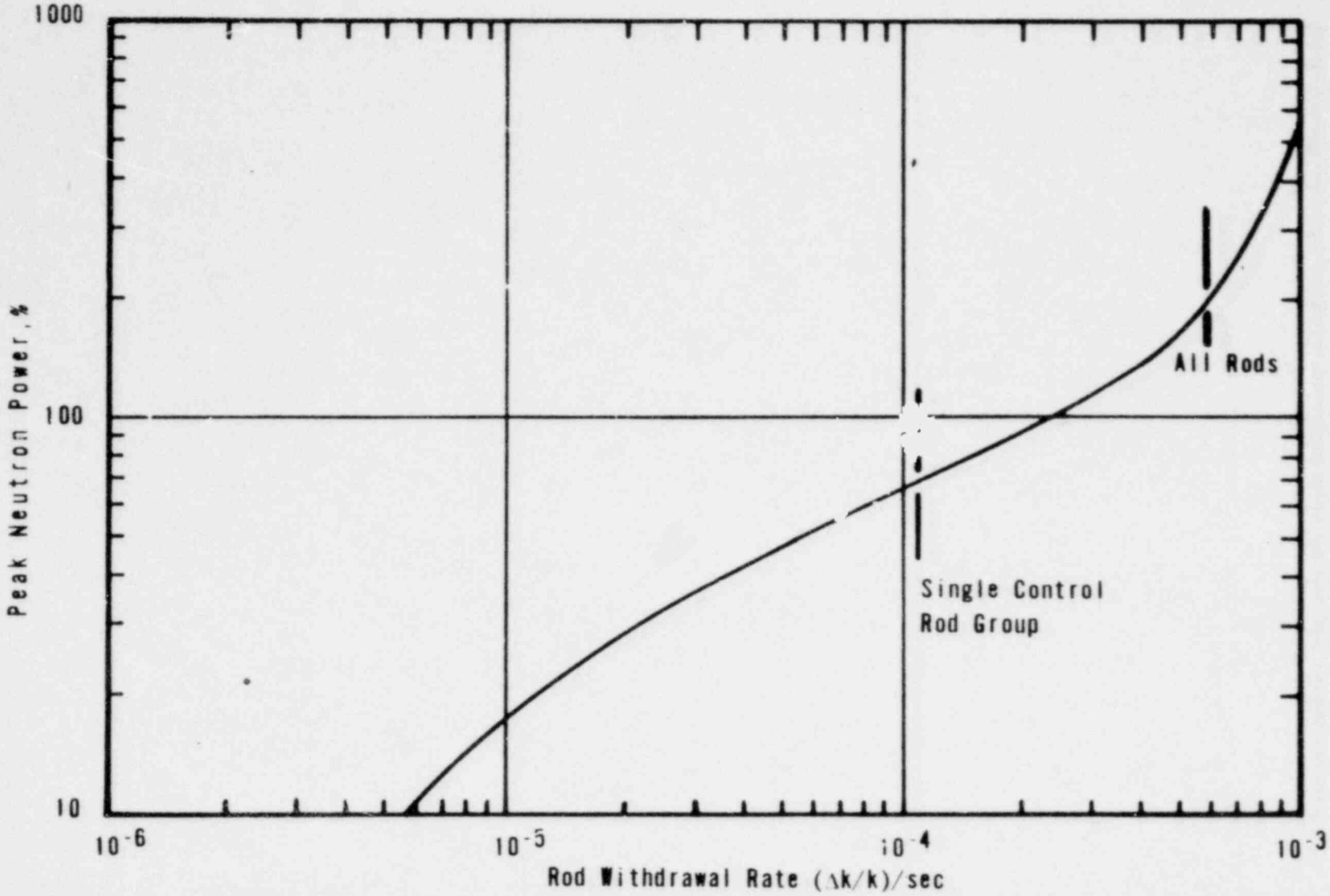

8800

DAVIS-BESSE NUCLEAR POWER STATION
PEAK NEUTRON POWER VERSUS ROD WITHDRAWAL RATE
FOR A STARTUP ACCIDENT FROM 10^{-9} RATED POWER
FIGURE 14-4

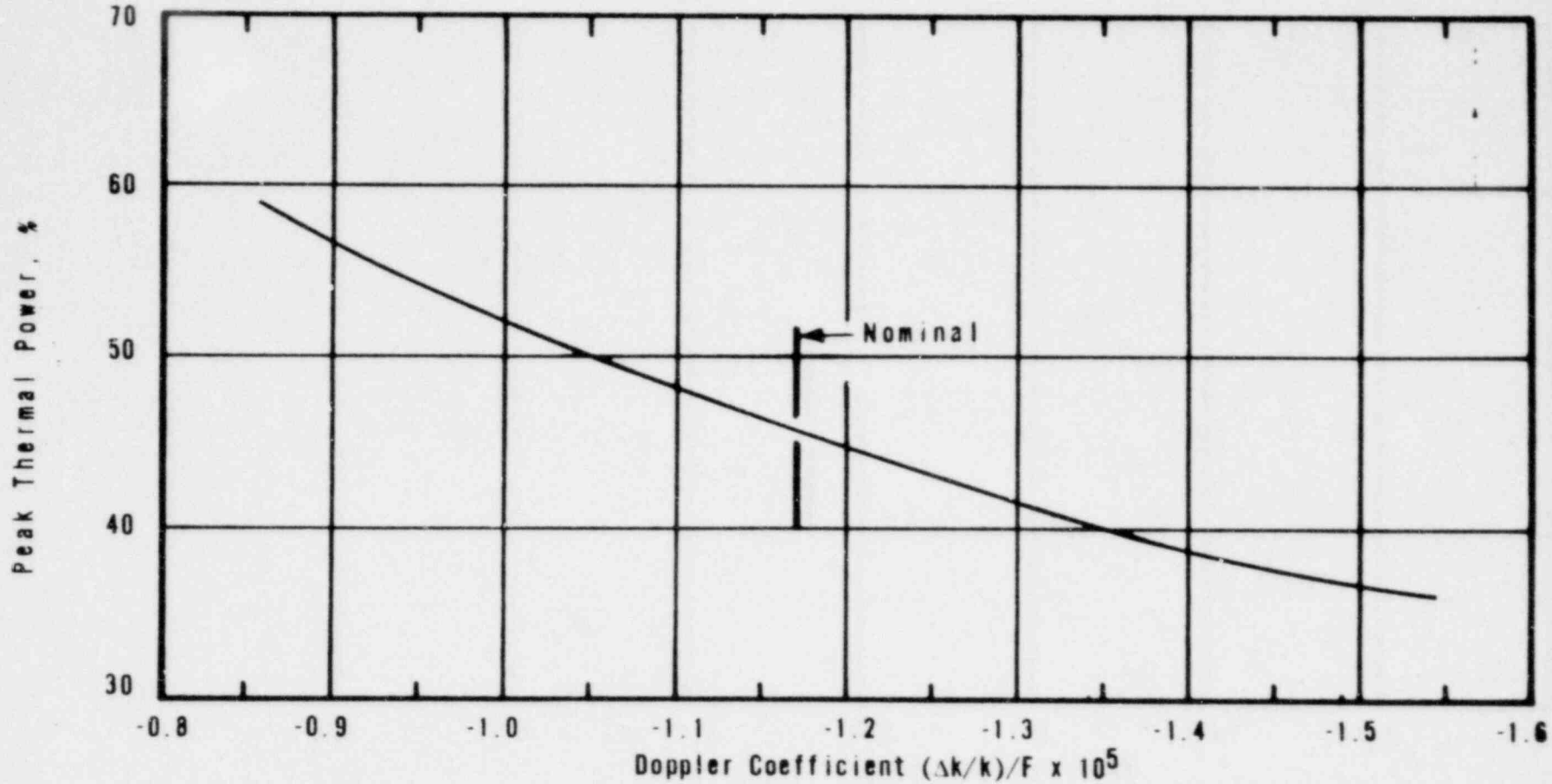

DAVIS-BESSE NUCLEAR POWER STATION
PEAK THERMAL POWER VERUS DOPPLER COEFFICIENT FOR
A STARTUP ACCIDENT USING A 1.5% $\Delta k/k$ ROD GROUP AT
1.89 X 10^{-4} ($\Delta k/k$) SEC FROM 10^{-9} RATED POWER
FIGURE 14-5

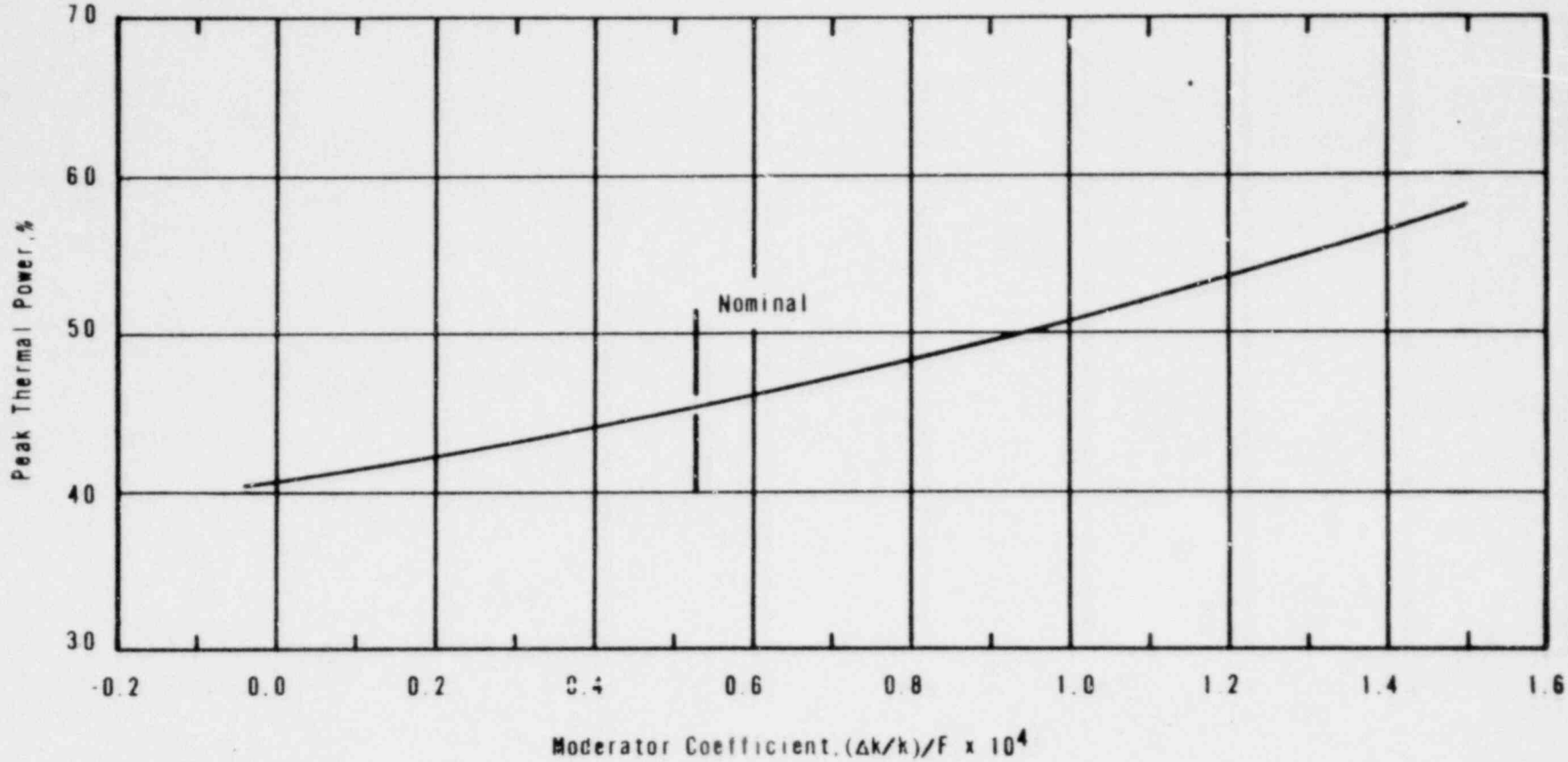

DAVIS-BESSE NUCLEAR POWER STATION
PEAK THERMAL POWER VERSUS MODERATOR COEFFICIENT FOR A STARTUP ACCIDENT USING A 1.5% Δk k ROD GROUP AT 1.09 X 10^{-4} (Δk k) SEC FROM 10^{-9} RATED POWER
FIGURE 14-6

0690

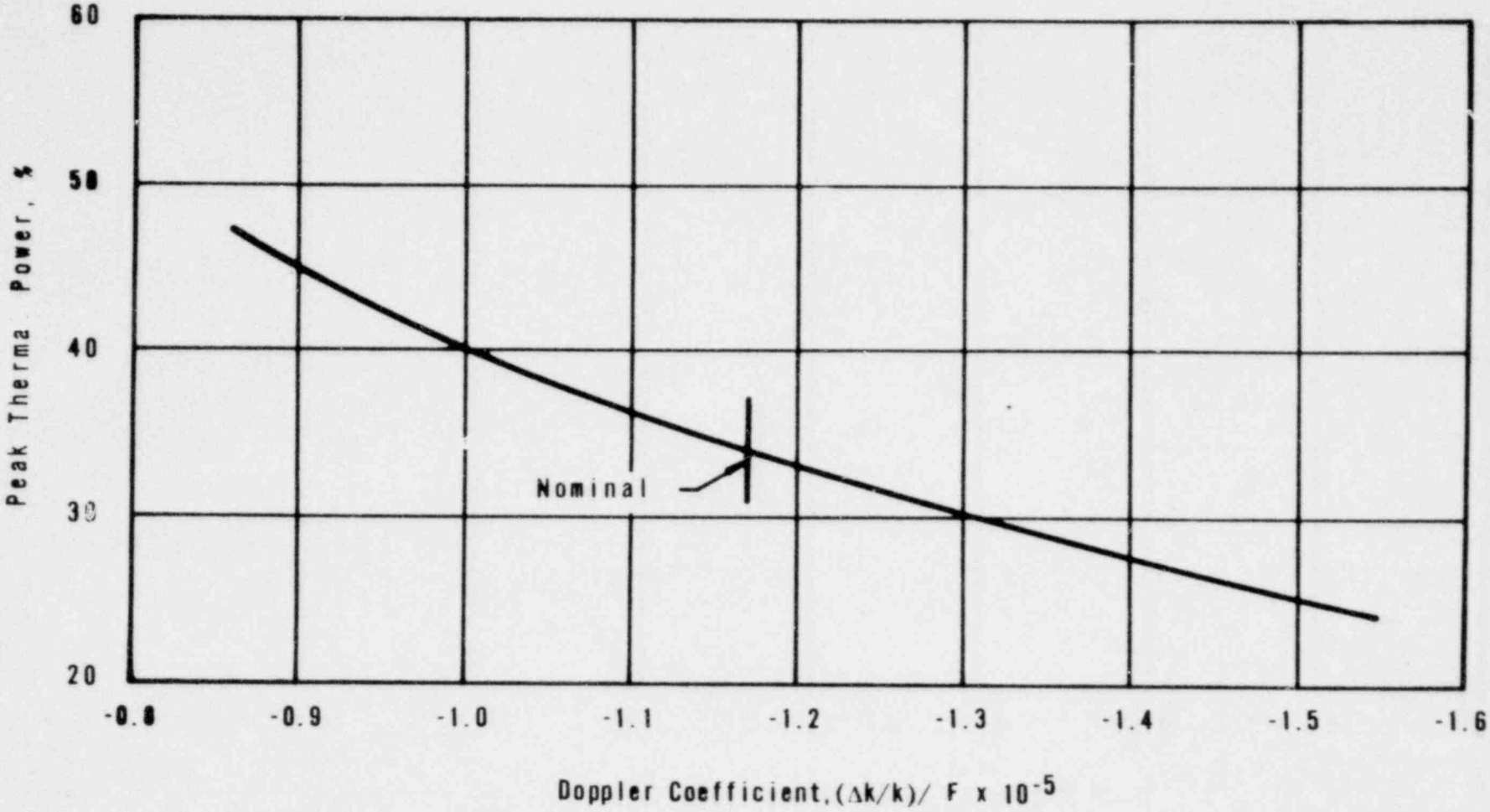

DAVIS-BESSE NUCLEAR POWER STATION
PEAK THERMAL POWER VERSUS DOPPLER COEFFICIENT
FOR A STARTUP ACCIDENT USING ALL RODS AT 5.8
X 10^{-4} (Δk k) SEC FROM 10^{-9} RATED POWER
FIGURE 14-7

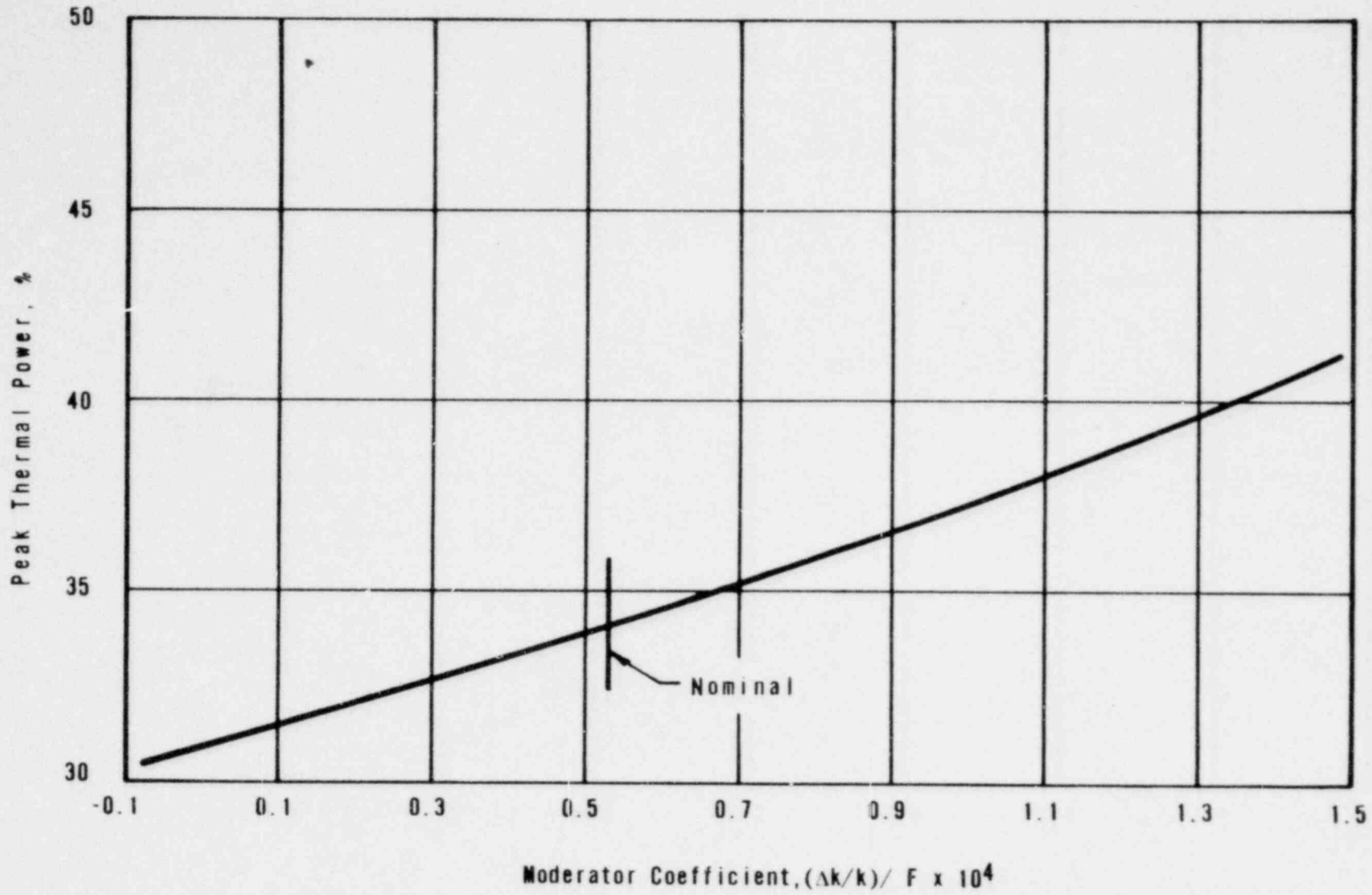

DAVIS-BESSE NUCLEAR POWER STATION
PEAK THERMAL POWER VERSUS MODERATOR COEFFICIENT
FOR A STARTUP ACCIDENT USING ALL RODS AT 5.8 X
10^{-4} (Δk/k) SEC FROM 10^{-9} RATED POWER
FIGURE 14-8

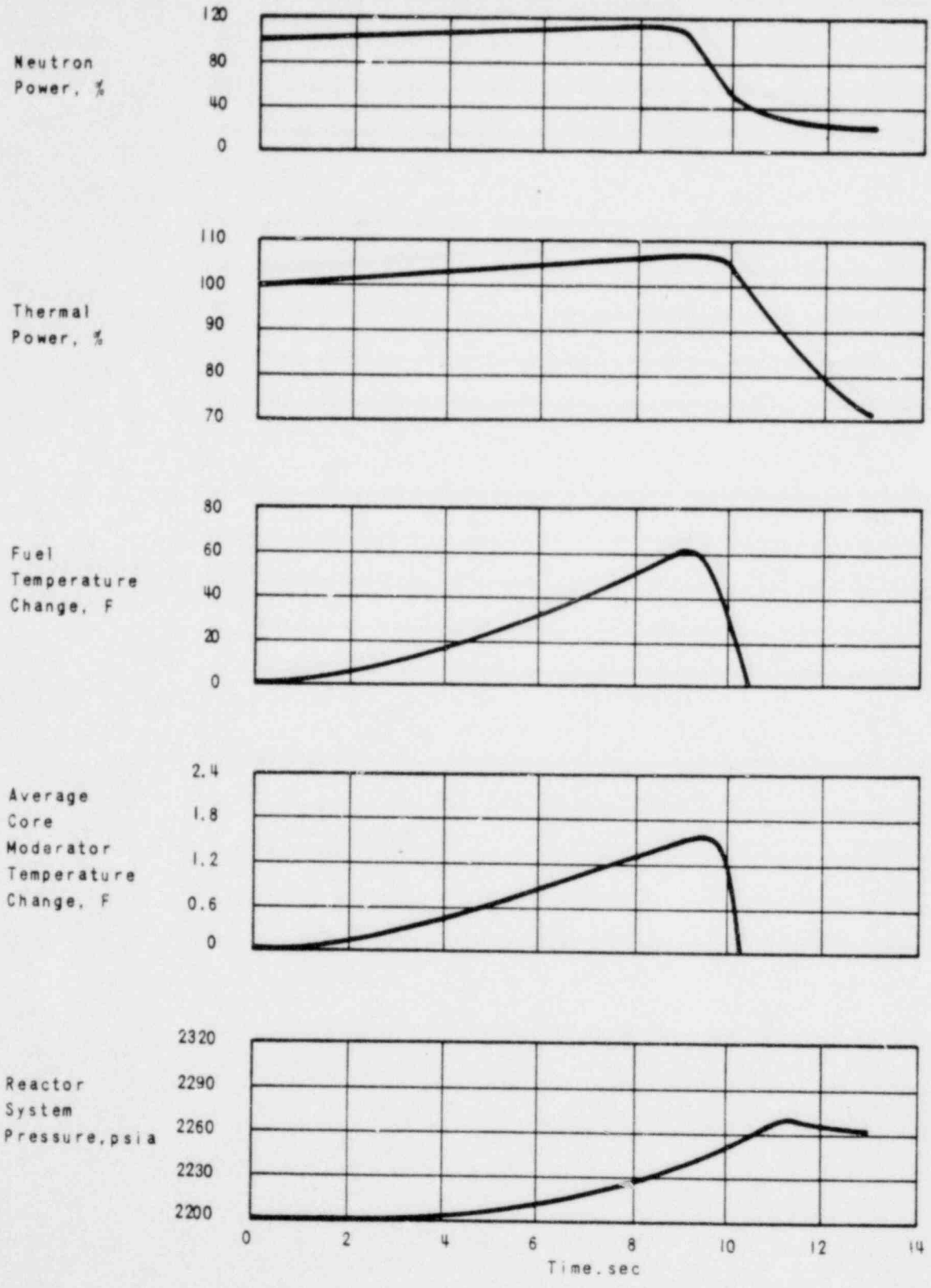

DAVIS-BESSE NUCLEAR POWER STATION
ROD WITHDRAWAL ACCIDENT FROM RATED POWER USING A 1.5% $\Delta k/k$ ROD GROUP AT 1.09×10^{-4} $(\Delta k/k)$/ SEC; HIGH FLUX REACTOR TRIP IS ACTUATED
FIGURE 14-9

0093

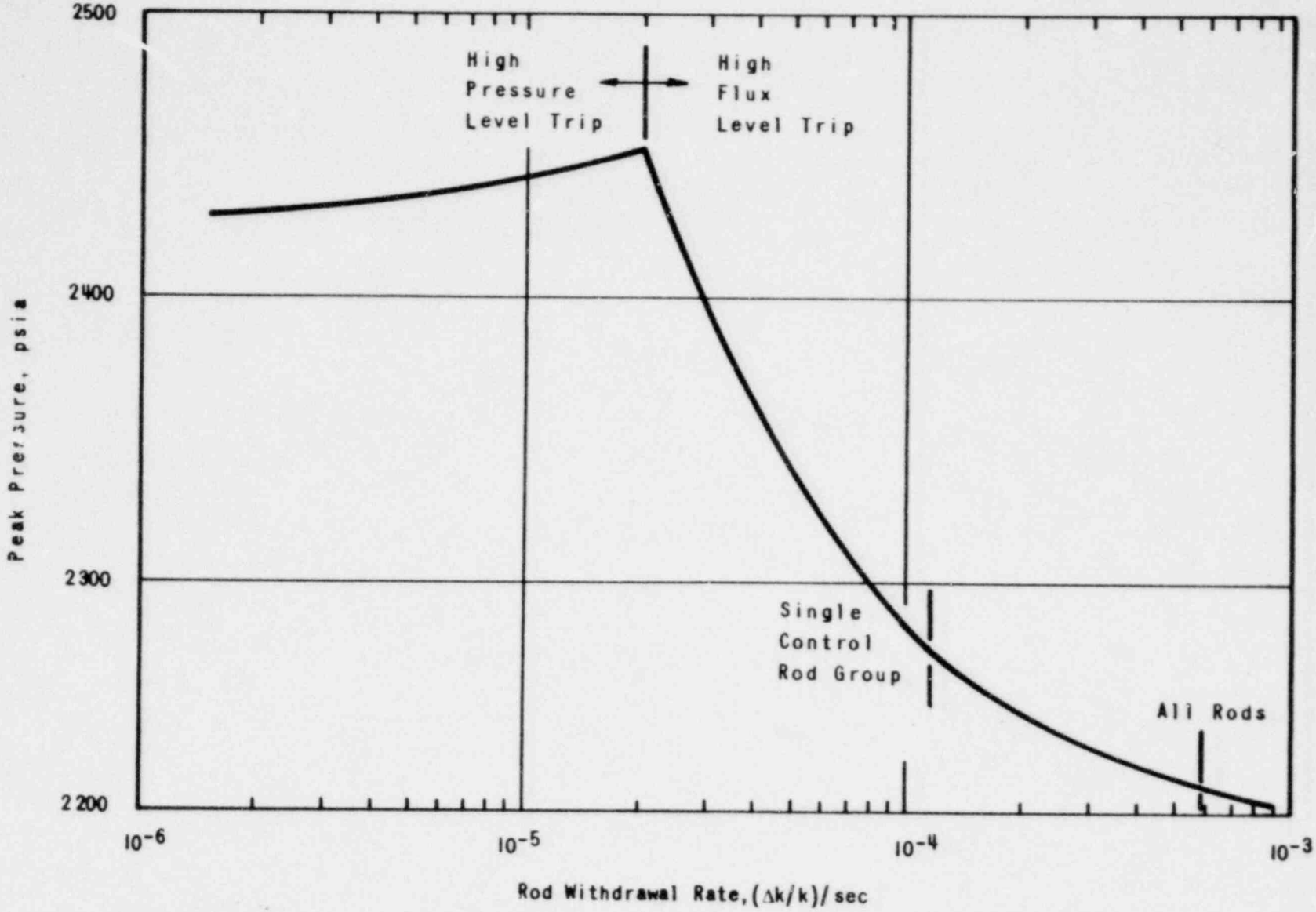

DAVIS-BESSE NUCLEAR POWER STATION
PEAK PRESSURE VERSUS ROD WITHDRAWAL RATE FOR
A ROD WITHDRAWAL ACCIDENT FROM RATED POWER
FIGURE 14-10

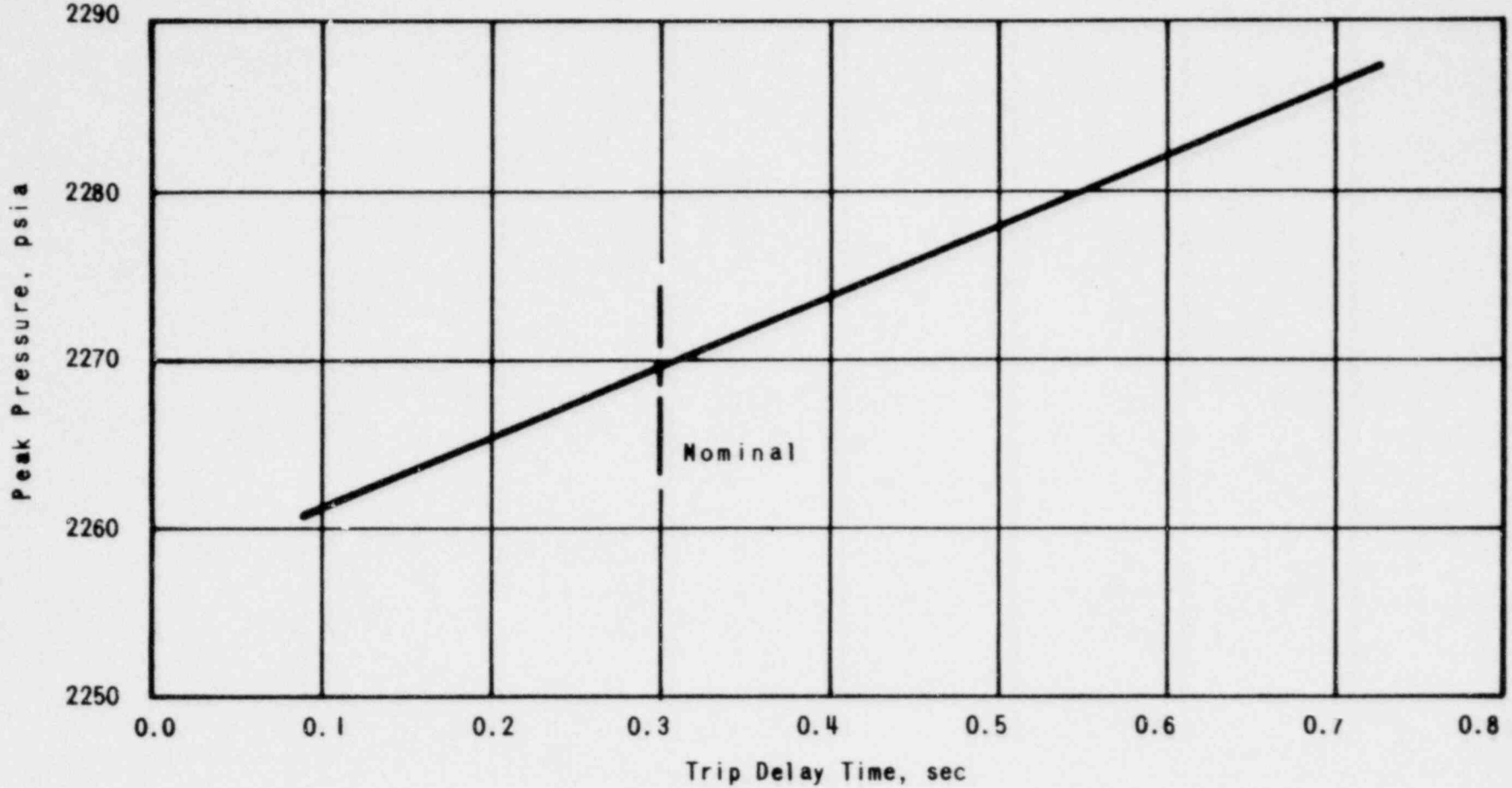

DAVIS-BESSE NUCLEAR POWER STATION
PEAK PRESSURE VERSUS TRIP DELAY TIME FOR A ROD WITHDRAWAL ACCIDENT FROM RATED POWER USING A 1.5% Δk k ROD GROUP
FIGURE 14-11

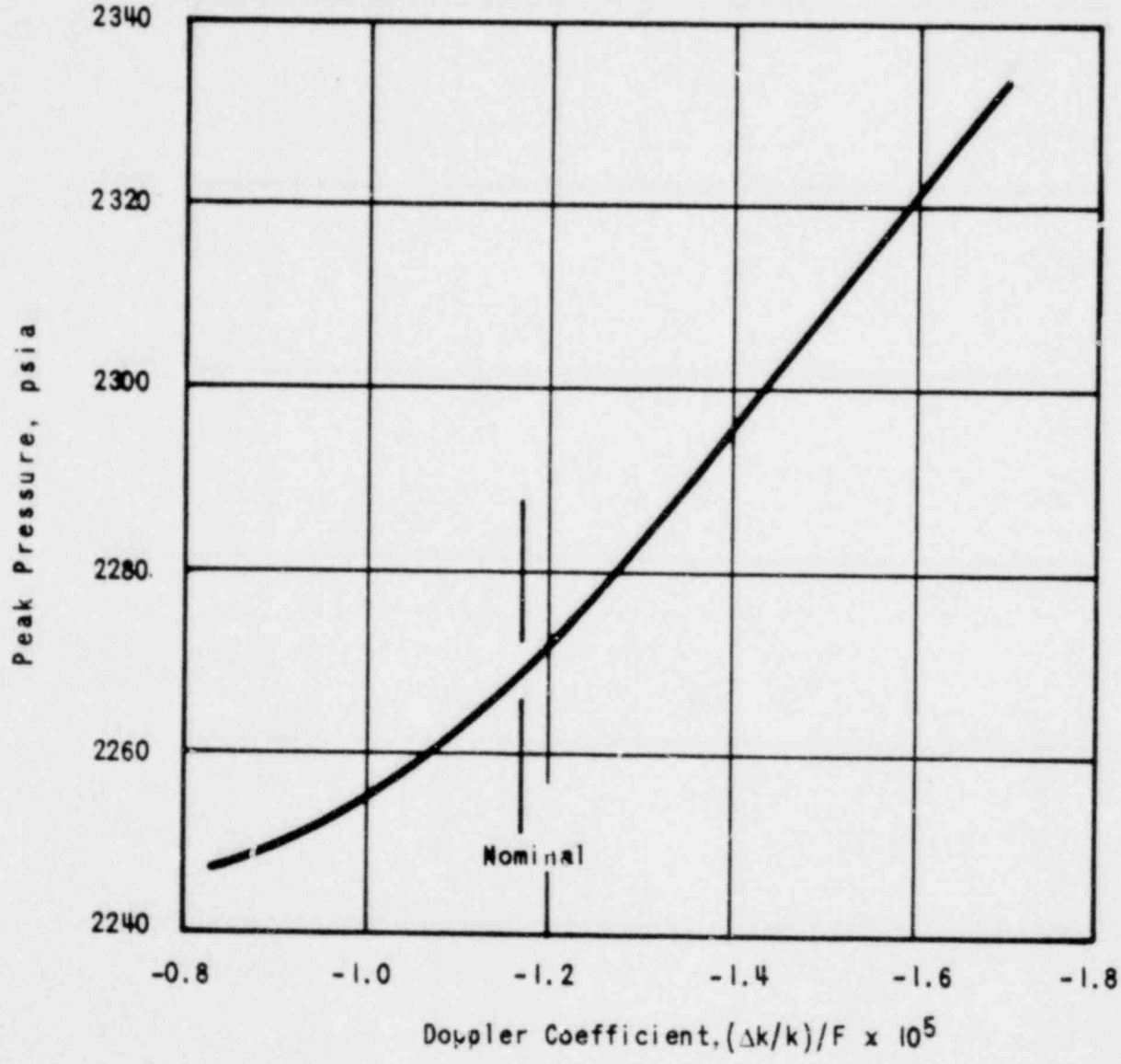

DAVIS-BESSE NUCLEAR POWER STATION
PEAK PRESSURE VERSUS DOPPLER COEFFICIENT FOR
A ROD WITHDRAWAL ACCIDENT FROM RATED POWER
USING A 1.5% Δk k ROD GROUP
FIGURE 14-12

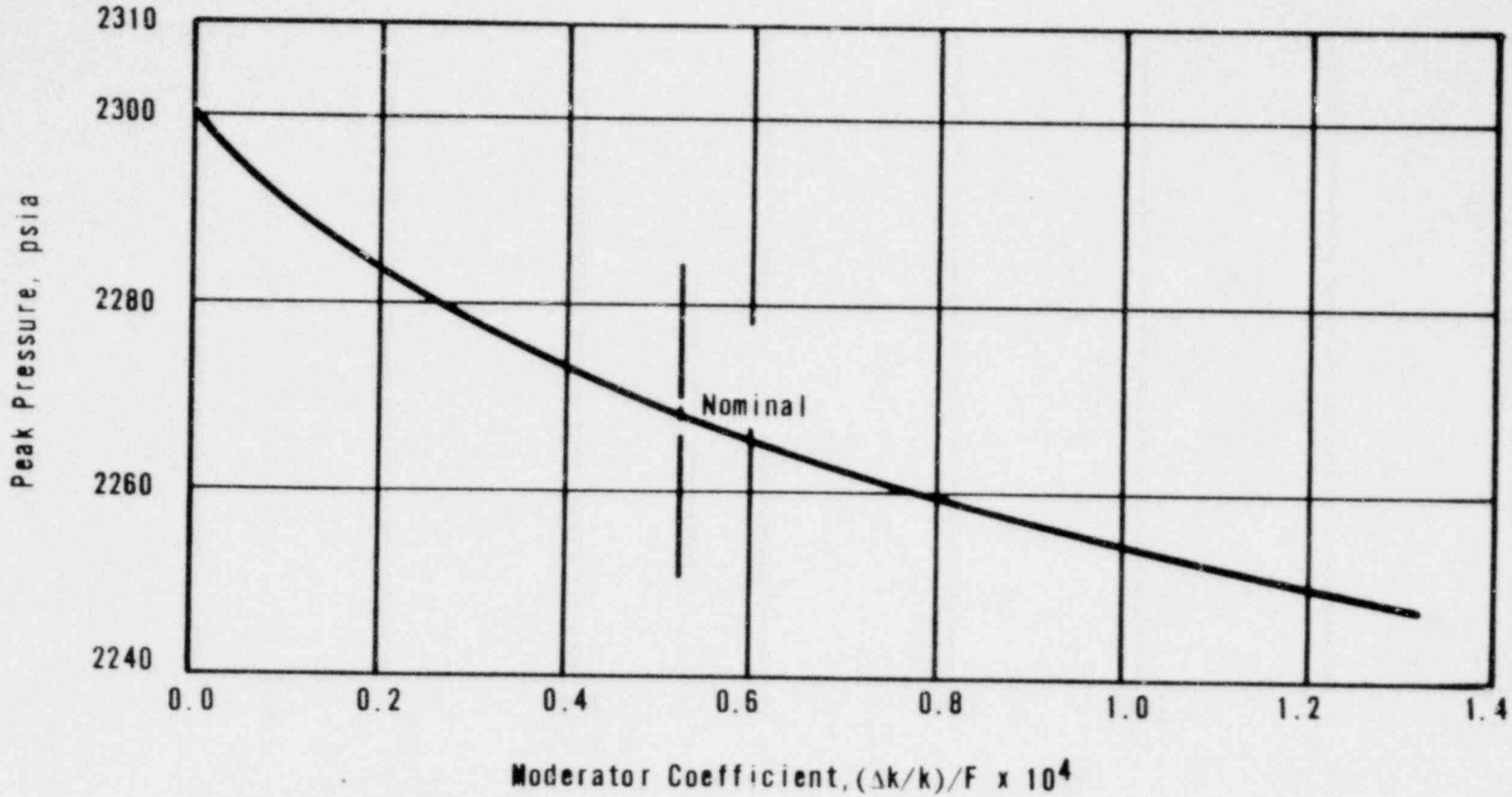

DAVIS-BESSE NUCLEAR POWER STATION
PEAK PRESSURE VERSUS MODERATOR COEFFICIENT FOR A ROD WITHDRAWAL ACCIDENT FROM RATED POWER USING A 1.5% Δk k ROD GROUP
FIGURE 14-13

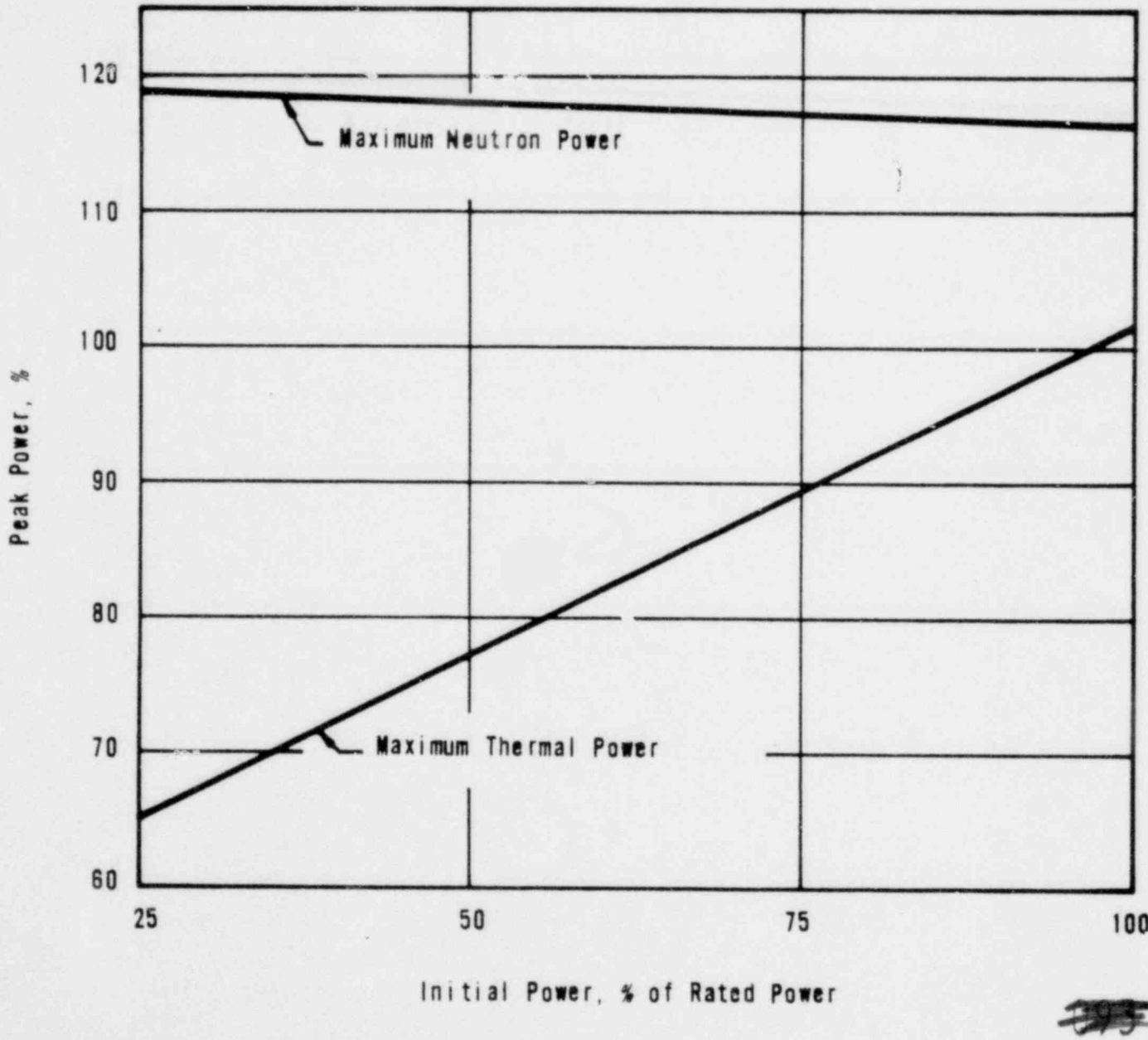

DAVIS-BESSE NUCLEAR POWER STATION
MAXIMUM NEUTRON AND THERMAL POWER FOR AN
ALL-ROD WITHDRAWAL ACCIDENT FROM VARIOUS
INITIAL POWER LEVELS
FIGURE 14-14

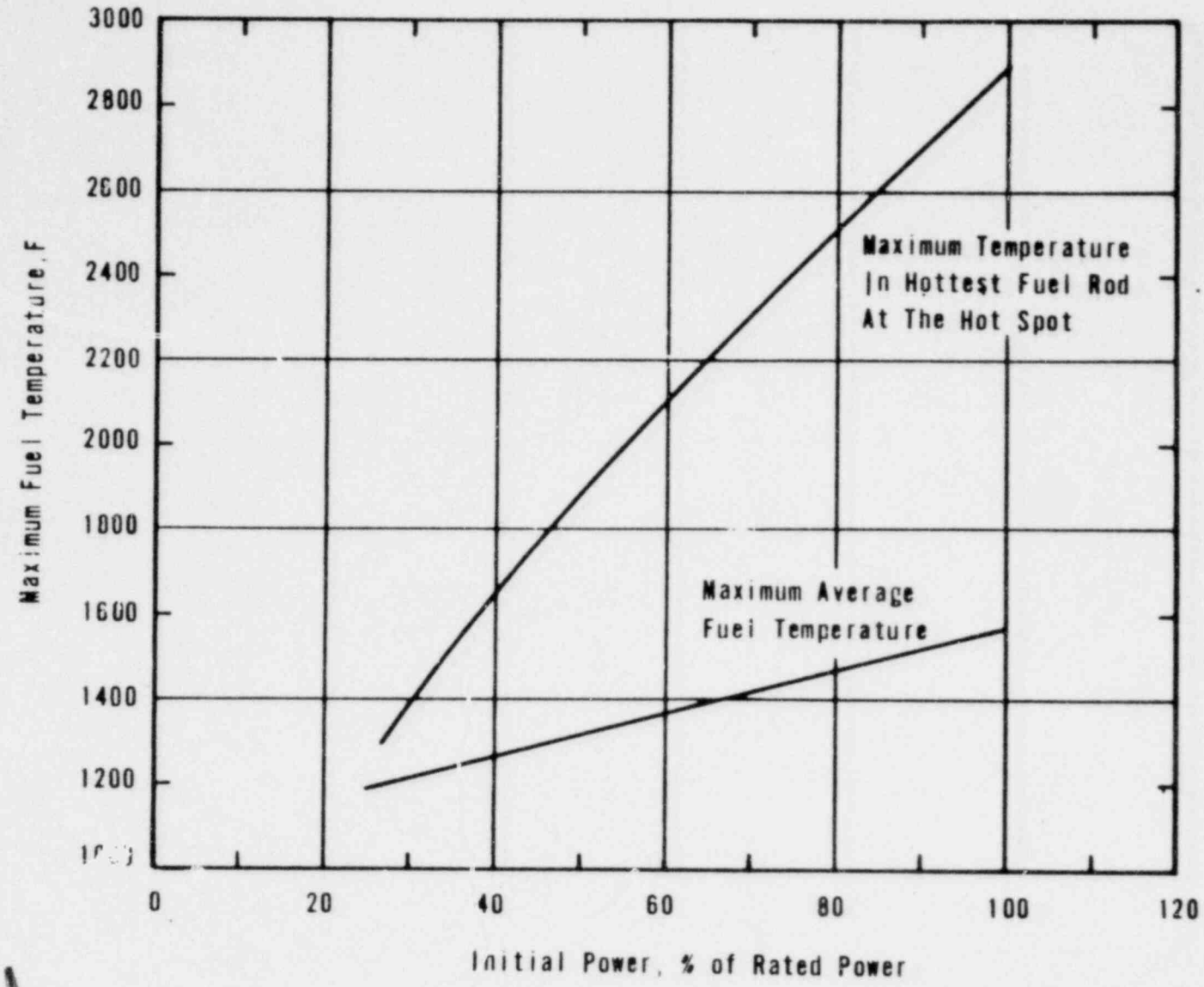

DAVIS-BESSE NUCLEAR POWER STATION
PEAK FUEL TEMPERATURE IN AVERAGE ROD AND HOT SPOT FOR AN ALL-ROD WITHDRAWAL ACCIDENT FROM VARIOUS INITIAL POWER LEVELS
FIGURE 14-15

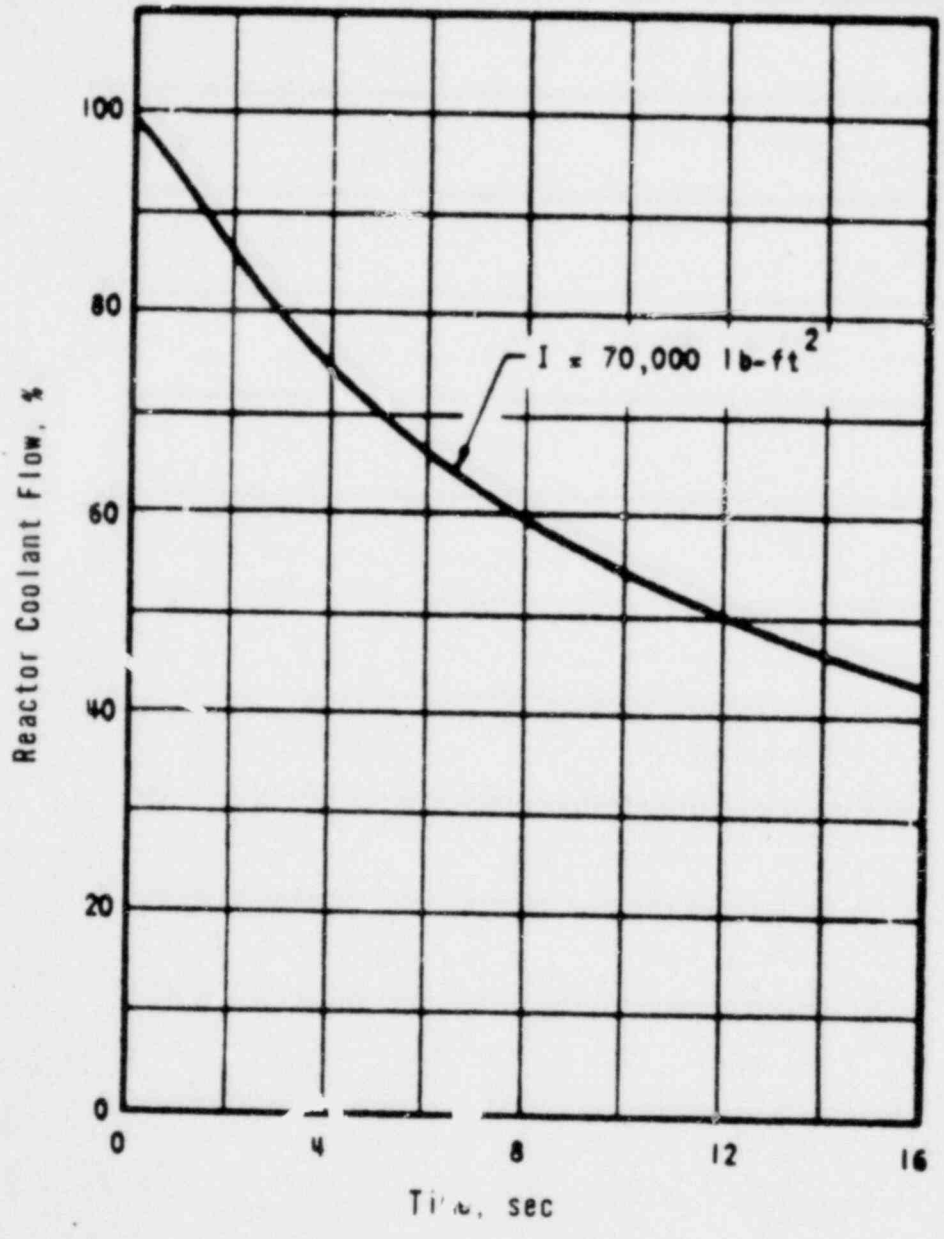

DAVIS-BESSE NUCLEAR POWER STATION
PER CENT REACTOR COOLANT FLOW AS A
FUNCTION OF TIME AFTER LOSS OF PUMP
POWER
FIGURE 14-16

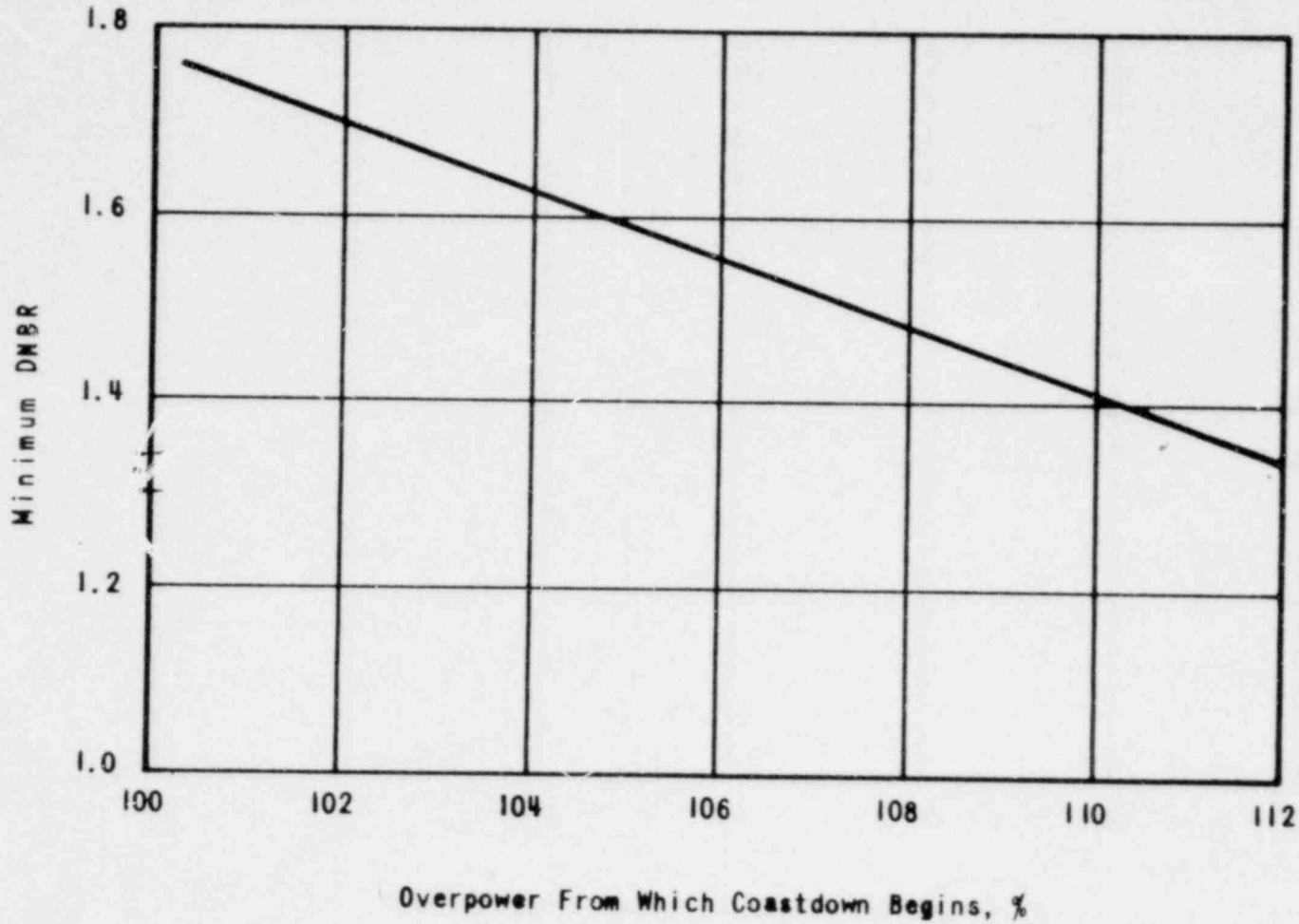

DAVIS-BESSE NUCLEAR POWER STATION
MINIMUM DNBR WHICH OCCURS DURING COASTDOWN
FROM VARIOUS INITIAL POWER LEVELS
FIGURE 14-17

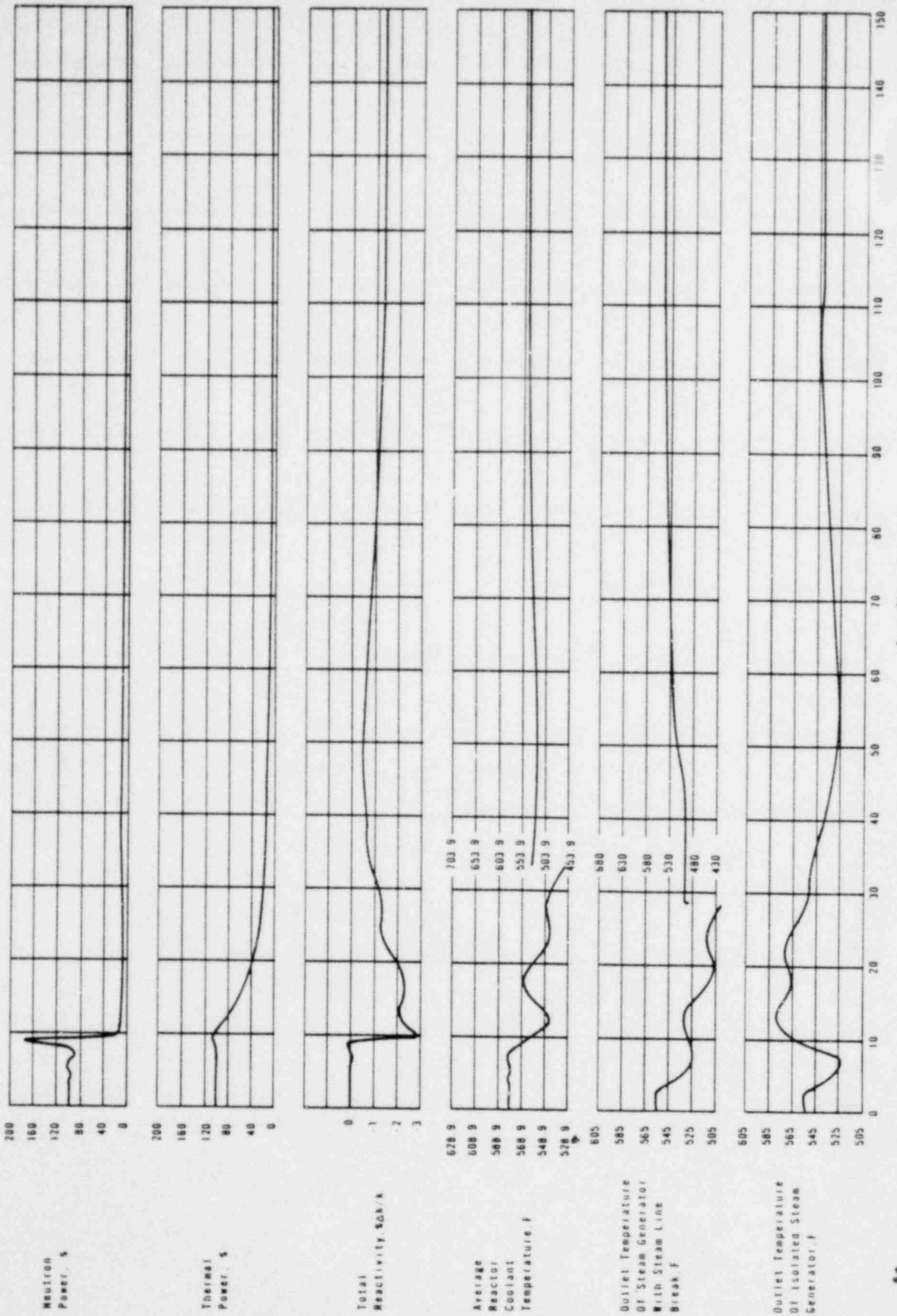

DAVIS-BESSE NUCLEAR POWER STATION
DOUBLE-ENDED RUPTURE OF 34-IN STEAM LINE BETWEEN STEAM GENERATOR AND STEAM STOP VALVE (WITH FEEDWATER ISOLATION)
FIGURE 14-18

0102

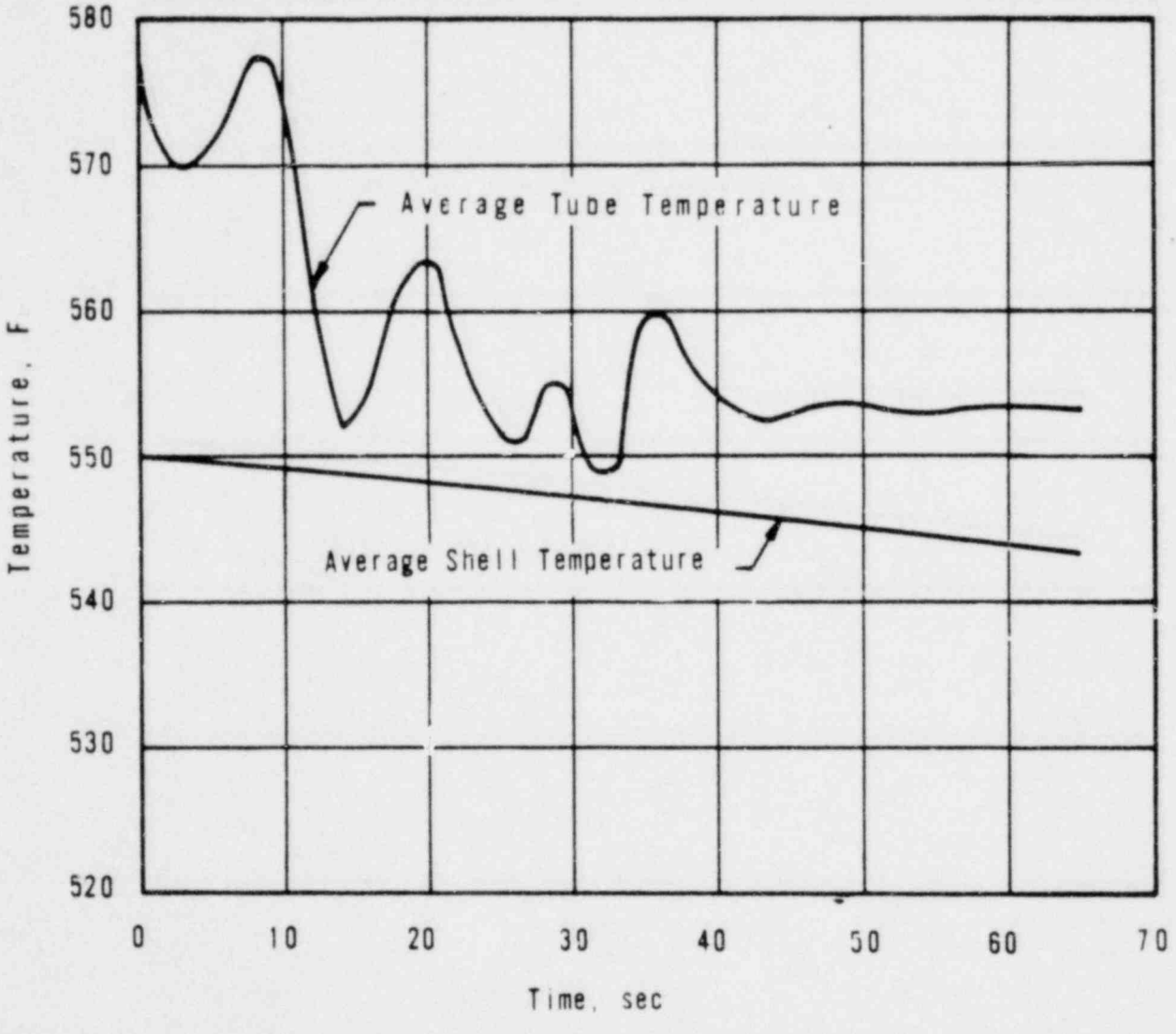

DAVIS-BESSE NUCLEAR POWER STATION
AVERAGE STEAM GENERATOR SHELL AND TUBE
TEMPERATURE VERSUS TIME AFTER ASSUMED
STEAM LINE BREAK
FIGURE 14-19

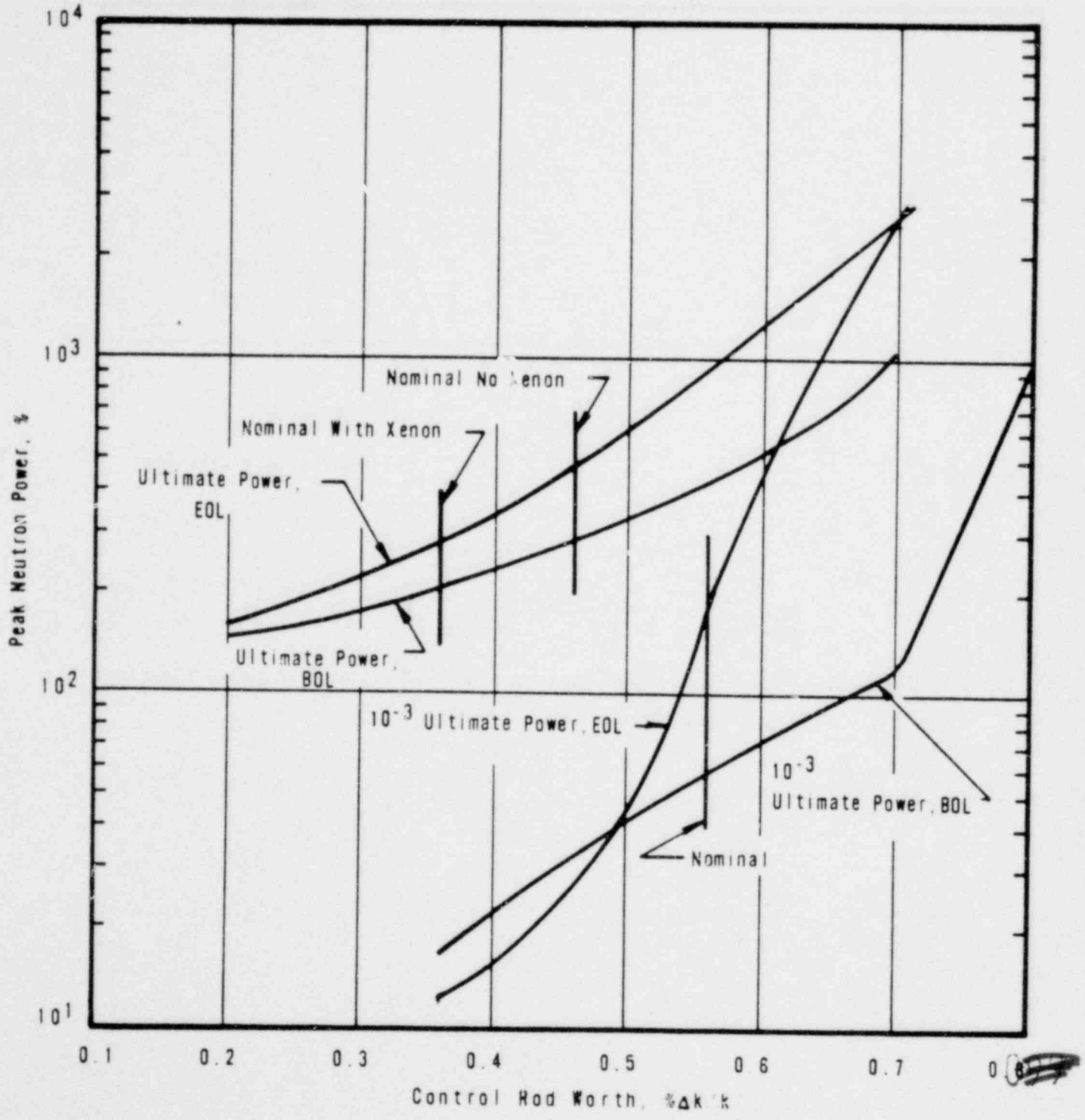

DAVIS-BESSE NUCLEAR POWER STATION
PEAK NEUTRON POWER VARIATION
WITH EJECTED CONTROL ROD WORTH
FIGURE 14-20

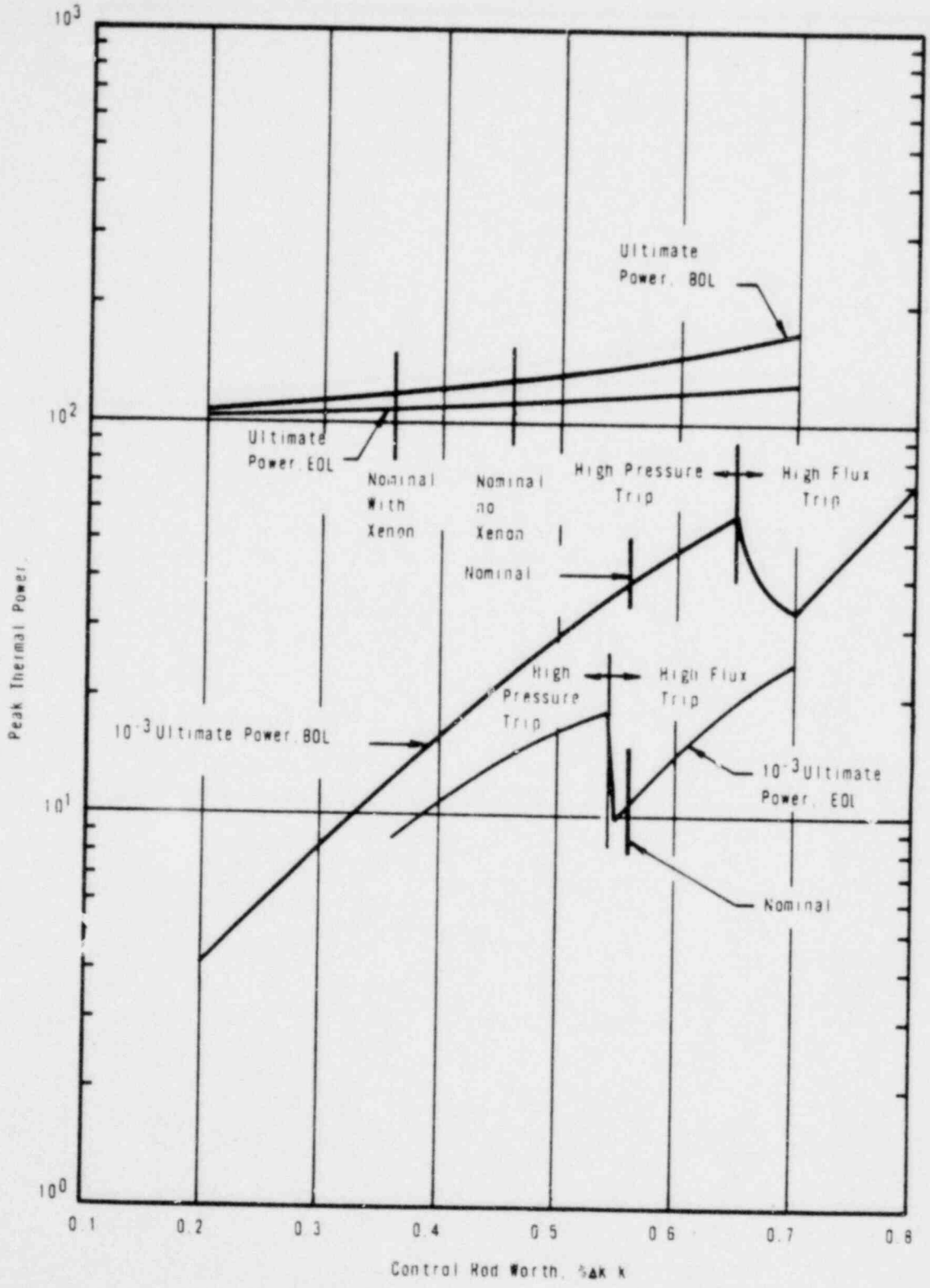

DAVIS-BESSE NUCLEAR POWER STATION
PEAK THERMAL POWER AS A FUNCTION
OF EJECTED CONTROL ROD WORTH
FIGURE 14-21

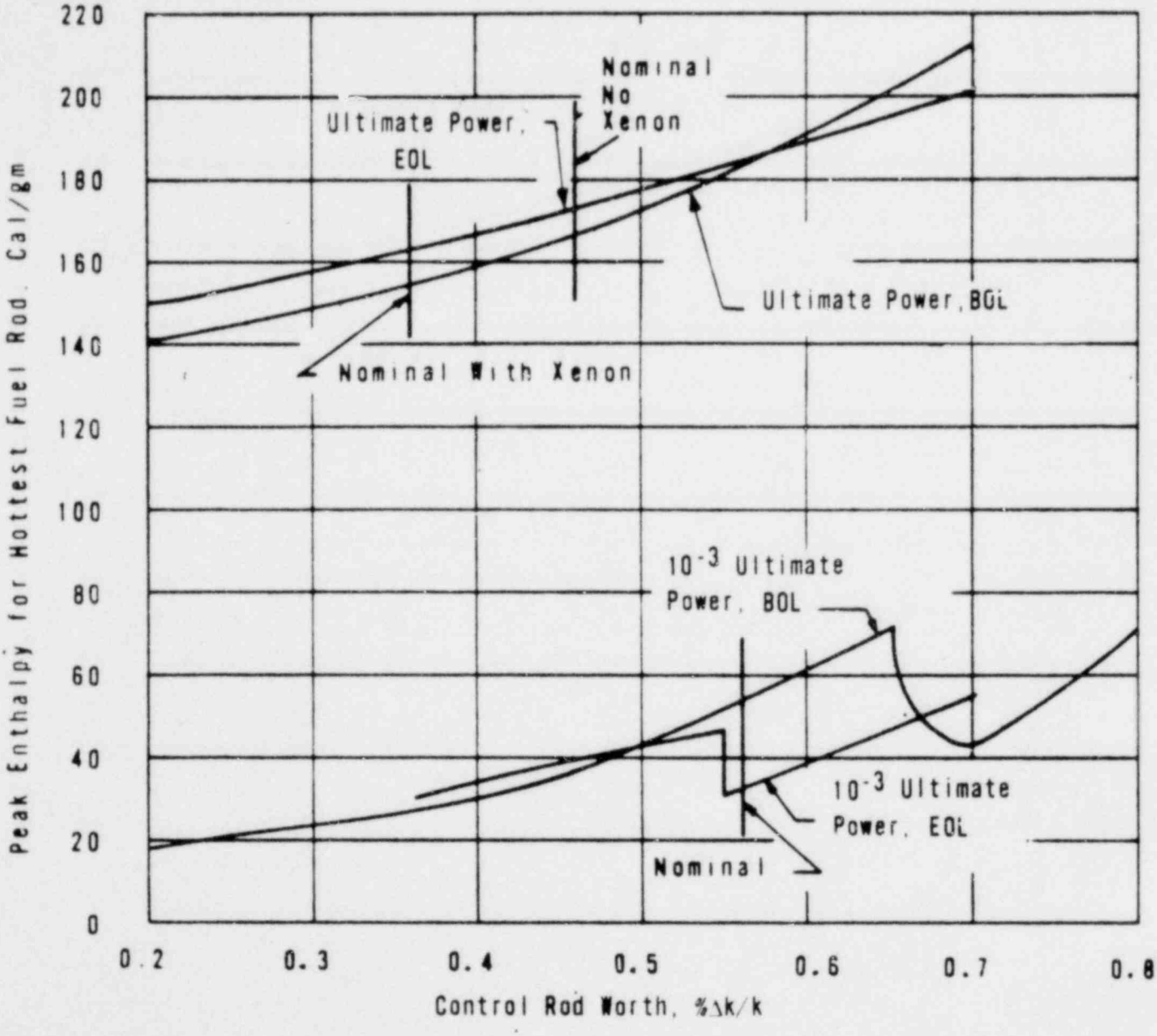

DAVIS-BESSE NUCLEAR POWER STATION
PEAK ENTHALPY OF HOTTEST FUEL ROD
VERSUS EJECTED CONTROL ROD WORTH
FIGURE 14-22

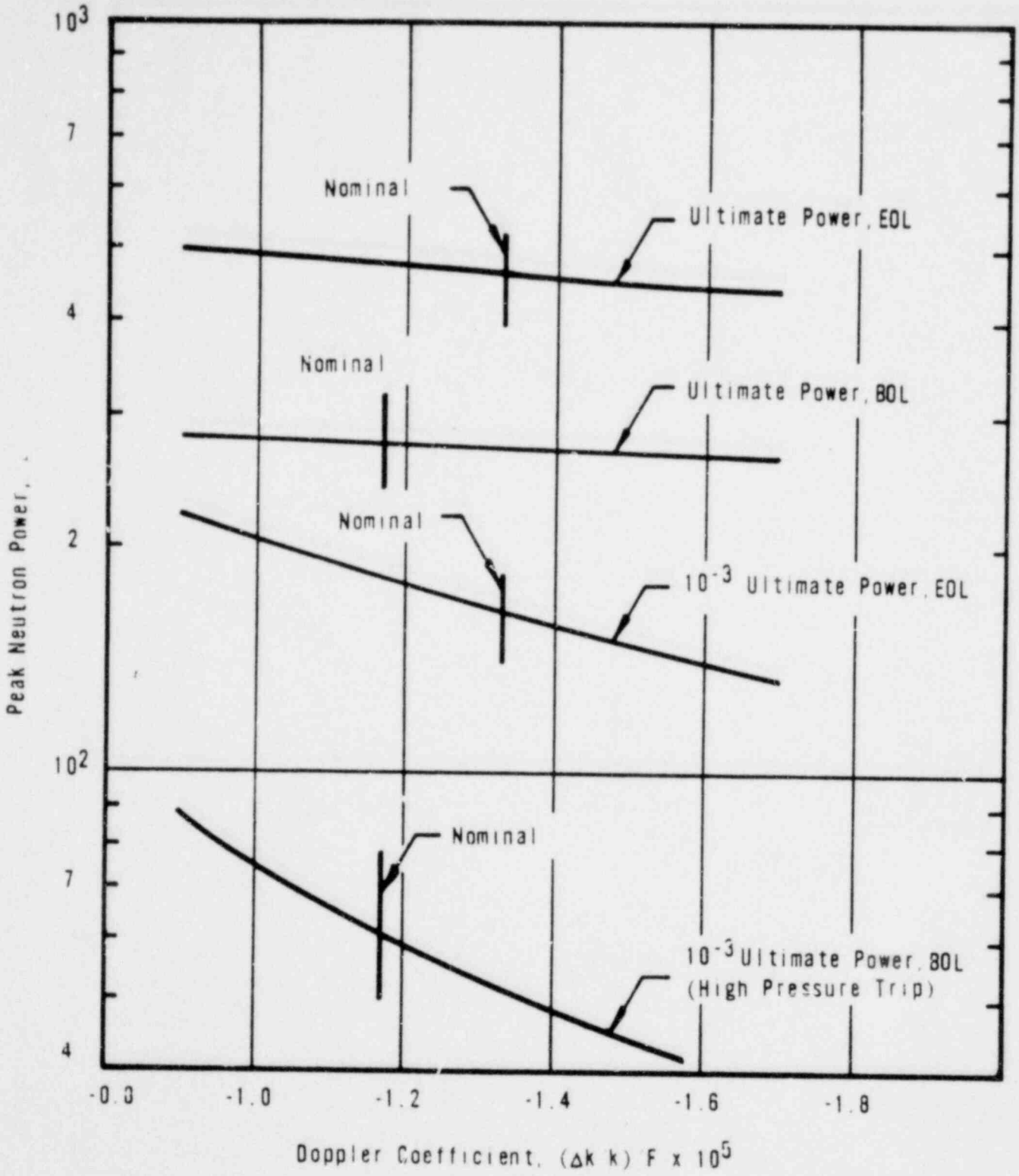

DAVIS-BESS NUCLEAR POWER STATION
EFFECT ON PEAK NEUTRON POWER OF VARYING THE DOPPLER COEFFICIENT
FOR AN EJECTED ROD WORTH OF 0.56% $\Delta k\ k$ AT 10^{-3} ULTIMATE POWER AND
0.46% $\Delta k\ k$ ULTIMATE POWER
FIGURE 14-23

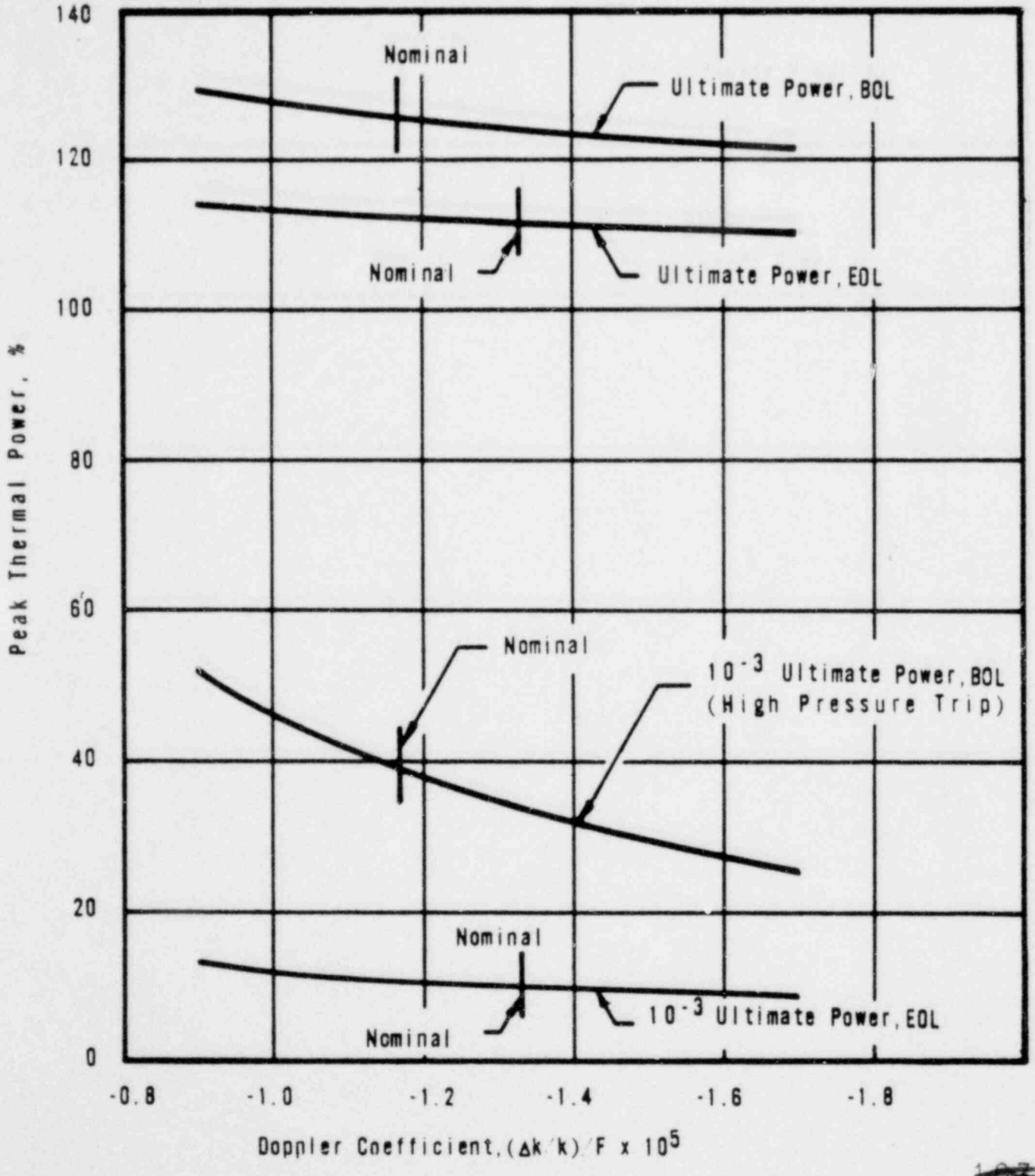

DAVIS-BESSE NUCLEAR POWER STATION
EFFECT ON PEAK THERMAL POWER OF VARYING THE DOPPLER COEFFICIENT
FOR AN EJECTED ROD WORTH OF 0.56% Δk k AT 10^{-3} ULTIMATE POWER AND
0.46% Δk k AT ULTIMATE POWER
FIGURE 14-24

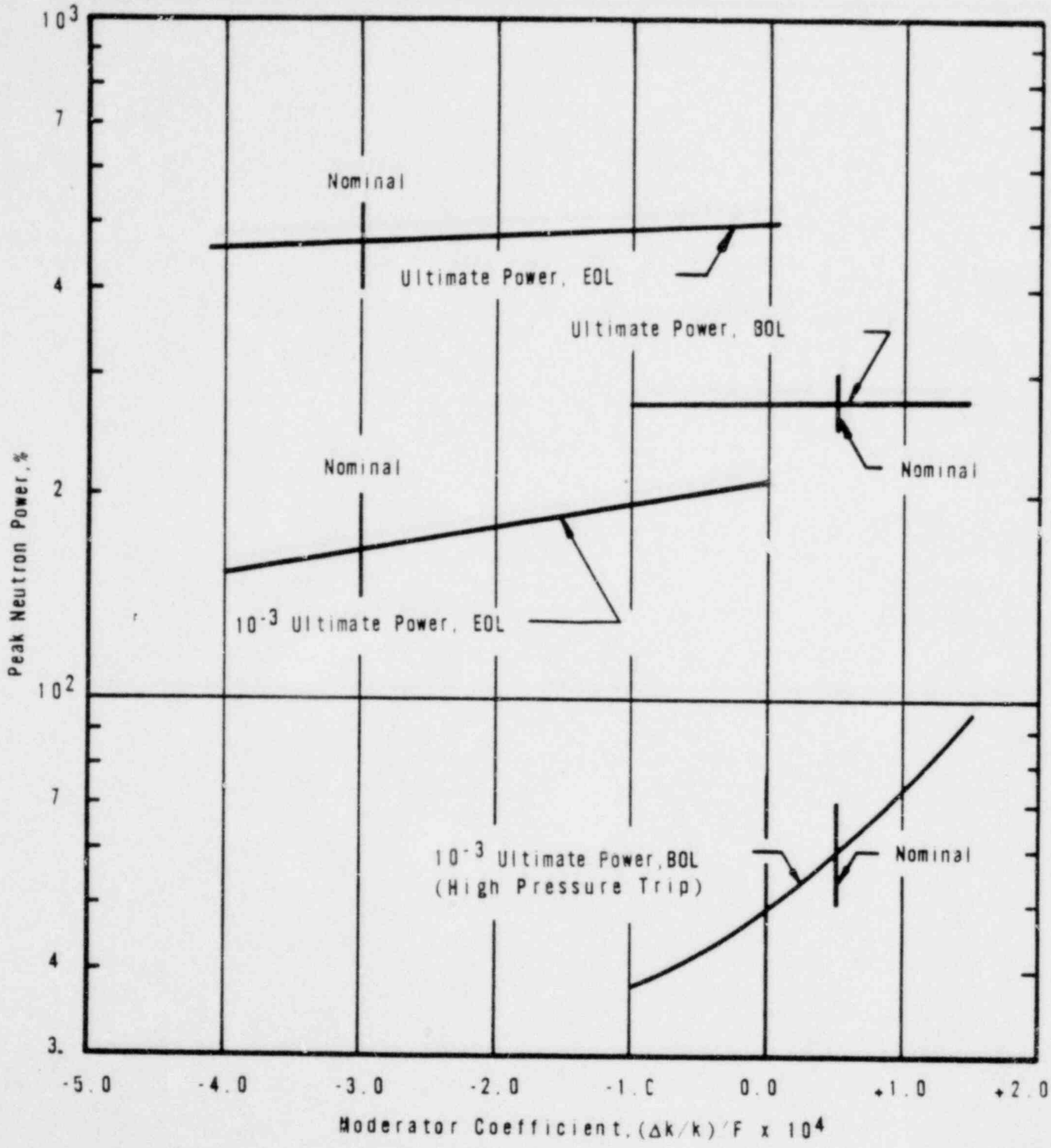

DAVIS-BESSE NUCLEAR POWER STATION
EFFECT ON PEAK NEUTRON POWER OF VARYING THE MODERATOR COEFFICIENT FOR AN EJECTED ROD WORTH OF 0.56% Δk k AT 10^{-3} ULTIMATE POWER AND 0.46% Δk/k AT ULTIMATE POWER
FIGURE 14-25

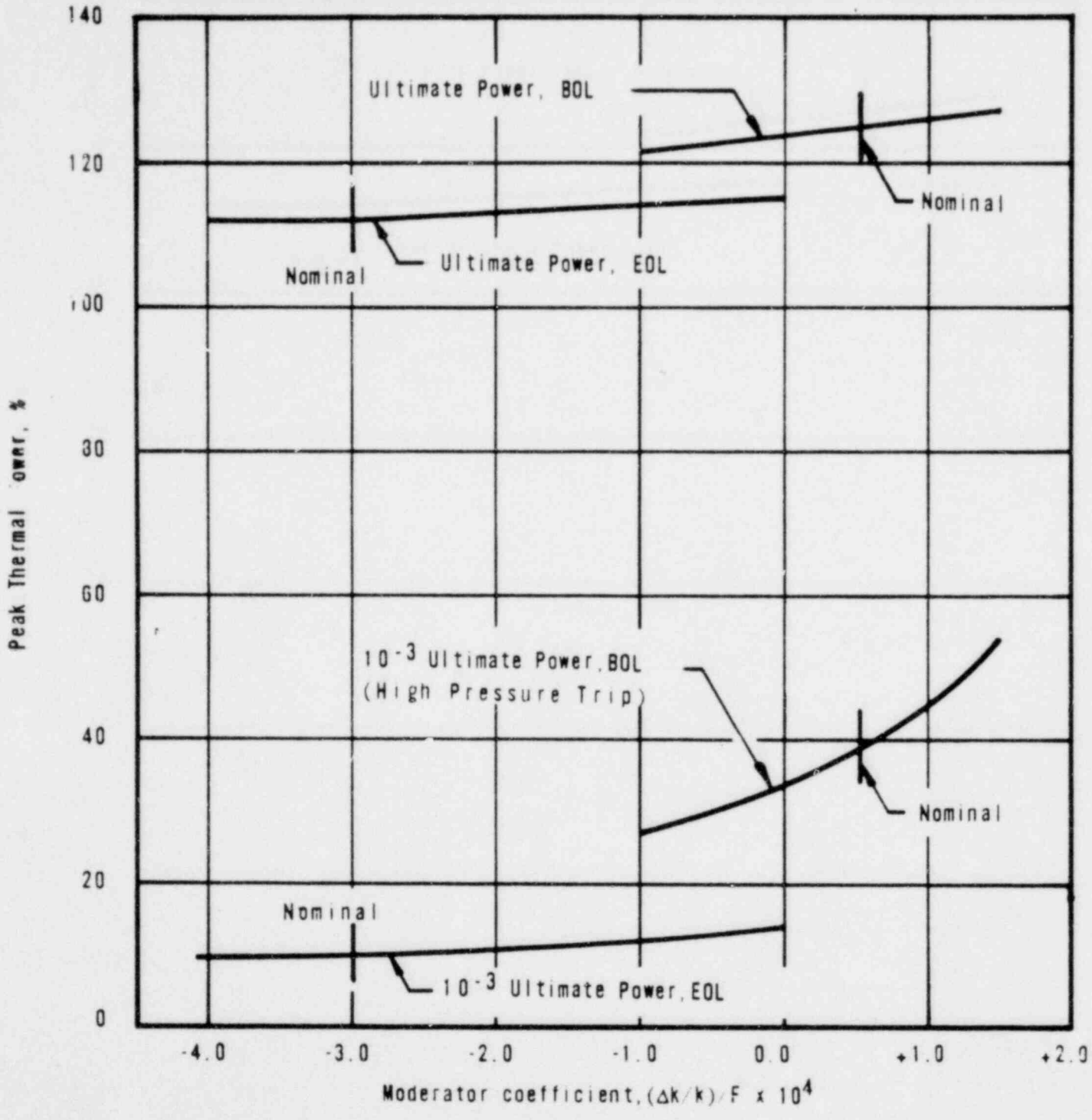

DAVIS-BESSE NUCLEAR POWER STATION
EFFECT ON PEAK THERMAL POWER OF VARYING THE MODERATOR COEFFICIENT FOR AN EJECTED ROD WORTH OF 0.56% Δk k AT 10^{-3} ULTIMATE POWER AND 0.46% Δk k AT ULTIMATE POWER
FIGURE 14-26

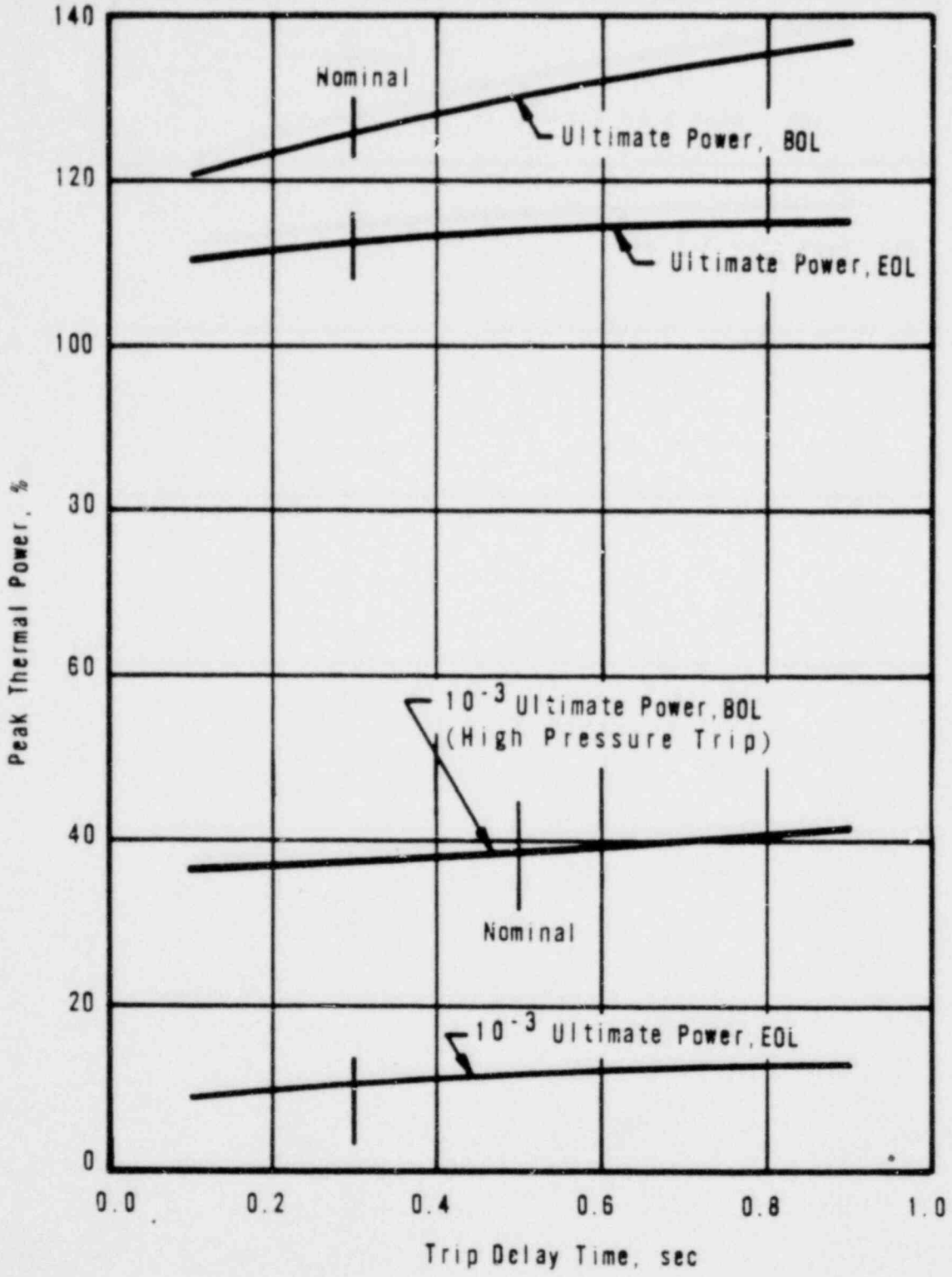

DAVIS-BESSE NUCLEAR POWER STATION
EFFECT ON PEAK THERMAL POWER OF VARYING THE TRIP DELAY TIME FOR AN EJECTED ROD WORTH OF 0.56% Δk k AT 10^{-3} ULTIMATE POWER AND 0.46% Δk k AT ULTIMATE POWER
FIGURE 14-27

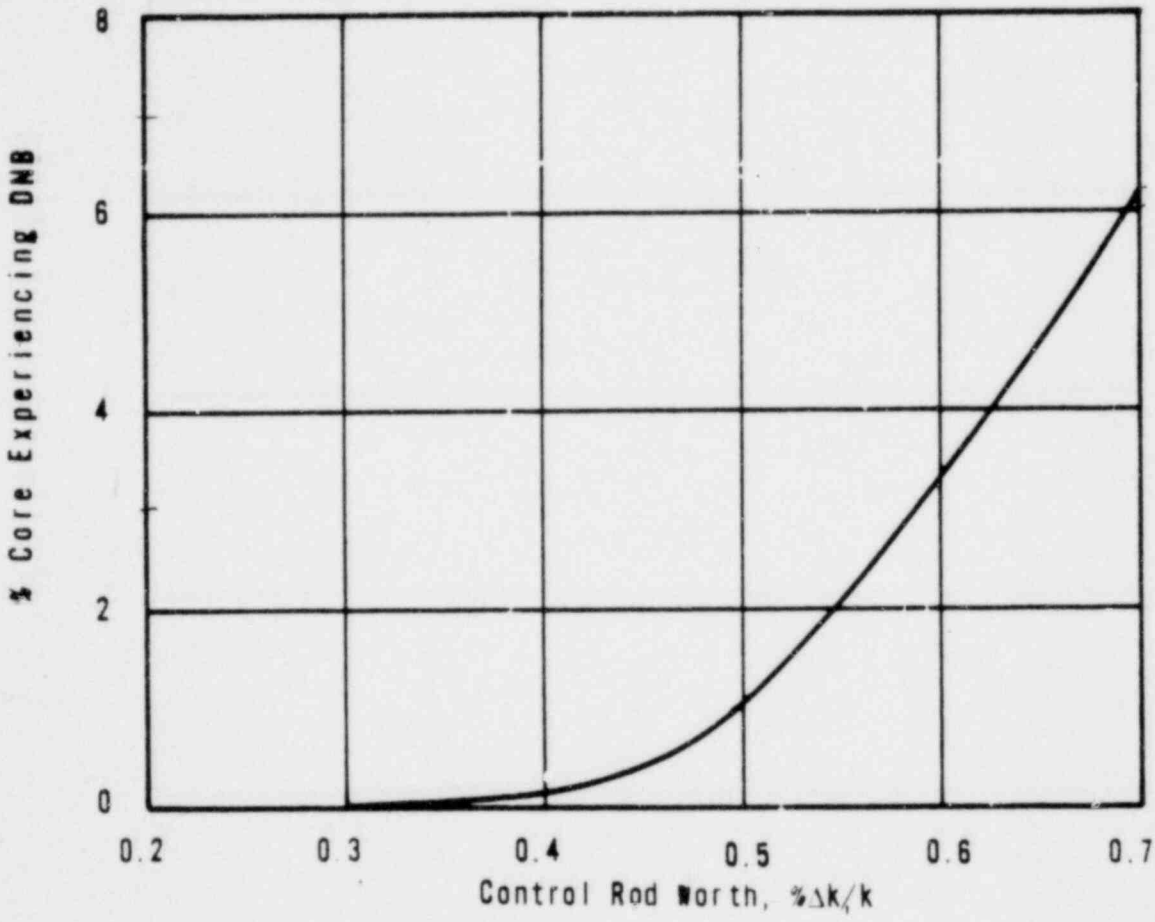

DAVIS-BESSE NUCLEAR POWER STATION
PER CENT CORE EXPERIENCING DNB AS
A FUNCTION OF EJECTED CONTROL ROD
WORTH AT ULTIMATE POWER, BOL
FIGURE 14-28

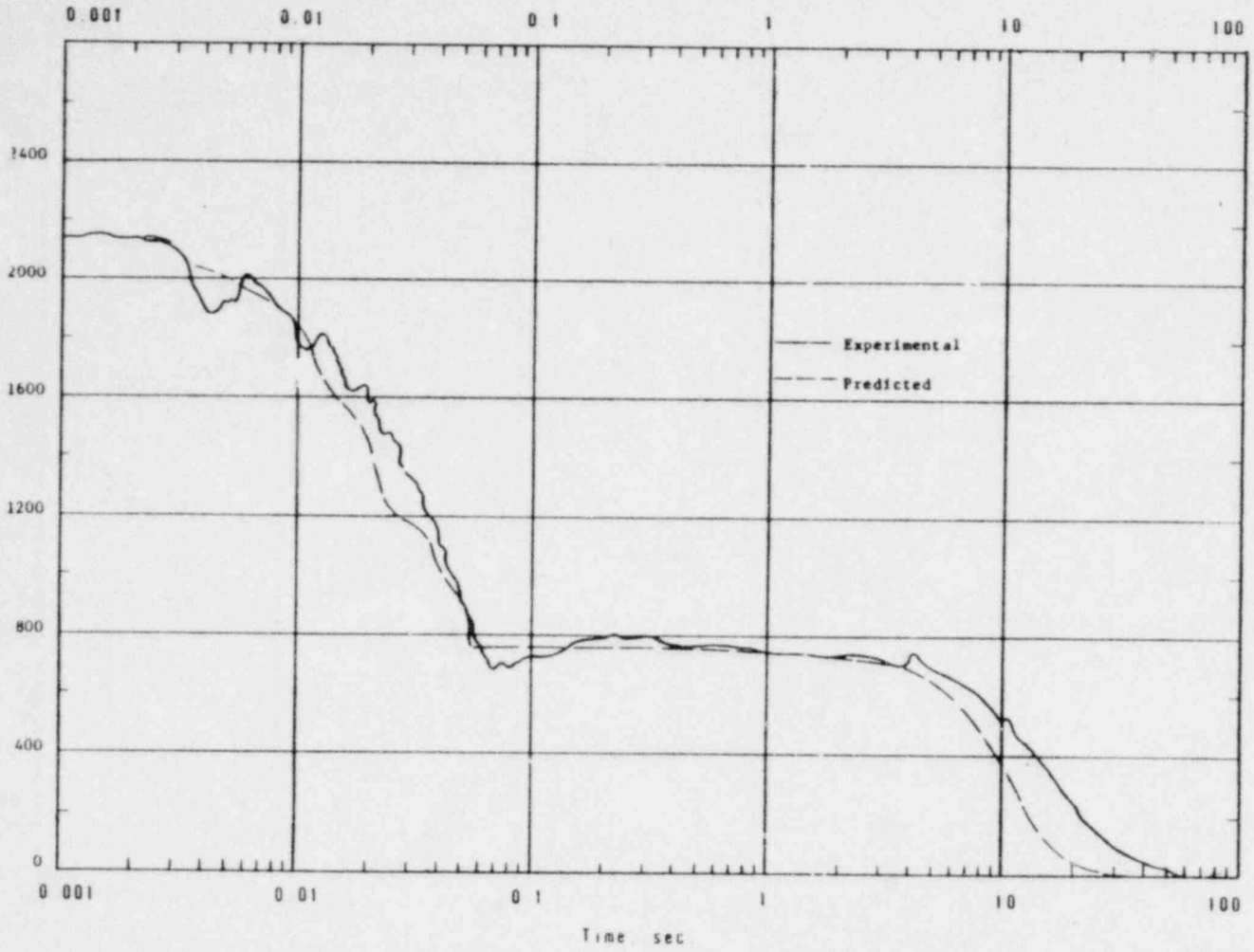

DAVIS-BESSE NUCLEAR POWER STATION
LOFT SEMISCALE BLOWDOWN TEST
NO. 54 - VESSEL PRESSURE VERSUS TIME
FIGURE 14-29

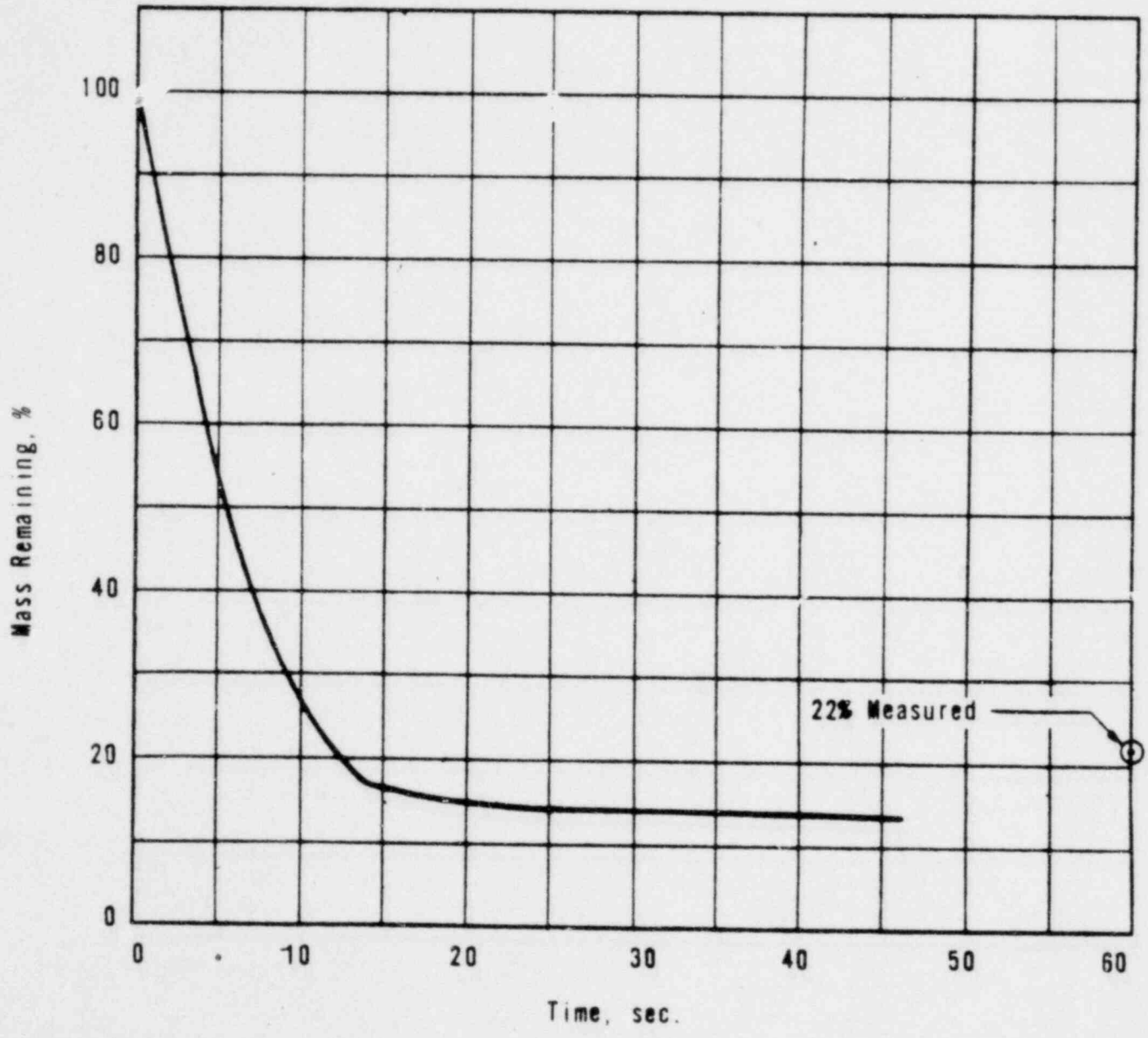

DAVIS-BESSE NUCLEAR POWER STATION
PREDICTED PER CENT MASS REMAINING
VERSUS TIME - LOFT TEST NO. 546
FIGURE 14-30

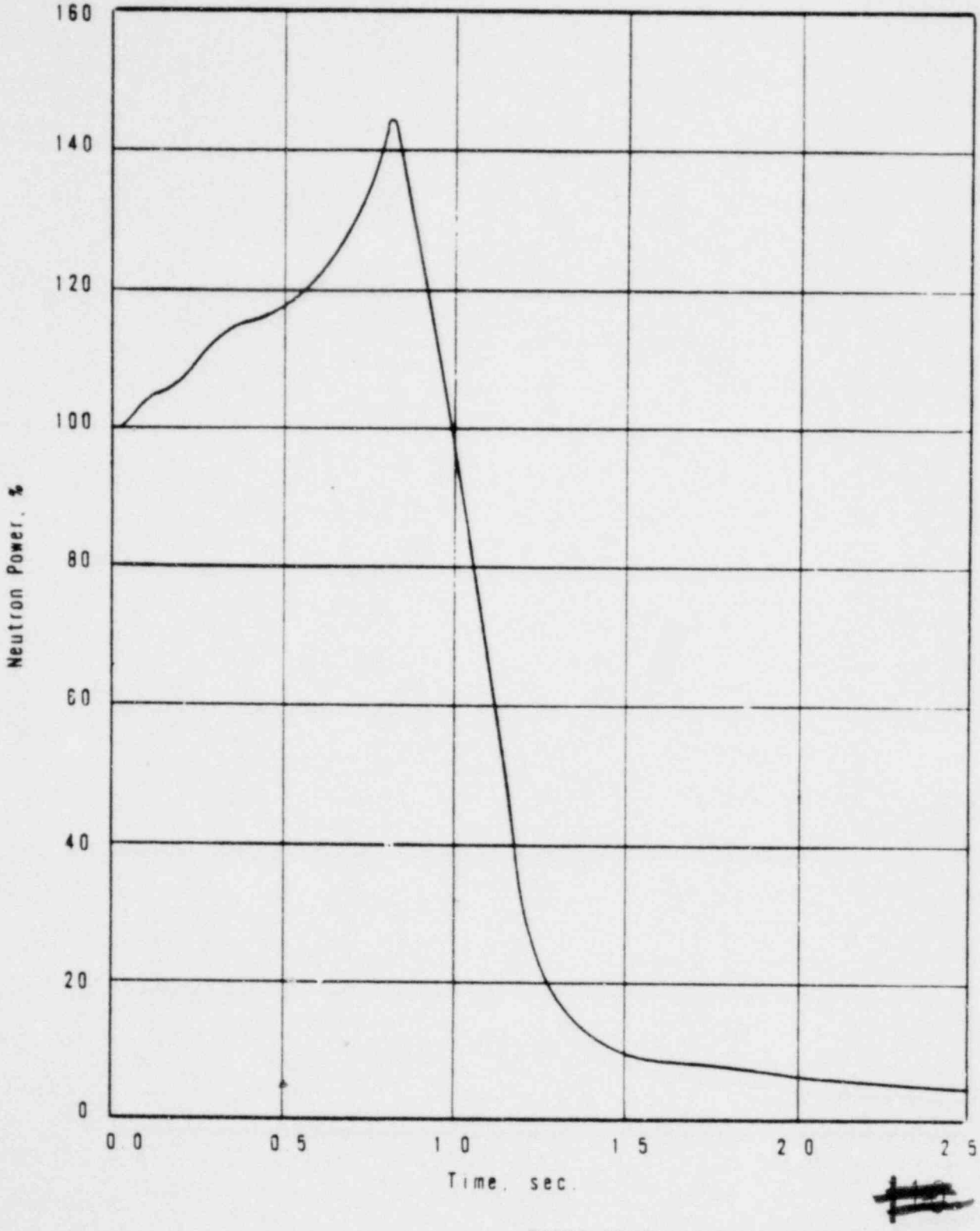

DAVIS-BESSE NUCLEAR POWER STATION
NEUTRON POWER VERSUS TIME FOR A
36-IN. I.D. DOUBLE-ENDED, HOT LEG
PIPE RUPTURE AT ULTIMATE POWER
WITHOUT TRIP
FIGURE 14-31
AMENDMENT NO. 1

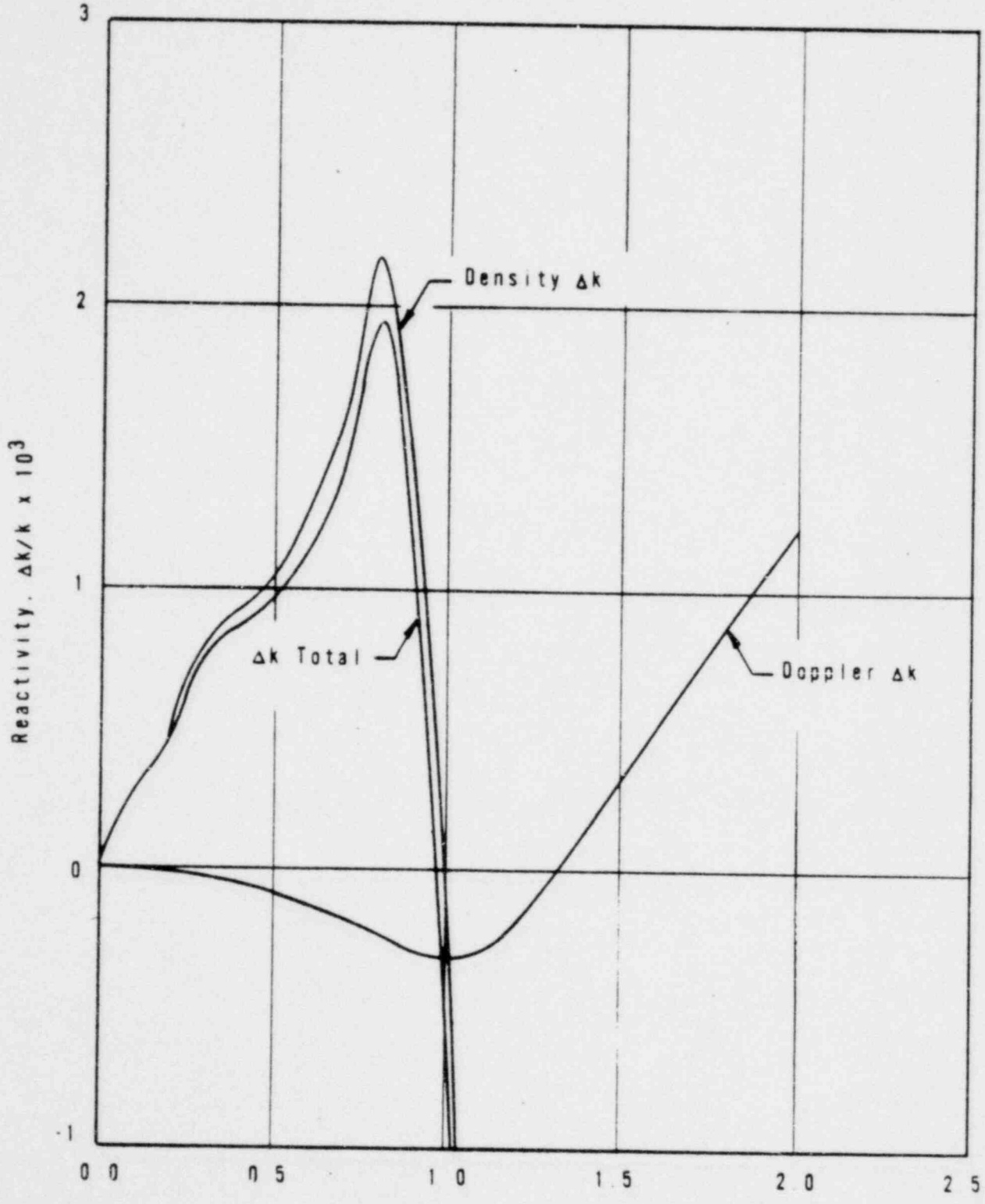

DAVIS-BESSE NUCLEAR POWER STATION
REACTIVITY VERSUS TIME FOR A 36-IN.
ID. DOUBLE-ENDED HOT LEG PIPE
RUPTURE AT ULTIMATE POWER WITHOUT TRIP
FIGURE 14-32

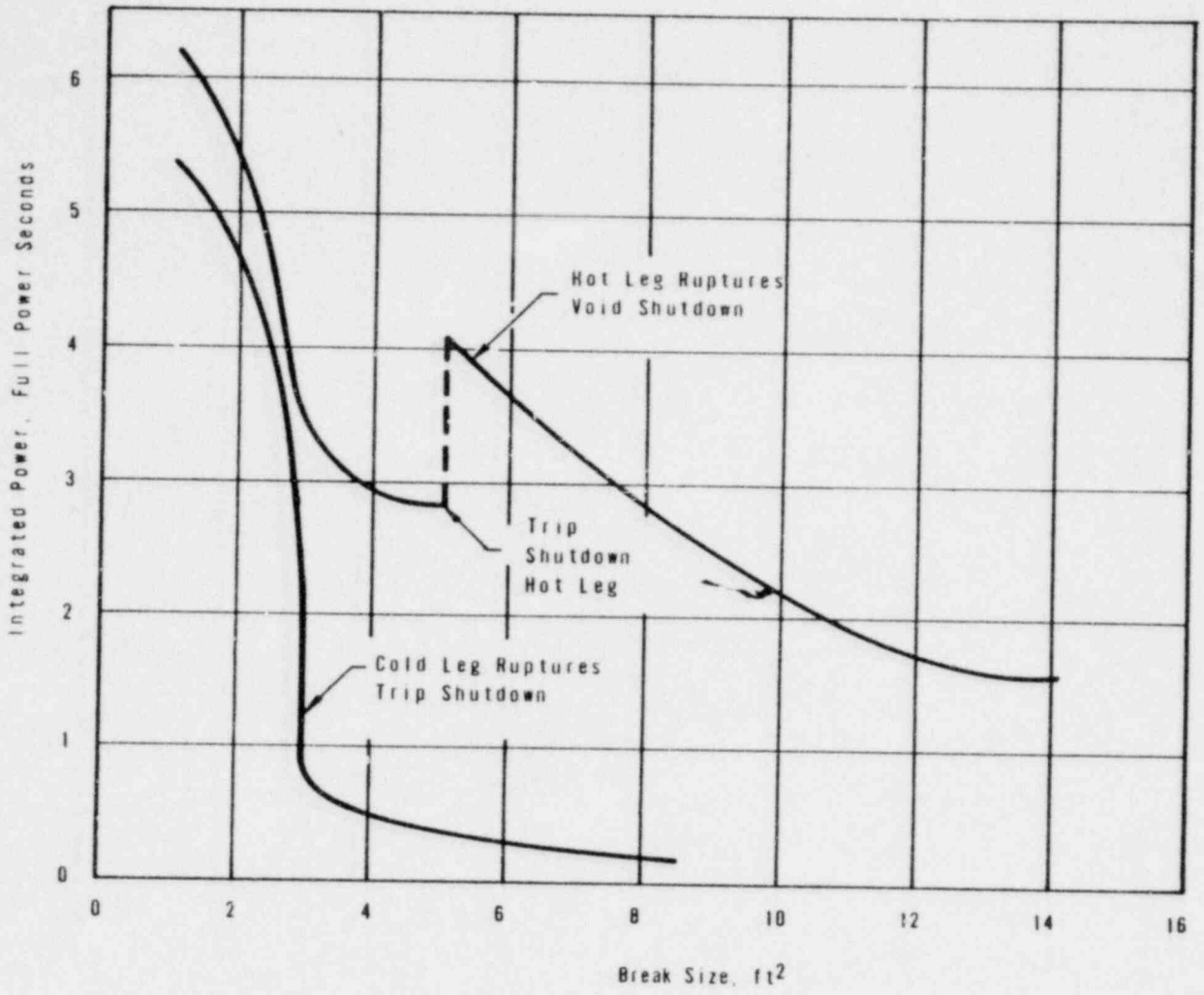

DAVIS-BESSE NUCLEAR POWER STATION
INTEGRATED POWER VERSUS BREAK SIZE
FOR A SPECTRUM OF RUPTURE SIZES
FIGURE 14-33

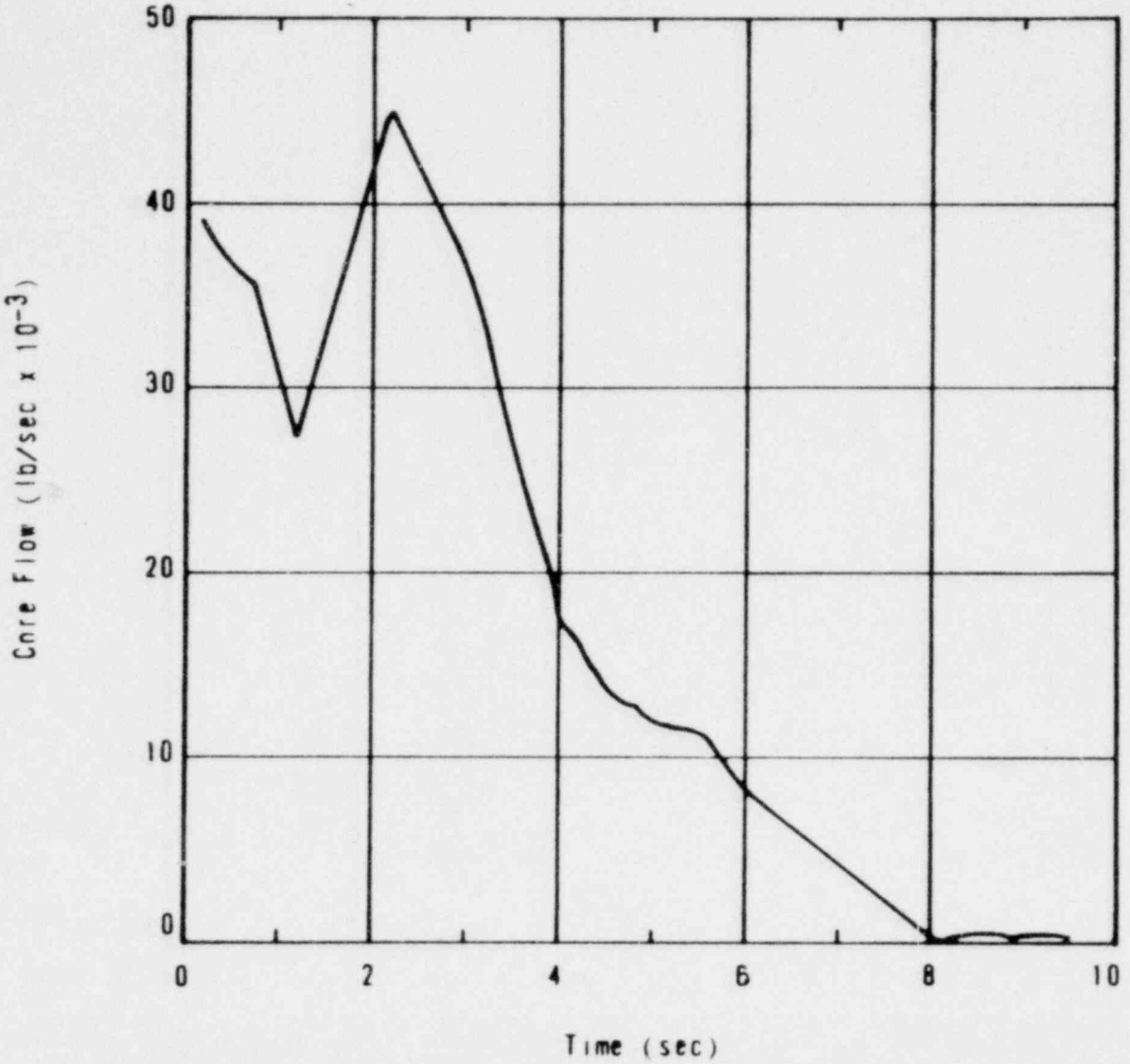

DAVIS BESSE NUCLEAR POWER STATION
CORE FLOW VERSUS TIME FOR A 36 IN
ID DOUBLE ENDED HOT LEG PIPE RUPTURE
FIGURE 14-34

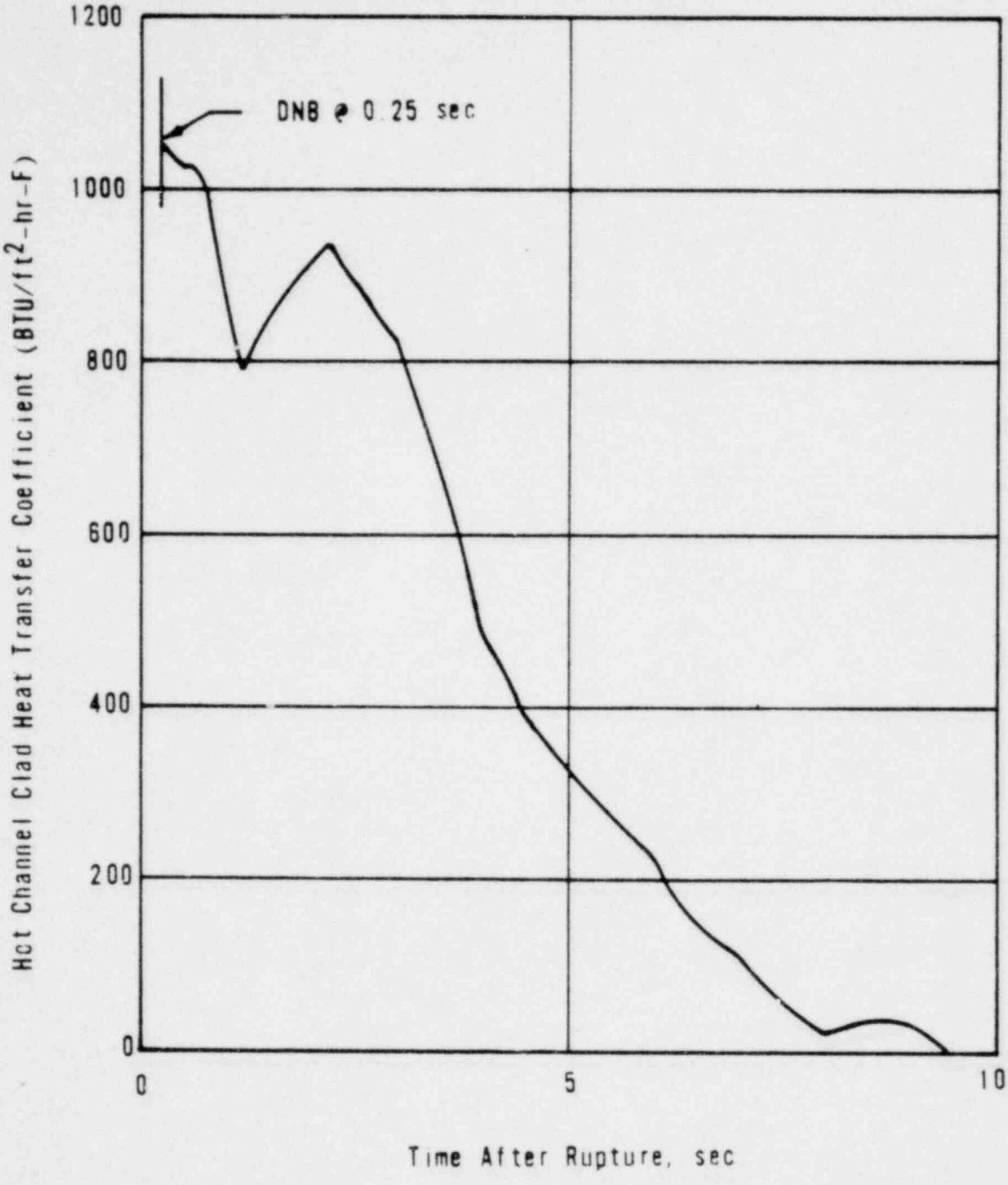

DAVIS-BESSE NUCLEAR POWER STATION
HOT CHANNEL CLAD SURFACE HEAT TRANSFER COEFFICIENT AFTER DNB VERSUS TIME FOR A 36-IN I.D. DOUBLE-ENDED, HOT LEG PIPE RUPTURE
FIGURE 14-35

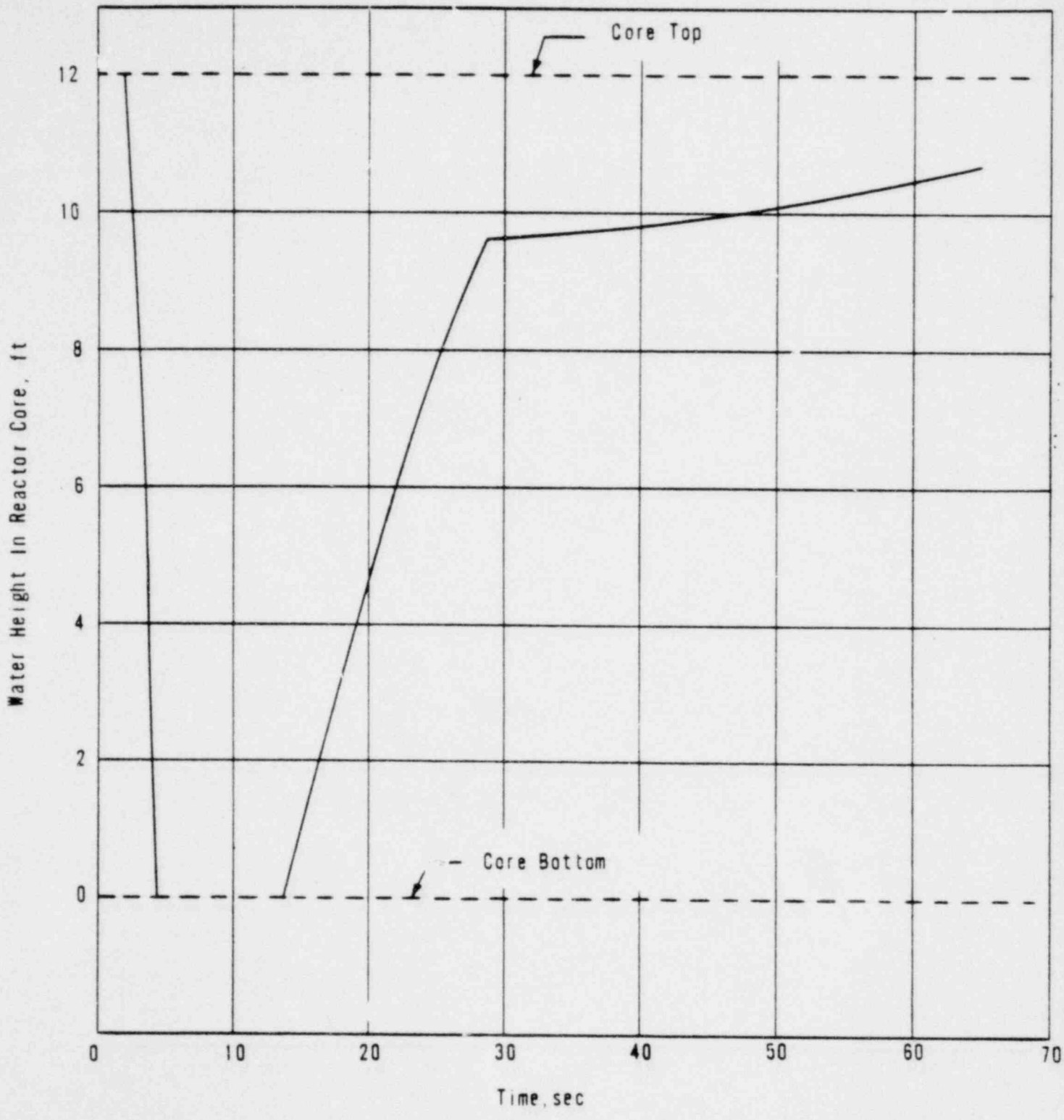

DAVIS-BESSE NUCLEAR POWER STATION
REACTOR VESSEL WATER HEIGHT VERSUS TIME FOR A
36-IN. ID, DOUBLE-ENDED, HOT LEG PIPE RUPTURE
FOR 600 PSIG CORE FLOODING TANK OPERATING
FIGURE 14-38

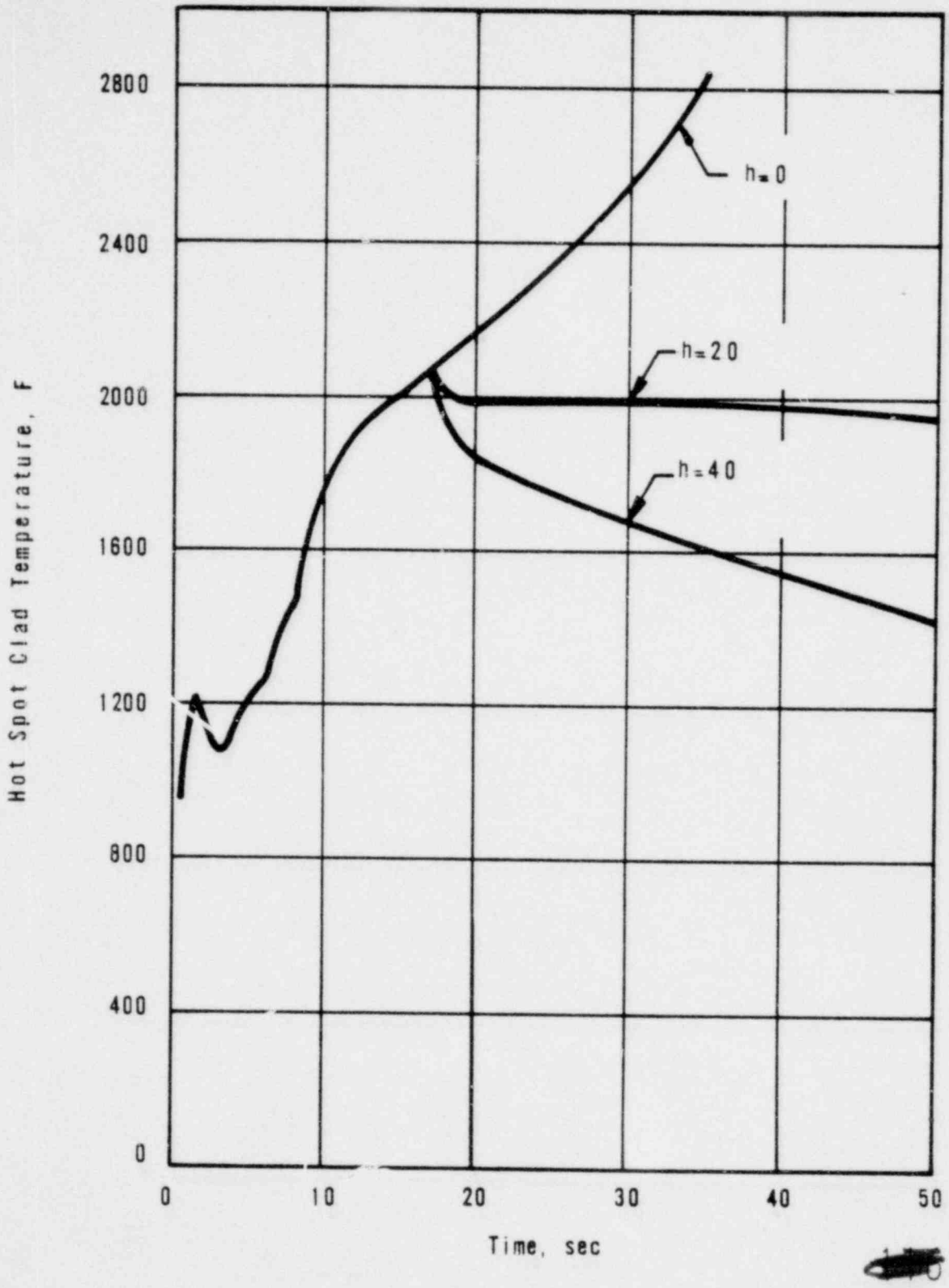

DAVIS-BESSE NUCLEAR POWER STATION
HOT SPOT CLAD TEMPERATURE VERSUS TIME FOR
A 36-IN. ID. DOUBLE-ENDED HOT LEG RUPTURE
AND VARIABLE QUENCH COEFFICIENT
FIGURE 14-37

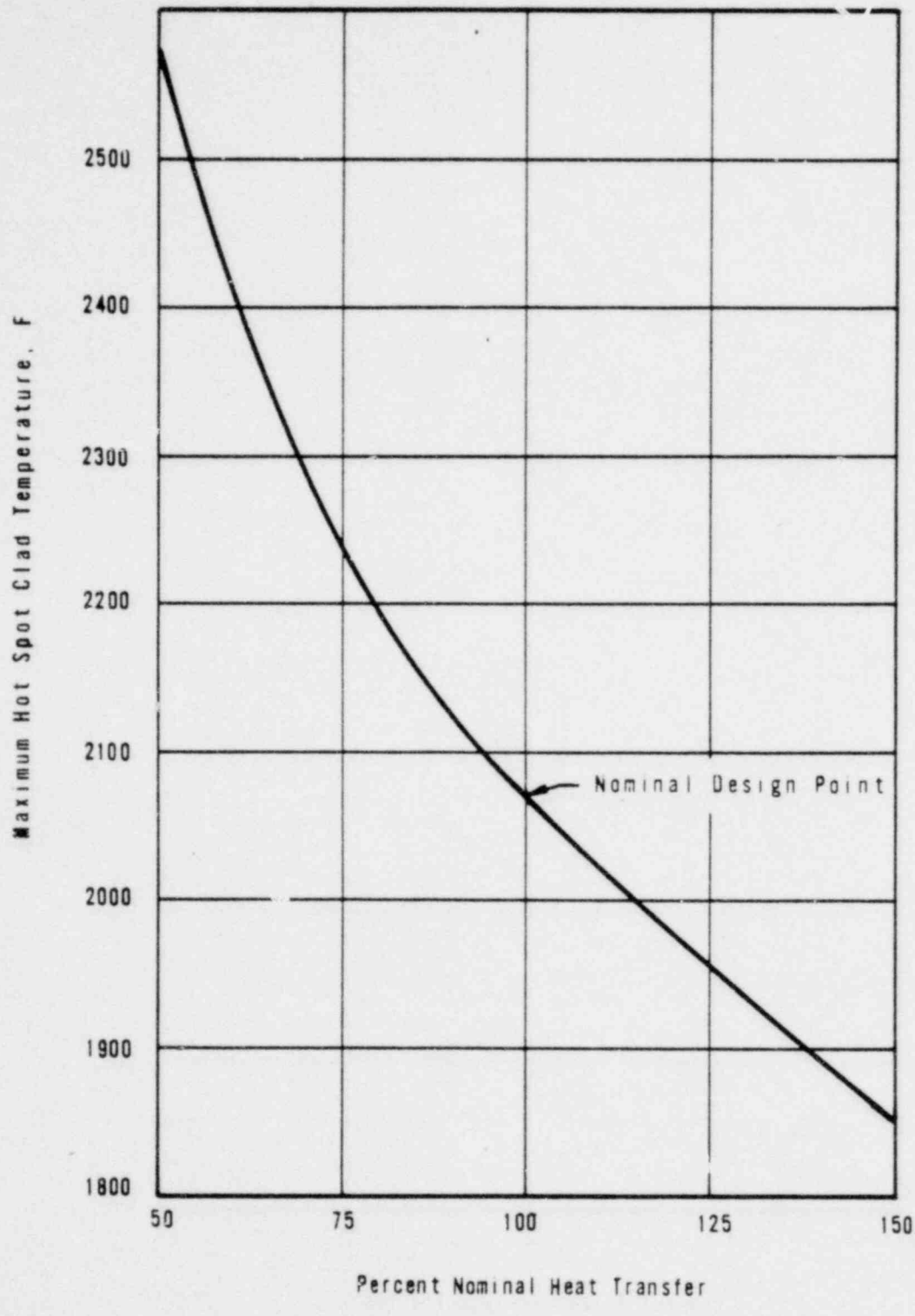

DAVIS-BESSE NUCLEAR POWER STATION
MAXIMUM HOT SPOT CLAD TEMPERATURE VERSUS VARIABLE HEAT TRANSFER COEFFICIENT AFTER DNB FOR A 36-IN. ID, DOUBLE-ENDED, HOT LEG RUPTURE
FIGURE 14-38

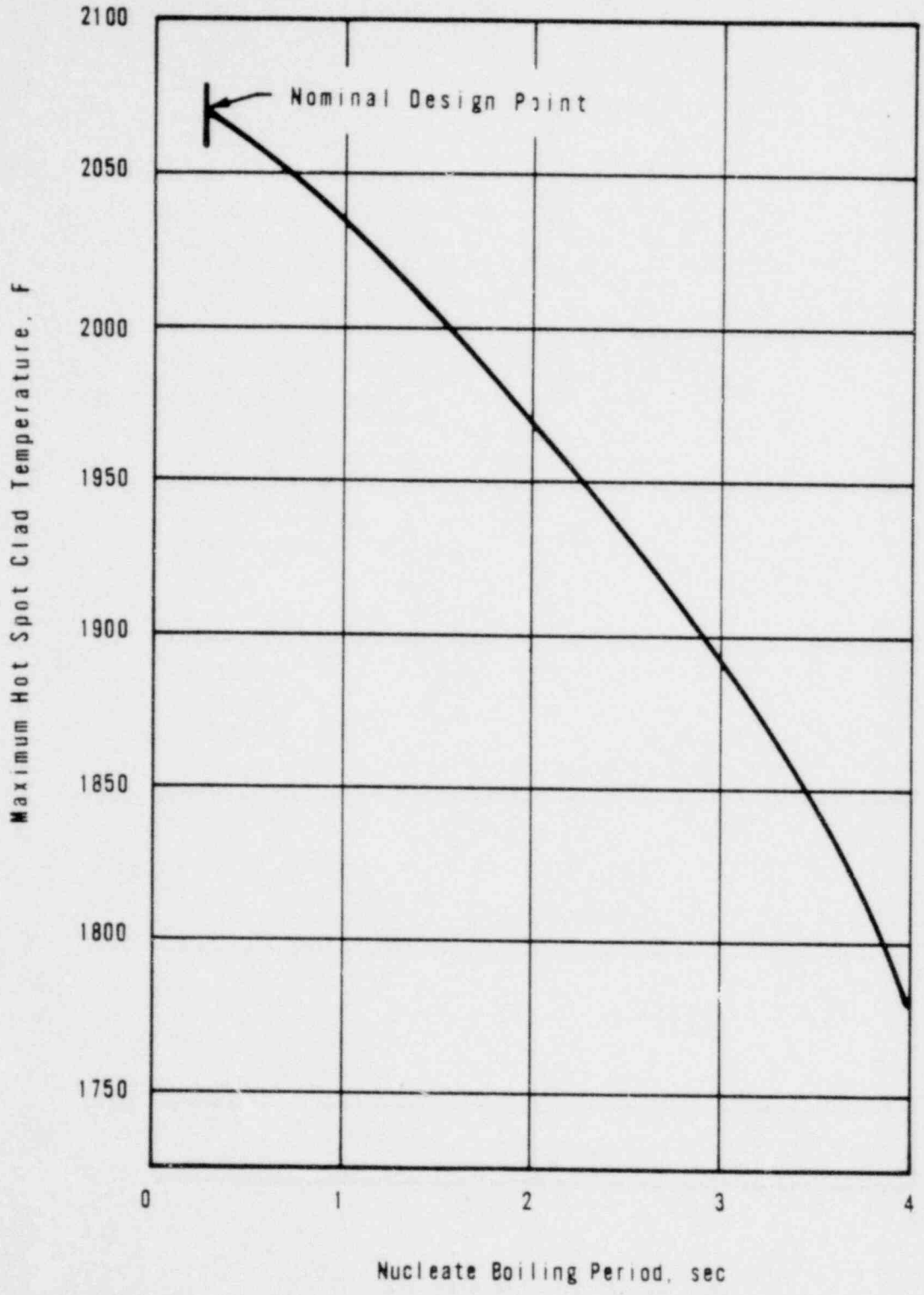

DAVIS-BESSE NUCLEAR POWER STATION
MAXIMUM HOT SPOT CLAD TEMPERATURE AS A FUNCTION OF TIME TO REACH DNB FOF A 36-IN. ID, DOUBLE-ENDED, HOT LEG RUPTURE
FIGURE 14-39

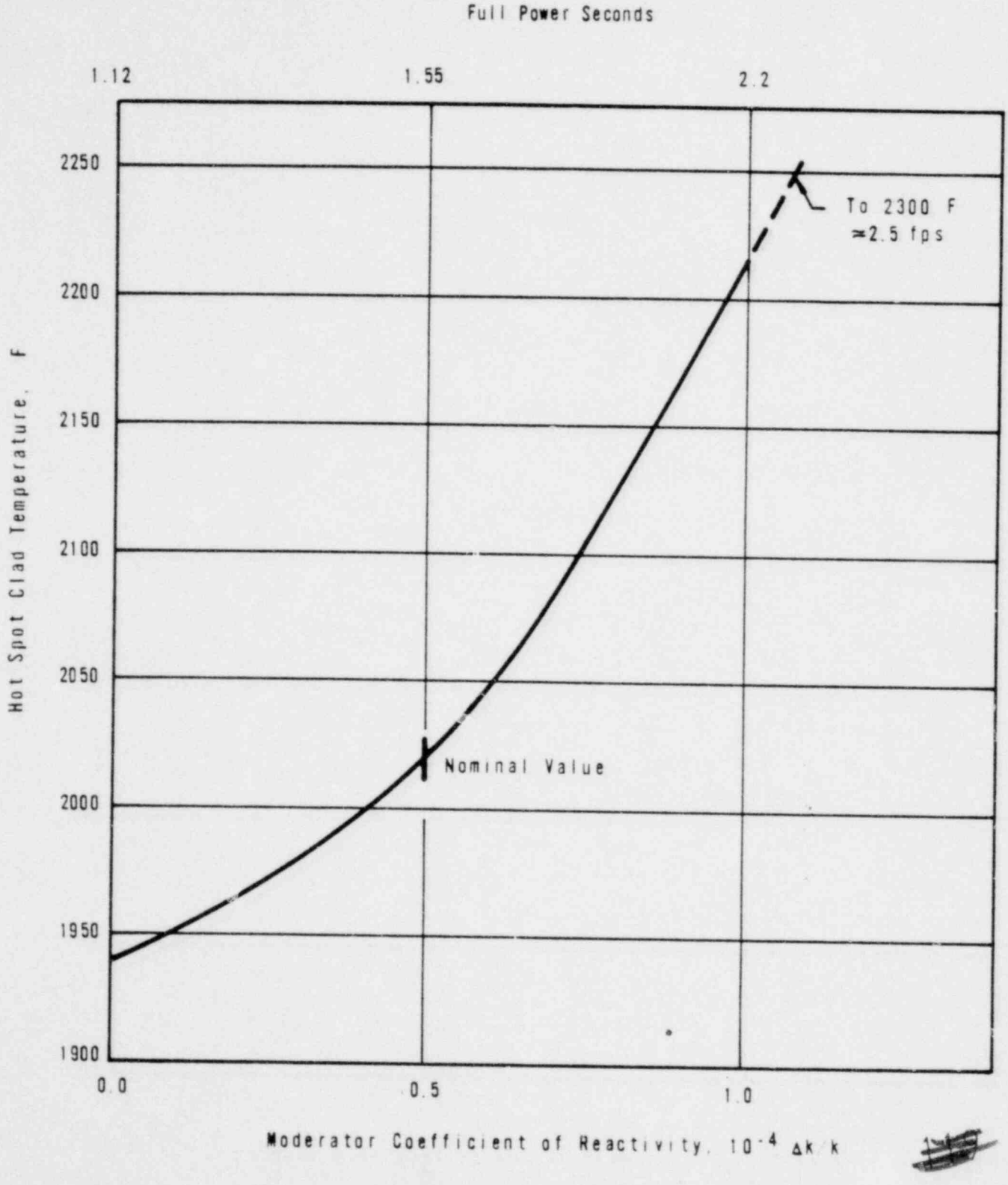

DAVIS-BESSE NUCLEAR POWER STATION
HOT SPOT CLAD TEMPERATURE AS A FUNCTION OF MODERATOR COEFFICIENT EFFECT ON VOID SHUTDOWN FOR A 36-IN. ID, DOUBLE-ENDED, HOT LEG PIPE RUPTURE.
FIGURE 14-40

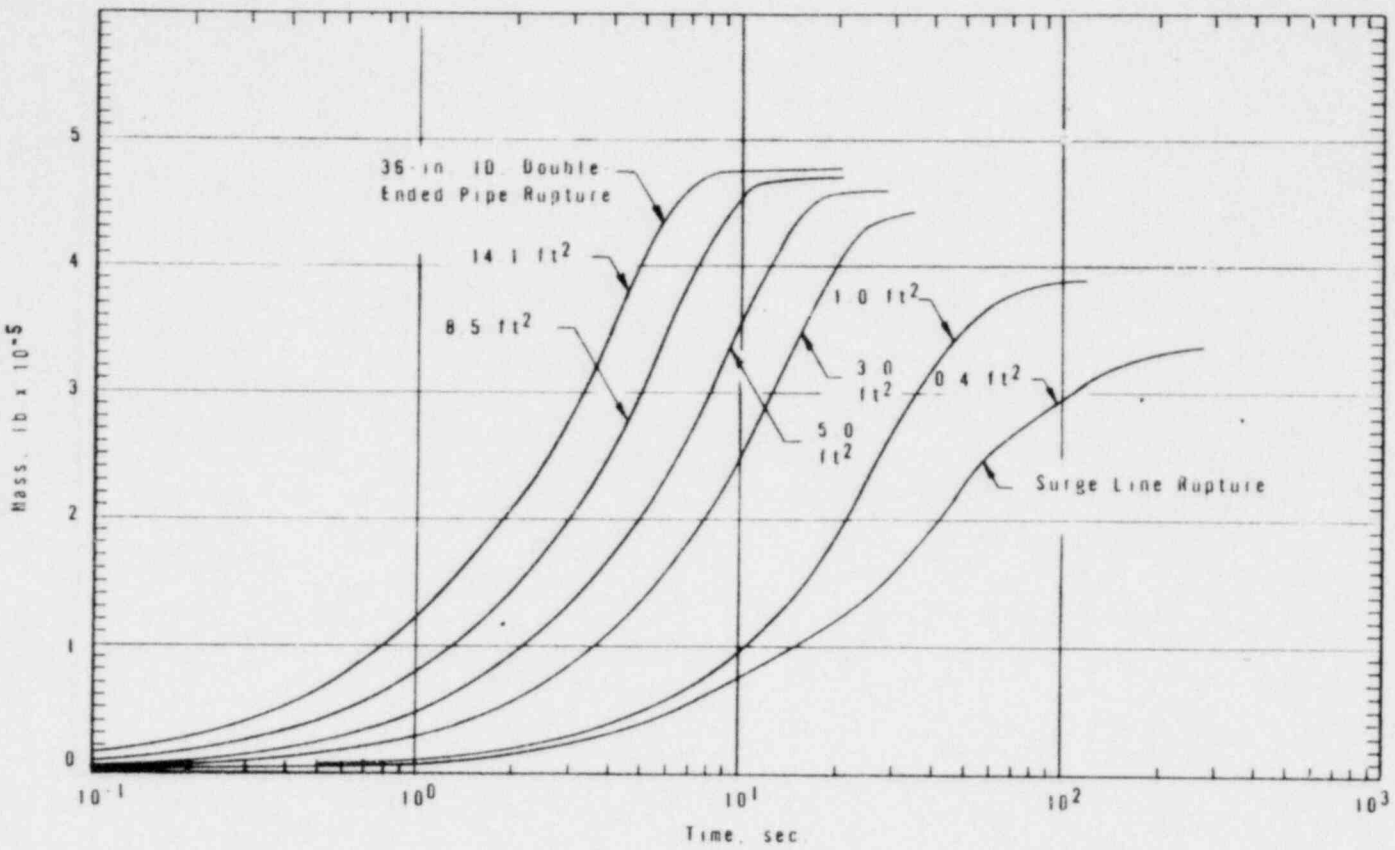

DAVIS-BESSE NUCLEAR POWER STATION
MASS RELEASED TO REACTOR
BUILDING FOR THE SPECTRUM
OF HOT LEG RUPTURES
FIGURE 14-41

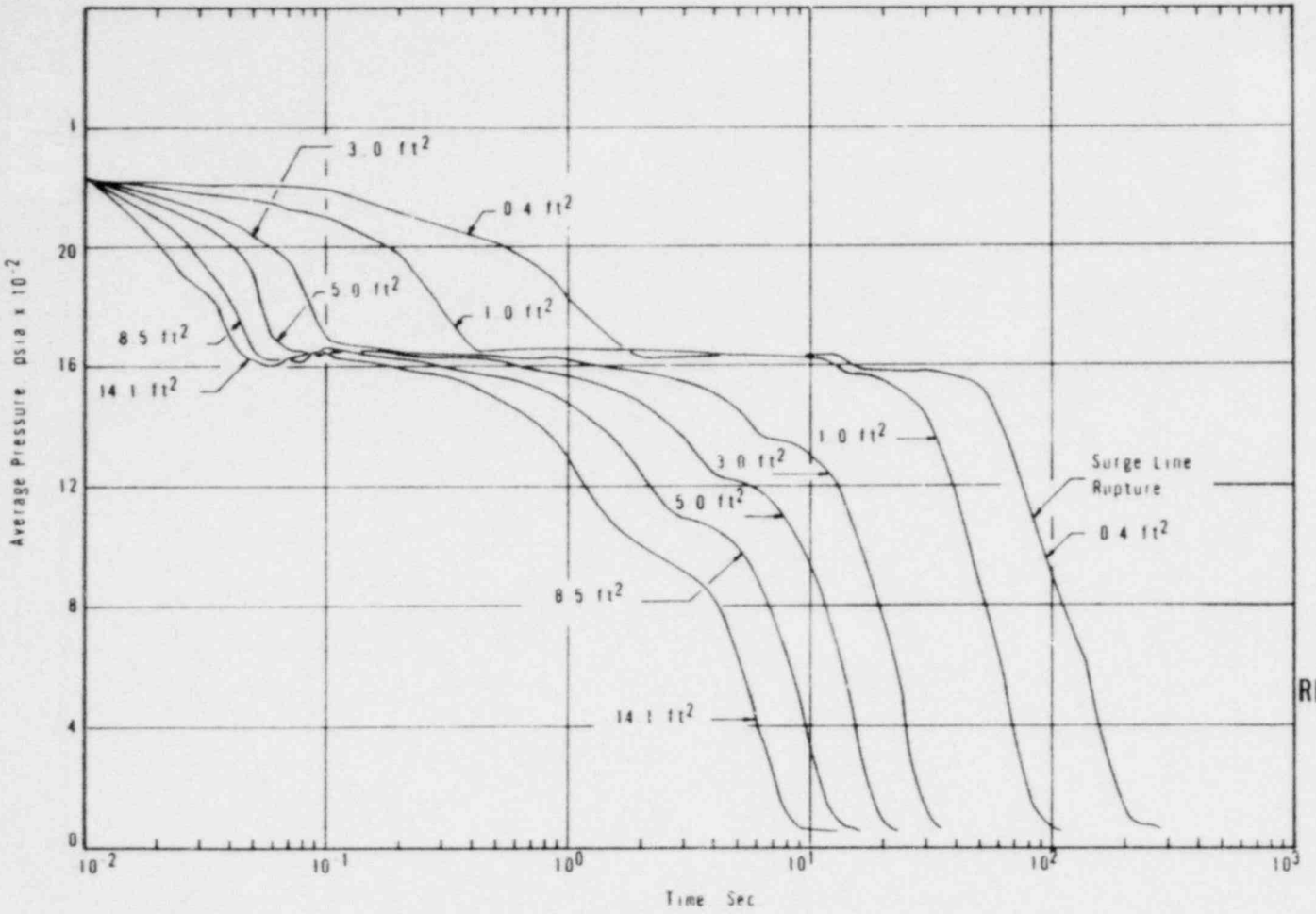

DAVIS-BESSE NUCLEAR POWER STATION
REACTOR COOLANT AVERAGE PRESSURE FOR THE SPECTRUM OF HOT LEG RUPTURES
FIGURE 14-42

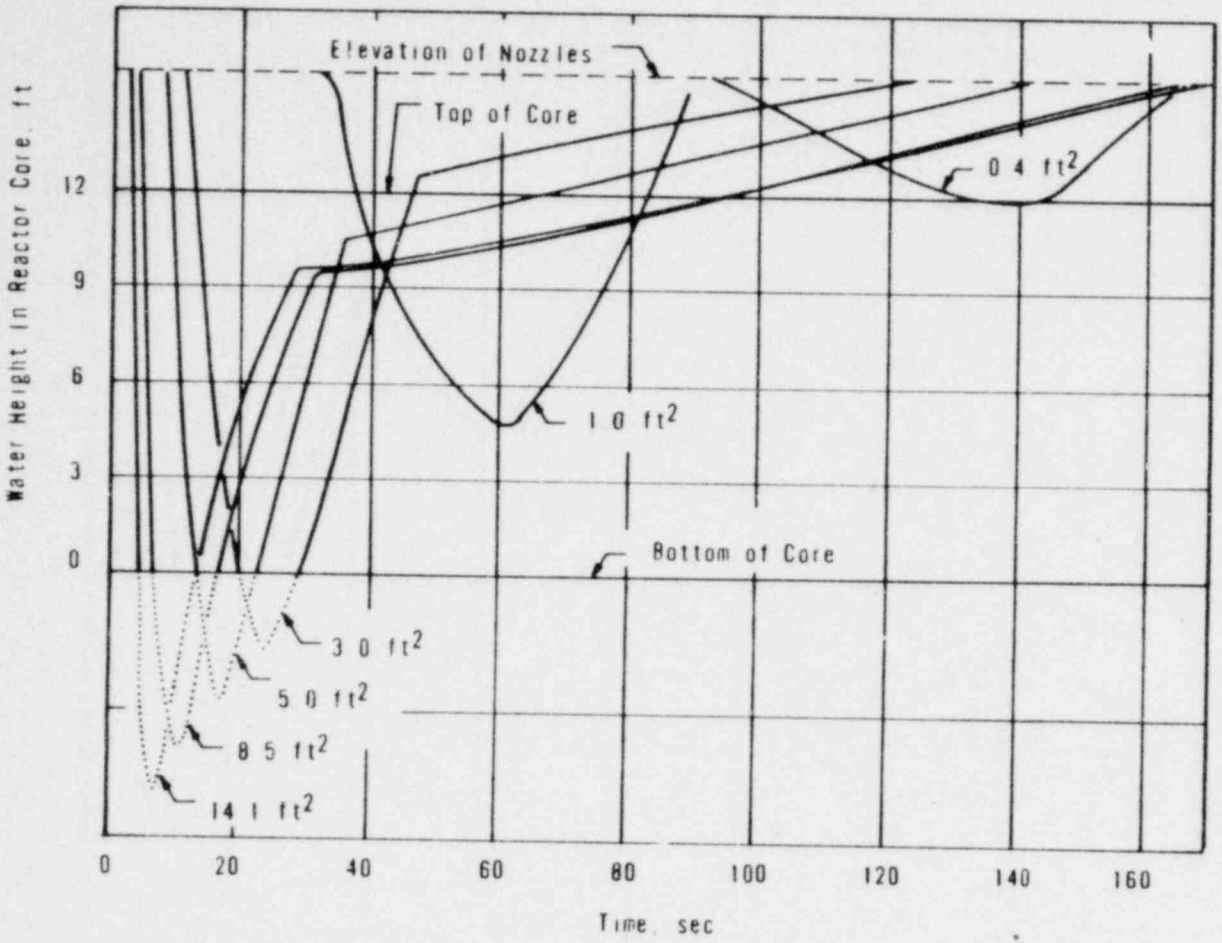

DAVIS-BESSE NUCLEAR POWER STATION
HOT LEG RUPTURES - REACTOR VESSEL WATER HEIGHT VERSUS TIME INCLUDING EFFECTS OF BOILOFF AND INJECTION
FIGURE 14-43

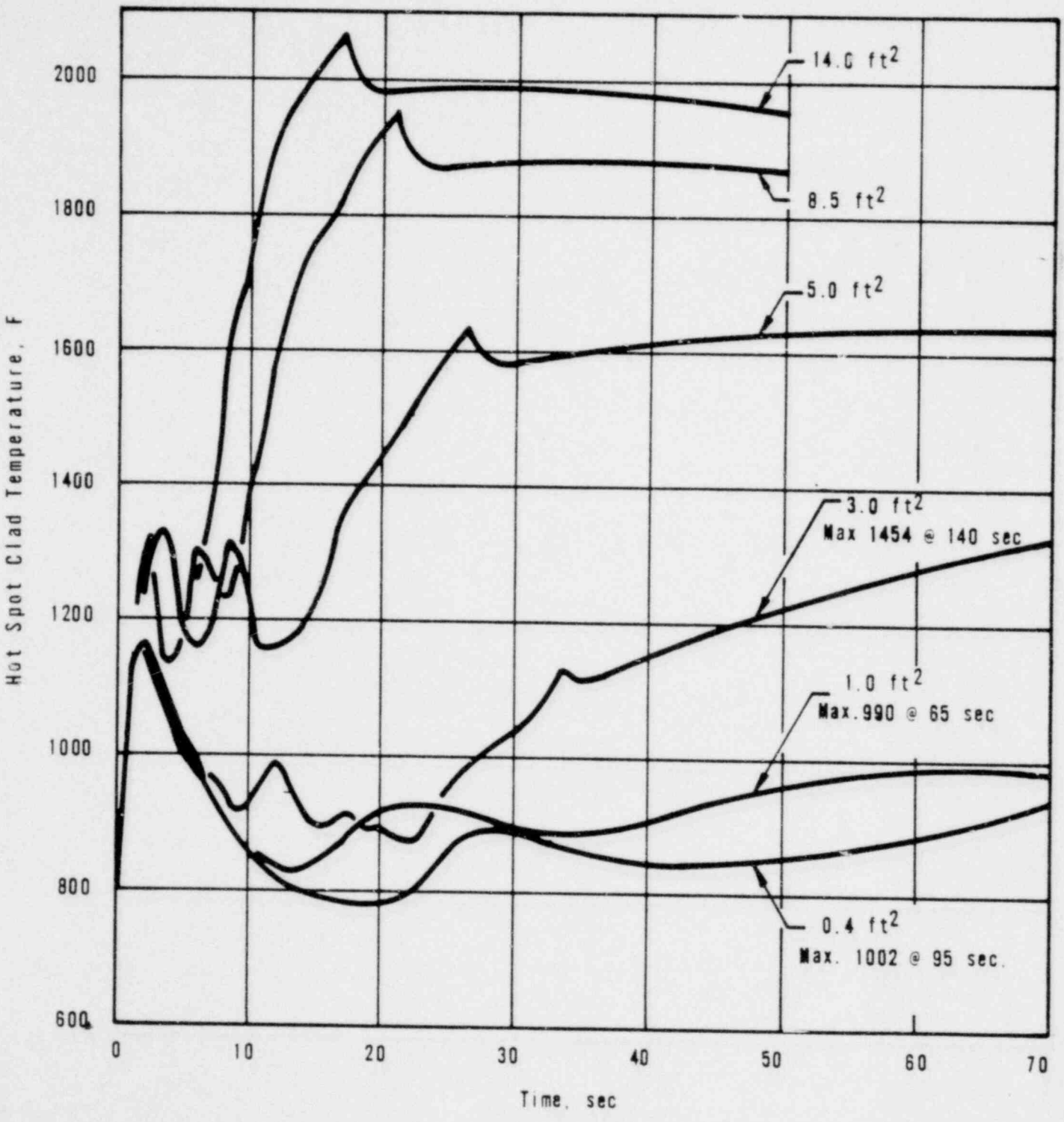

DAVIS-BESSE NUCLEAR POWER STATION
HOT SPOT CLADDING TEMPERATURE VERSUS TIME FOR SPECTRUM OF HOT LEG RUPTURES
FIGURE 14-44

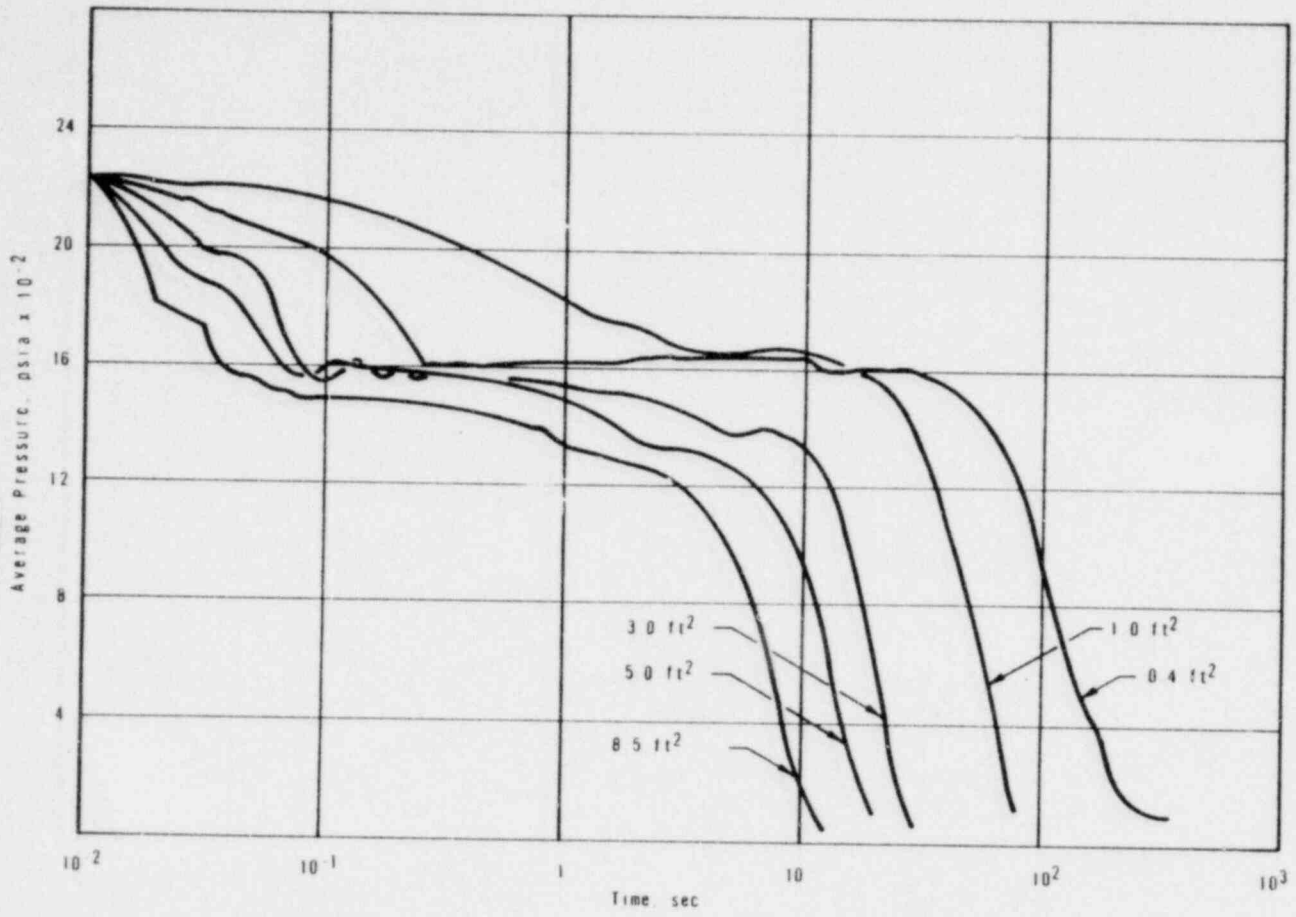

DAVIS-BESSE NUCLEAR POWER STATION
REACTOR COOLANT AVERAGE PRESSURE-
SPECTRUM OF COLD LEG RUPTURE SIZES
FIGURE 14-45

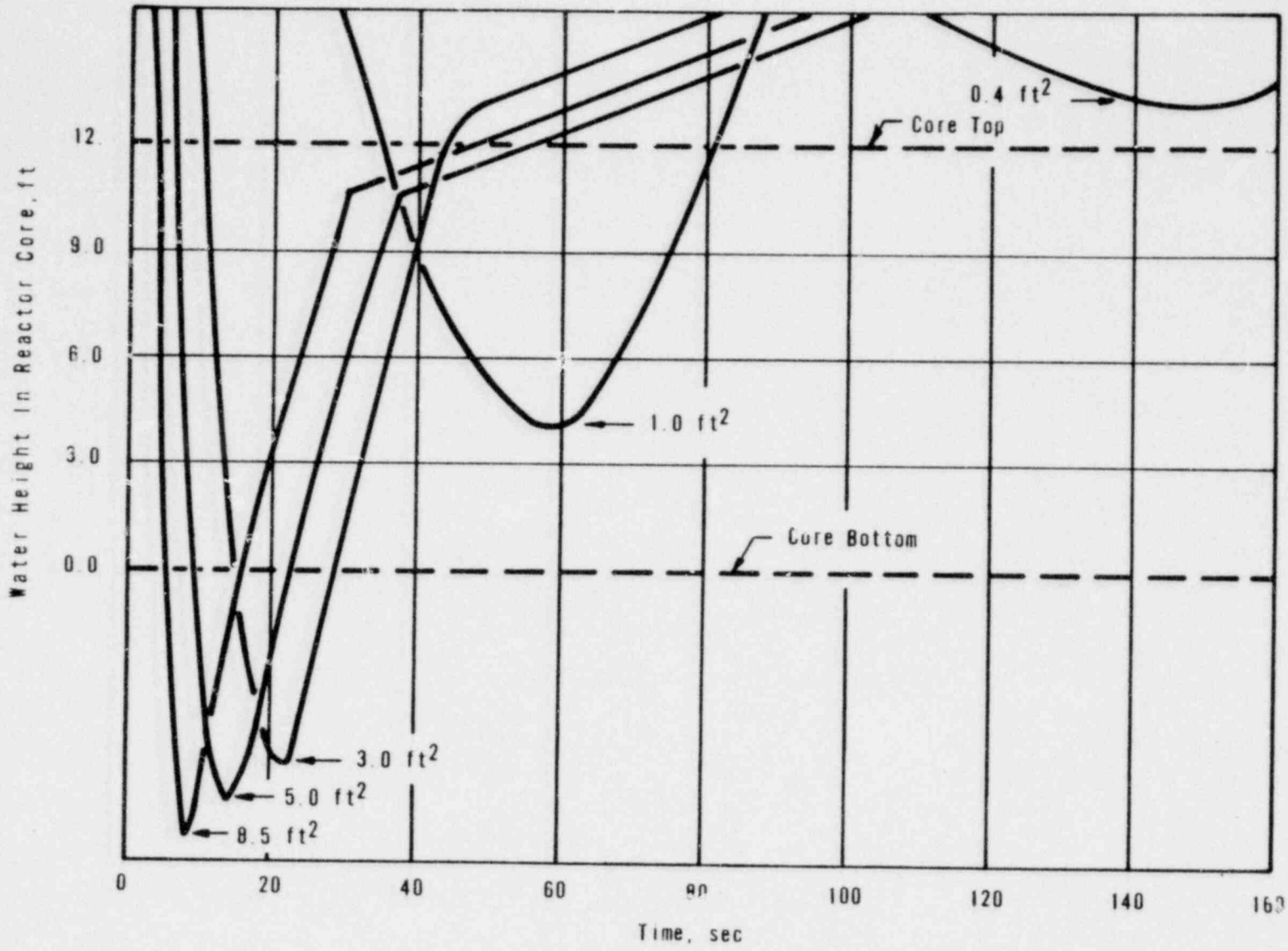

DAVIS-BESSE NUCLEAR POWER STATION
COLD LEG RUPTURES-REACTOR VESSEL WATER HEIGHT VERSUS TIME INCLUDING EFFECTS OF BOILOFF AND INJECTION
FIGURE 14-46

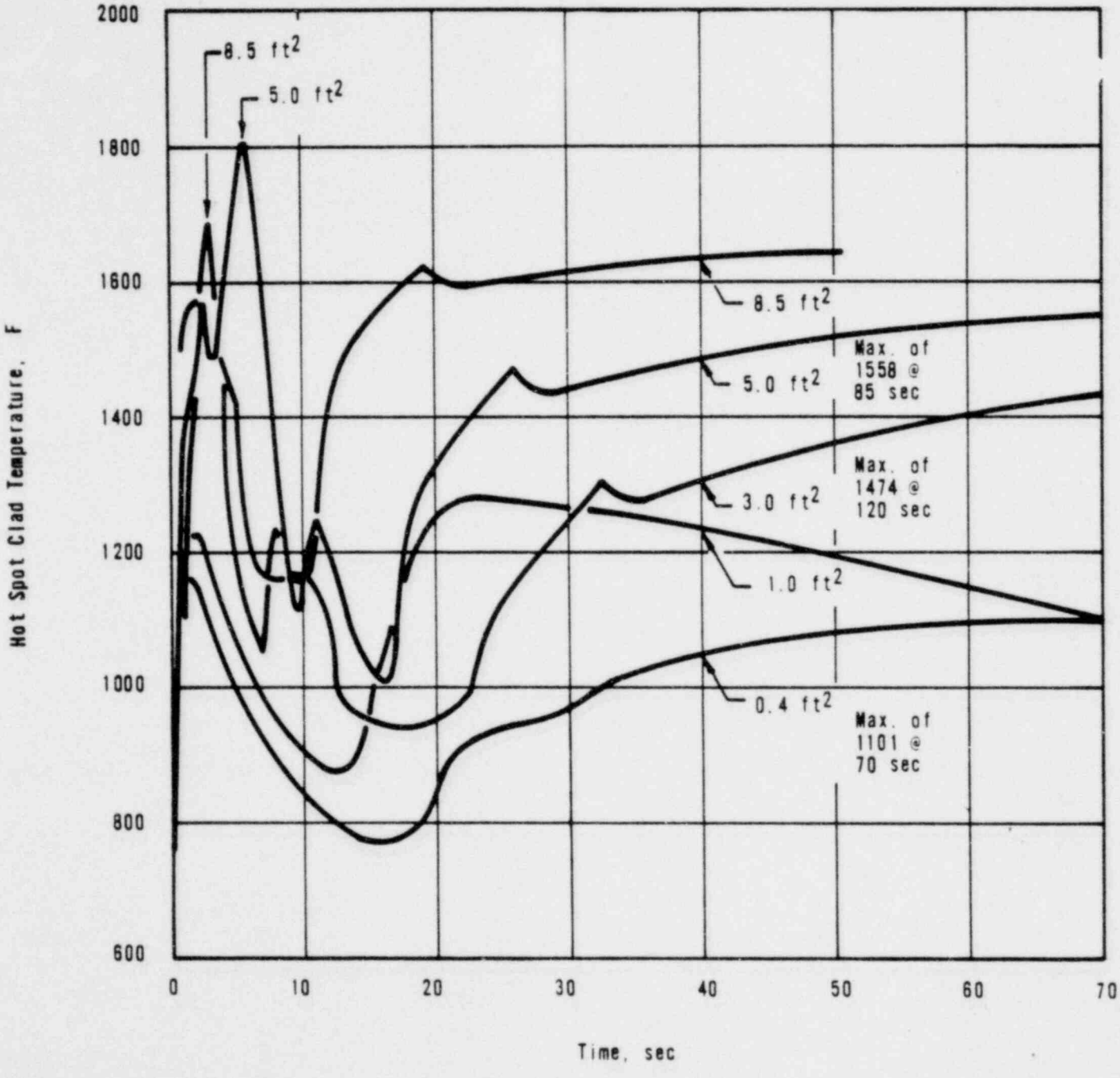

DAVIS-BESSE NUCLEAR POWER STATION
HOT SPOT CLADDING TEMPERATURE VERSUS
TIME FOR SPECTRUM OF COLD LEG RUPTURES
FIGURE 14-47

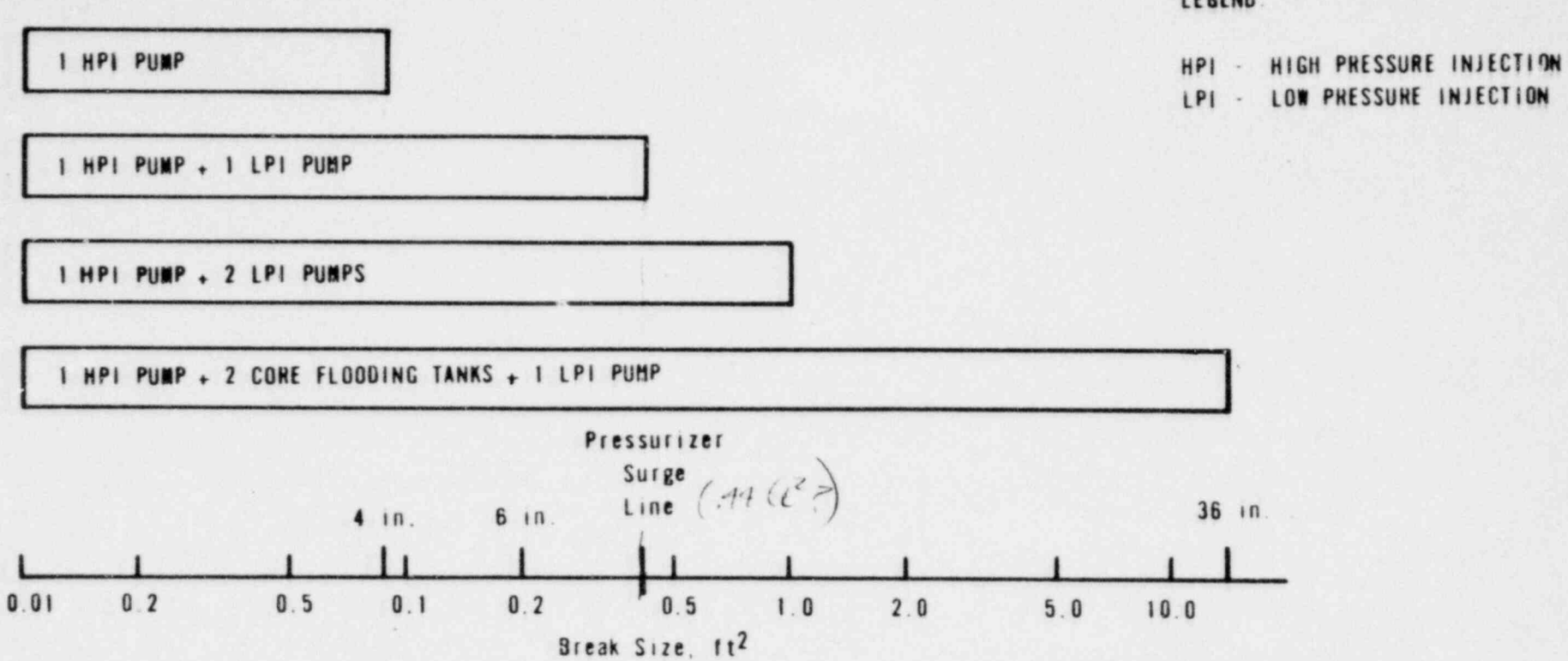

DAVIS-BESSE NUCLEAR POWER STATION
EMERGENCY CORE COOLING SYSTEMS CAPABILITY
TO MEET FUEL CLAD TEMPERATURE DESIGN LIMIT
FIGURE 14-48

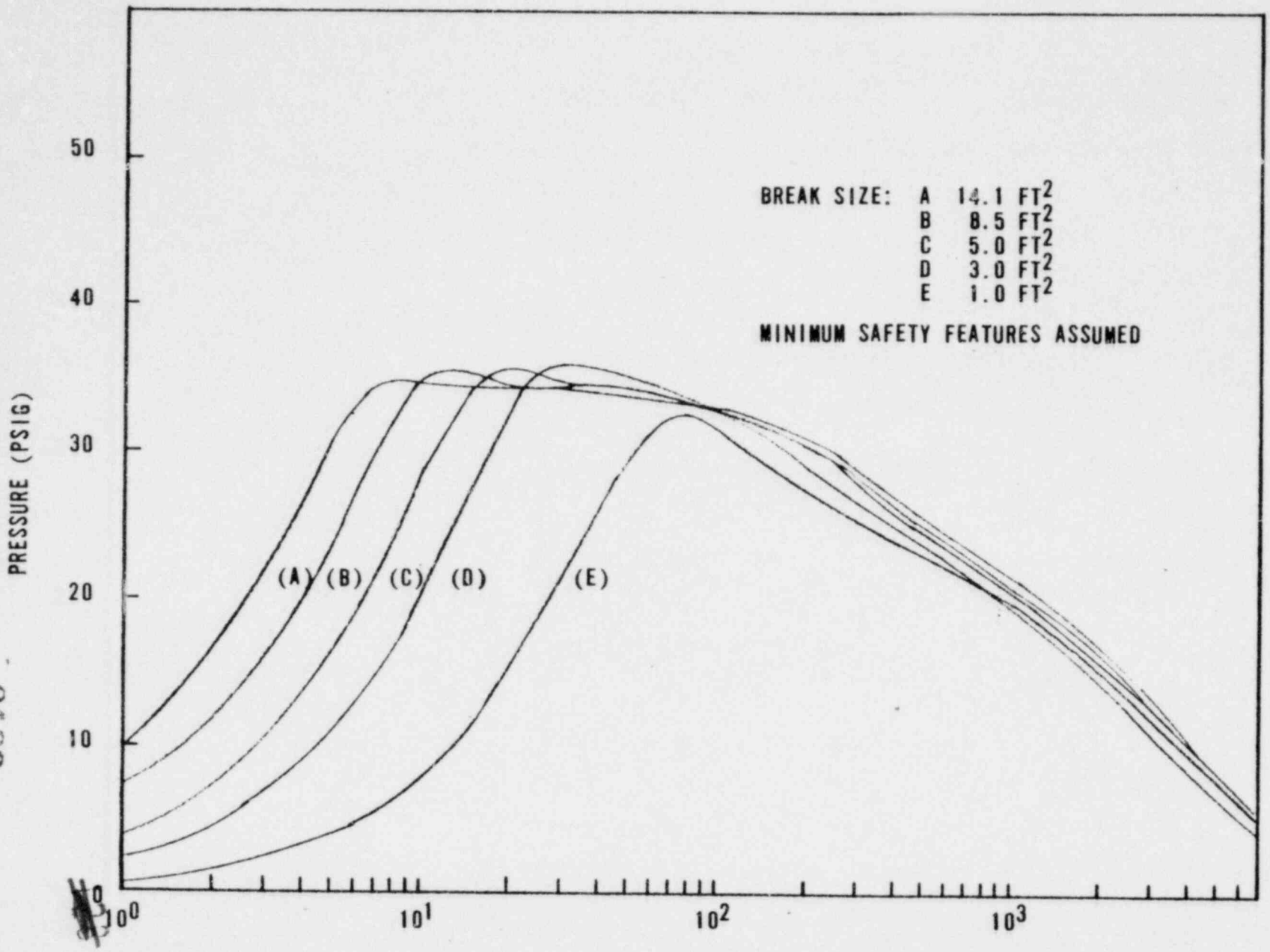

DAVIS-BESSE NUCLEAR POWER STATION
CONTAINMENT PRESSURE TRANSIENT CURVES
FIGURE 14-49

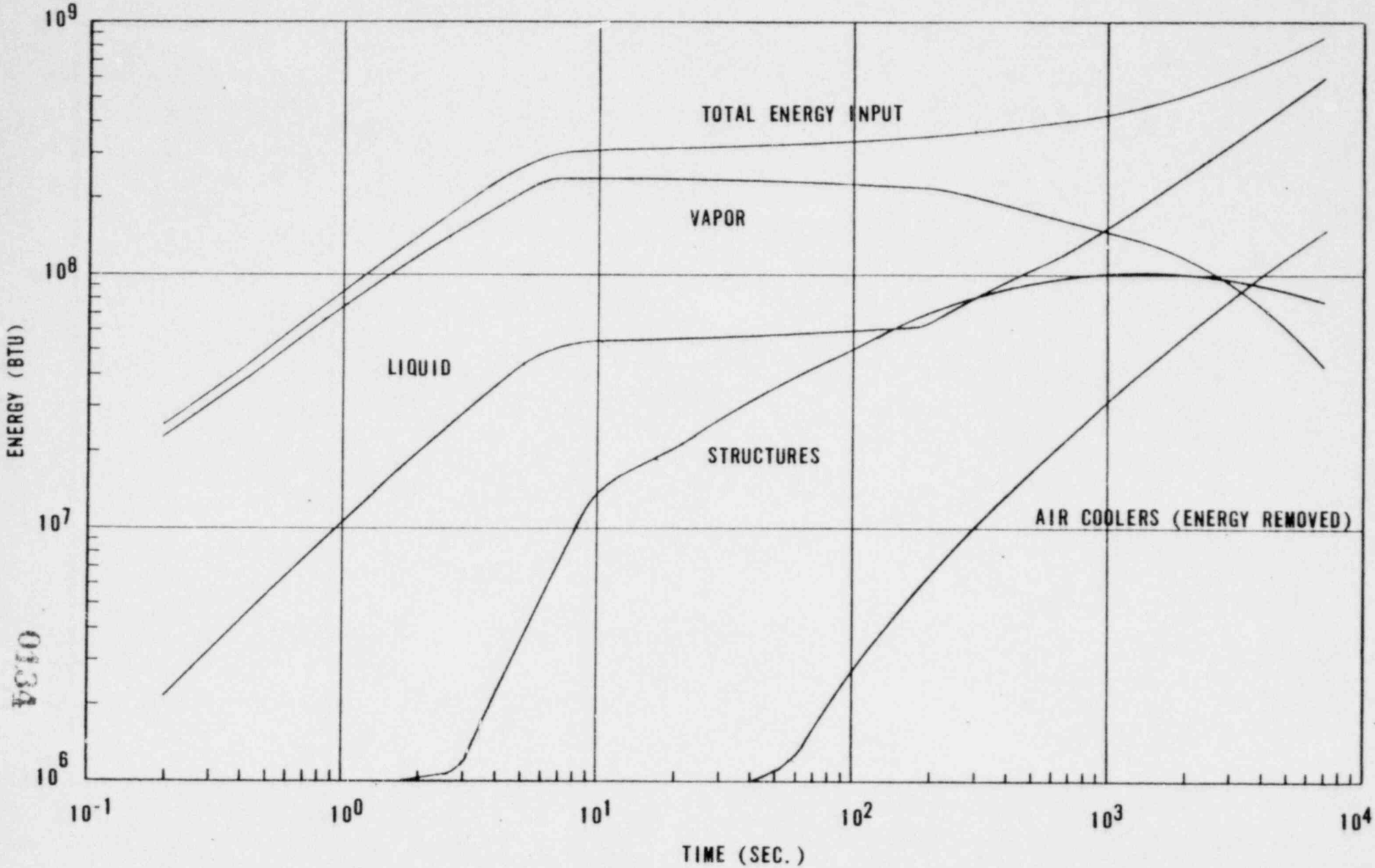

DAVIS-BESSE NUCLEAR POWER STATION
CONTAINMENT VESSEL HEAT BALANCE
14.1 SQ. FT. BREAK, MINIMUM SAFETY FEATURES
FIGURE 14-50

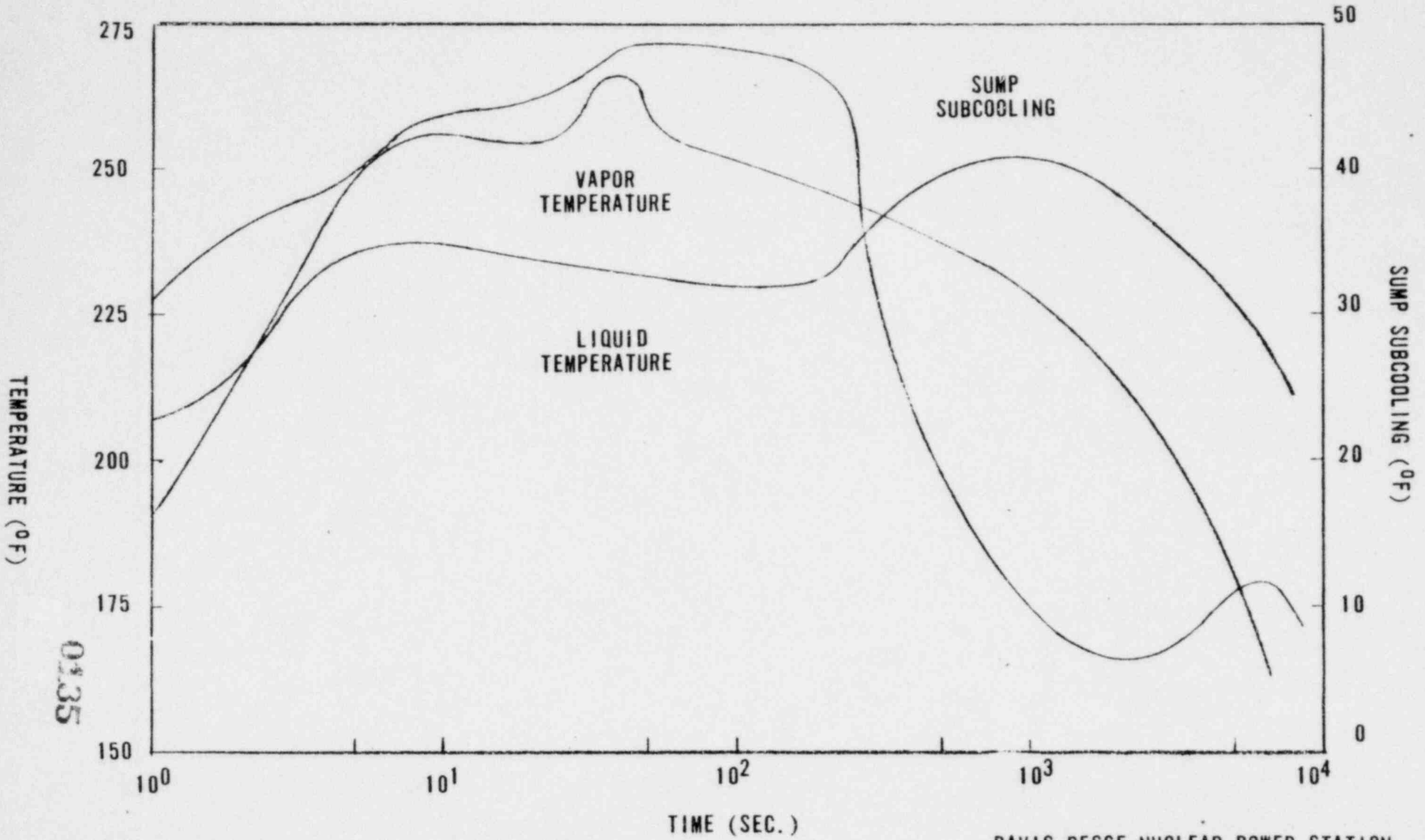

DAVIS-BESSE NUCLEAR POWER STATION
CONTAINMENT VESSEL
TEMPERATURE TRANSIENT AND SUMP SUBCOOLING TRANSIENT
14.1 Sq. FT. BREAK
FIGURE 14-51

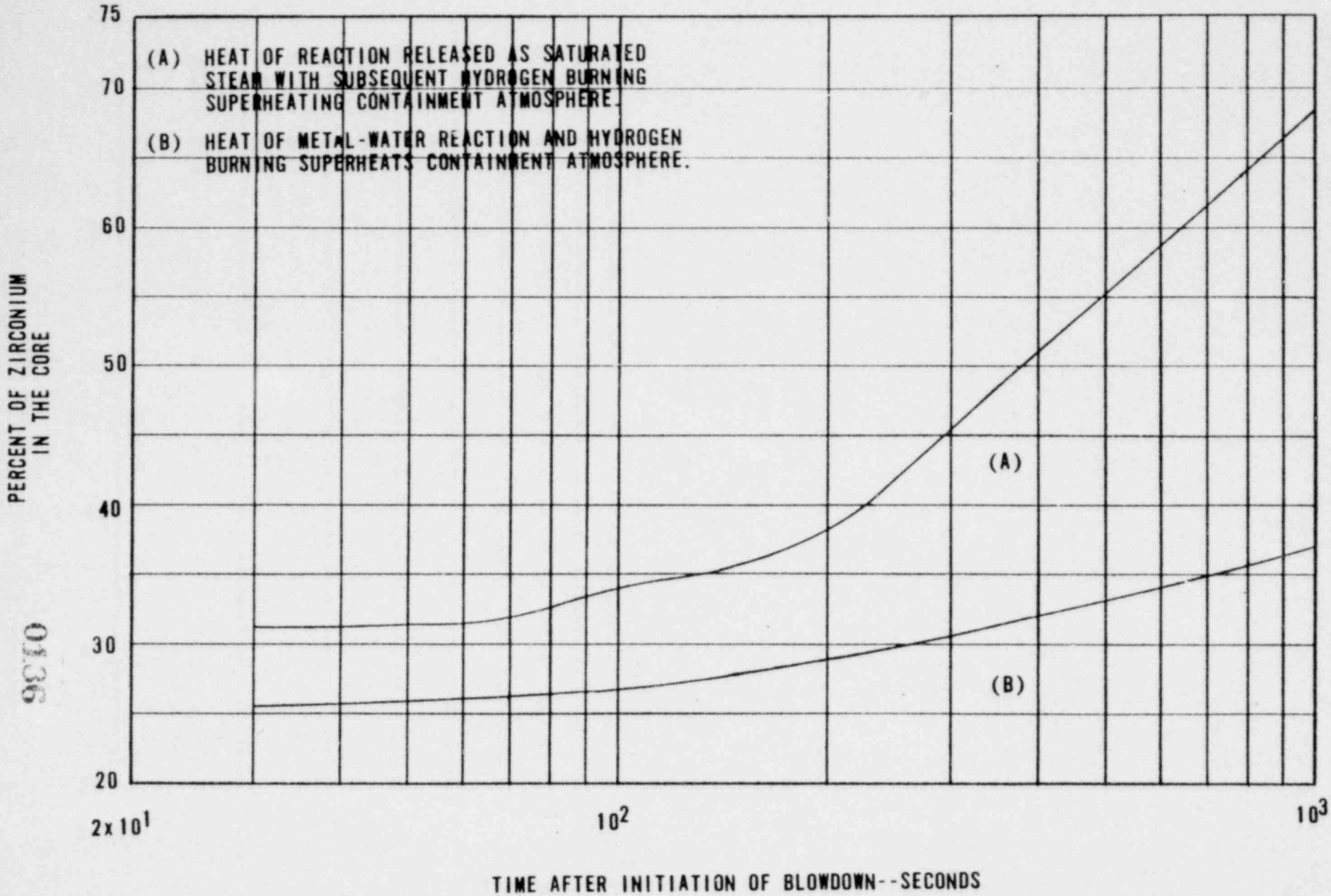

DAVIS-BESSE NUCLEAR POWER STATION
CONTAINMENT VESSEL METAL-WATER
REACTION CAPABILITY - 14.1 SQ. FT. BREAK
FIGURE 14-52

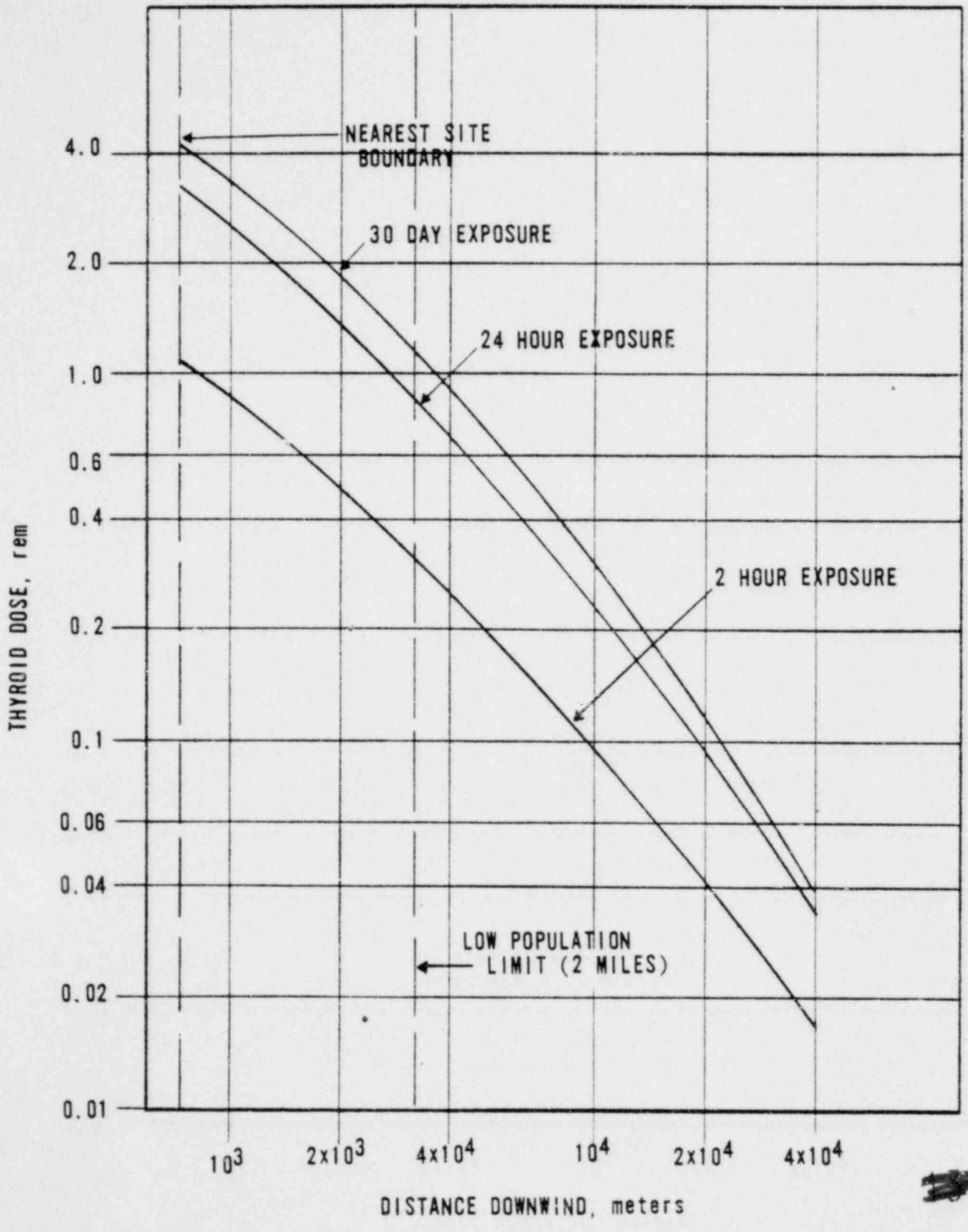

DAVIS-BESSE NUCLEAR POWER STATION
CUMULATIVE THYROID DOSE
LOSS OF COOLANT ACCIDENT
FIGURE 14-53

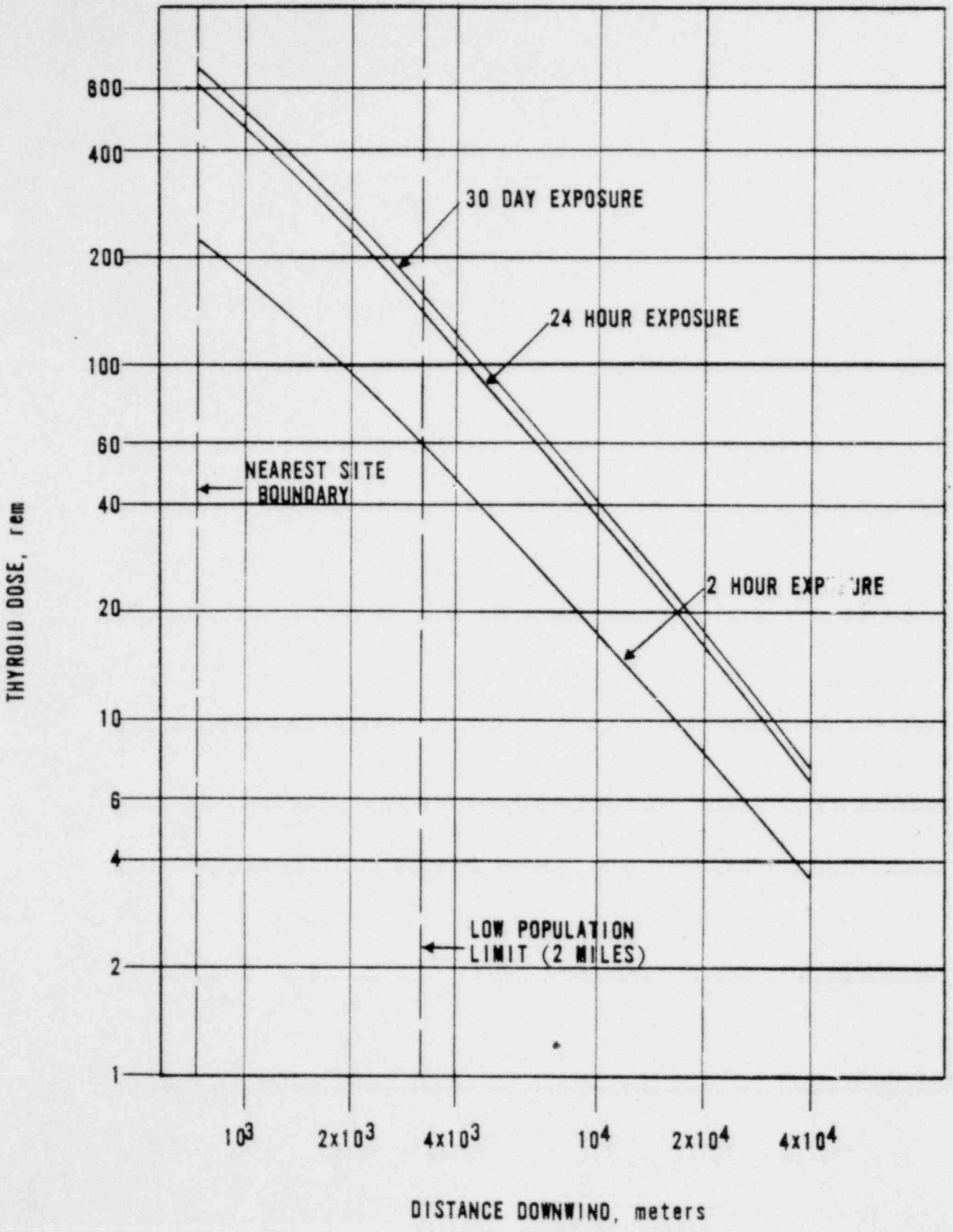

DAVIS-BESSE NUCLEAR POWER STATION
CUMULATIVE THYROID DOSE
MAXIMUM HYPOTHETICAL ACCIDENT
FIGURE 14-54

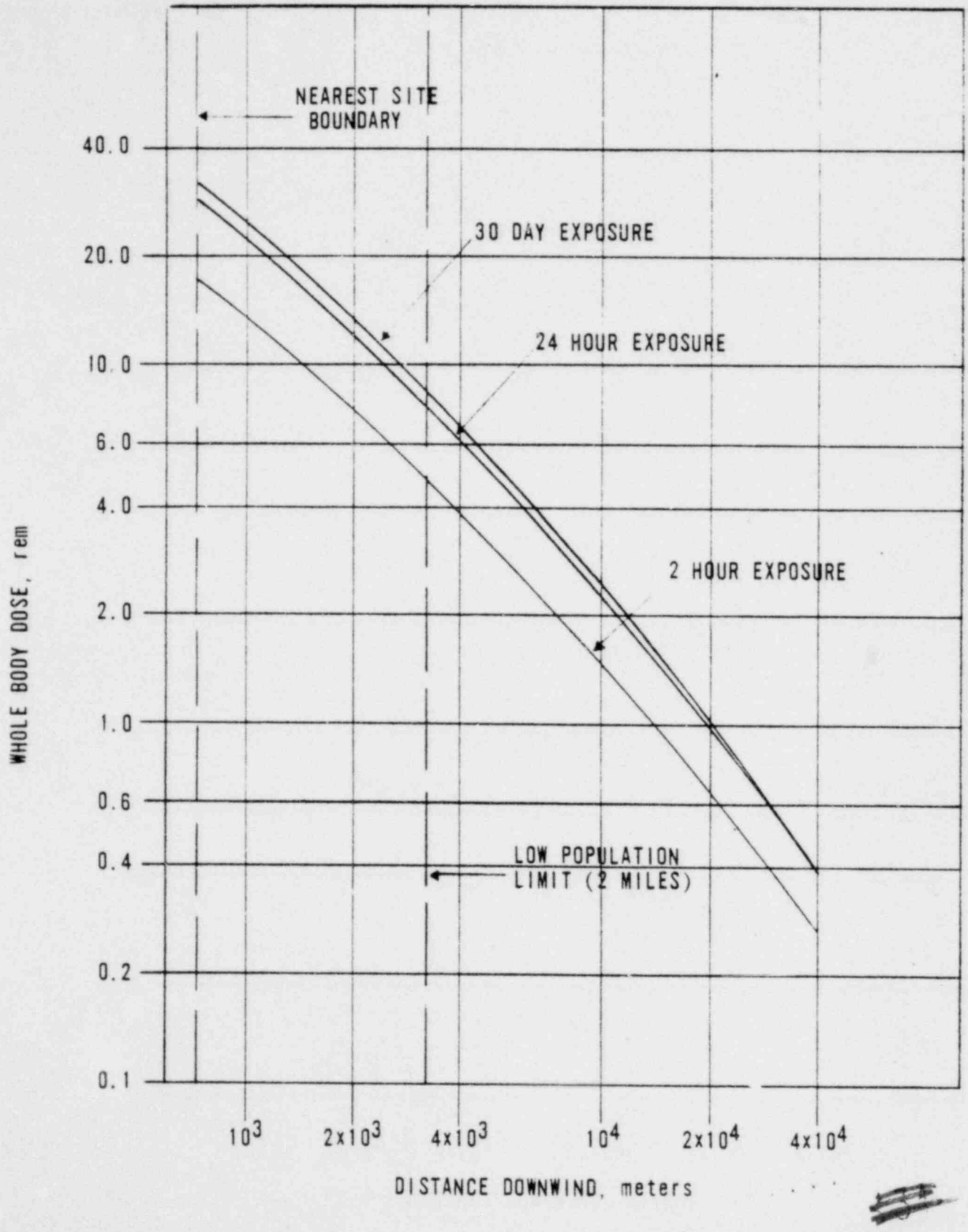

DAVIS-BESSE NUCLEAR POWER STATION
CUMULATIVE WHOLE BODY DOSE
MAXIMUM HYPOTHETICAL ACCIDENT
FIGURE 14-55